Martin Lysnæs-Larsen

Cooling potential assessment for automated window operation algorithms

Based on the ZEB laboratory building, evaluation of wind pressure coefficients and simulations in IDA ICE.

NTNU – Trondheim
Norwegian University of
Science and Technology

I

Acknowledgments

Trondheim, June 10th, 2022

Signature: ....

Department of Energy- and Process Engineering
Norwegian University of Science and Technology

II

Abstract

CO2 emissions and climate change have been an ever-increasingly important topic as global warming has already shown observable effects on the environment. More extreme weather, rising sea levels, and more frequent droughts and floods are some of the many implications. In this regard, the building sector also needs to prioritize the development of smart solutions that require less energy for building operation that also ensures a healthy indoor environment for its occupants. Zero-emission buildings (ZEB) are developed to assist this research process by being an arena where new and innovative components and solutions are developed and tested. In the Nordic climate, the development of energy reduction solutions has previously been based on increasing the insulation in the building body to reduce heat loss. However, the focus in recent years has been shifted, as buildings use less energy for heating and now see higher potential in energy savings by improving cooling performance – due to the well-insulated building bodies. The recently completed ZEB lab building, located at Trondheim at NTNU Gløshaugen, plans to utilize automated windows control as an energy-efficient cooling solution, and needs development before its implementation. This master thesis aims to find the ideal window control algorithms for this specific building by developing a Building Energy Model (BEM) of the ZEB lab, performing on-site measurements for wind pressure coefficients, and analyzing four proposed window control methods in the BEM.

On-site differential pressure measurements at the ZEB lab were conducted, which were utilized to calculate wind pressure coefficients (CP). A total of 15 differential pressure sensors were placed around the facades of the ZEB lab, which measured the pressure difference between the inside and outside of the facades for ten days. There were discovered some inaccuracies and issues with the collected data. However, after some simplifications, a new set of CPs based on the on-site measurements was established. Furthermore, this set of CPs was evaluated against the BEM software (IDA ICE) provided CP set, and it was concluded that the CP set based on the on-site measurements provided a better description of how the wind interacts with ZEB labs building body.

With the new set of CPs based on the on-site measurements, the BEM were simulated with four different heuristic-based window opening strategies to evaluate the respective cooling performance. It was found that all four proposed strategies gave satisfactory thermal comfort for the occupants, which were based on an assessment of the adaptive thermal comfort model and the recommendations from TEK17 §13-4. Furthermore, it was found that the strategies that utilize a fully open/closed window strategy gave a higher risk of draught, and an undesired oscillation between open/closing were found for some specific climatic circumstances. It was also found that night cooling did not provide enough improvement in thermal comfort (due to the small thermal mass of the ZEB lab) and is therefore not worth the investment in time required to develop and operate such a system. Therefore, it is concluded that out of the four heuristic window algorithm models that were evaluated, the one that utilized variable window opening area without night cooling is deemed the best option.

Norwegian summary

CO2-utslipp og klimaendringer har vært et stadig viktigere tema ettersom global oppvarming allerede har vist observerbare effekter på miljøet. Mer ekstremvær, stigende havnivåer og hyppigere tørker og flom er noen av de mange konsekvensene. I denne forbindelse må også byggesektoren prioritere utvikling av smarte løsninger som krever mindre energi til bygg-drift som også sikrer et sunt innemiljø for beboerne. Nullutslippsbygg (ZEB) er utviklet for å bistå denne forskningsprosessen ved å være en arena hvor nye og innovative komponenter og løsninger utvikles og testes. I det nordiske klimaet har utviklingen av energireduserende løsninger tidligere vært basert på å øke isolasjonen i bygningskroppen for å redusere varmetapet. Fokus de siste årene har imidlertid blitt flyttet, ettersom bygninger bruker mindre energi til oppvarming og nå ser et høyere potensial i energisparing ved å forbedre kjøleytelsen – på grunn av de godt isolerte bygningskroppene. Det nylig ferdigstilte ZEB-lab bygget, lokalisert i Trondheim ved NTNU Gløshaugen, planlegger å bruke automatisert vinduskontroll som en energieffektiv kjøleløsning, og trenger utvikling før implementering. Denne masteroppgaven tar sikte på å undersøke vinduskontrollalgoritme for denne spesifikke bygningen ved å utvikle en bygningsenergimodell (BEM) av ZEB-laboratoriet, utføre målinger på stedet for vindtrykkskoeffisienter og analysere fire foreslåtte vinduskontrollmetoder i BEM.

Det ble utført differensialtrykkmålinger på stedet ved ZEB-laboratoriet, som ble brukt til å beregne vindtrykkskoeffisienter (Cp). Totalt ble det plassert 15 differansetrykksensorer rundt fasadene til ZEB-laben, som målte trykkforskjellen mellom inn- og utside av fasadene i ti dager. Det ble oppdaget noen unøyaktigheter og problemer med de innsamlede dataene. Etter noen forenklinger ble det imidlertid etablert et nytt sett med CP basert på målingene på stedet. Videre ble dette settet med CP-er evaluert mot BEM-programvaren (IDA ICE) levert Cp-sett, og det ble konkludert med at Cp-settet basert på målingene på stedet ga en bedre beskrivelse av hvordan vinden interagerer med ZEB-laboratoriets bygningskropp.

Med det nye settet med CP-er basert på målingene på stedet, ble BEM simulert med fire forskjellige heuristisk-baserte vindusåpningsstrategier for å evaluere den respektive kjøleytelsen. Det ble funnet at alle fire foreslåtte strategier ga tilfredsstillende termisk komfort for beboerne, som var basert på en vurdering av den adaptive termiske komfortmodellen og anbefalingene fra TEK17 §13-4. Videre ble det funnet at strategiene som utnytter en strategi for fullt åpent/lukket vindu ga høyere risiko for trekk, og det ble funnet en uønsket svingning mellom åpen/lukking for noen spesifikke klimatiske forhold. Det ble også funnet at nattkjøling ikke ga nok forbedring i termisk komfort (på grunn av den lille termiske massen til ZEB-laboratoriet) og er derfor ikke verdt investeringen i tid som kreves for å utvikle og drifte et slikt system. Derfor konkluderes det med at av de fire heuristiske vindusalgoritmemodellene som ble evaluert, anses den som benyttet variabelt vindusåpningsområde uten nattkjøling som det beste alternativet.

Table of Contents

List of Figures

VIII

List of Tables

Nomenclature

A – Area (m^2)

C – Flow coefficient (-)

C_d – Discharge coefficient (-)

C_p – Pressure Coefficient (-)

g – Acceleration from gravity (m/s^2)

m' – Mass flow rate (kg/h)

N_k - Total distinct leakage of air (-)

P – Pressure (Pa)

Q – Airflow rate (m^3/h)

T – Air temperature (°C)

U – Air speed (m/s)

V – Volume (m^3)

W – External work rate

z – Height (m)

ρ – Mass density (kg/m^3)

Abbreviations

ACH – Air Changes per Hour

AHU – Air Handling Unit

AI – Artificial intelligence

AIVC – Air Infiltration and Ventilation Centre

BEM – Building Energy Modeling

CAD – Computer-Aided Design

CAV – Constant Air Volume

DCV – Demand Controlled Ventilation

DP – Differential Pressure

HVAC – Heating, Ventilation, and Air Conditioning

IAQ – Indoor Air Quality

IDA ICE – Simulation Software

ML – Machine Learning

NTNU – Norwegian University of Science and Technology

NV – Natural Ventilation

PMV – Predictive Mean Vote

PPD – Predicted Percentage Dissatisfied

PV – Photovoltaics

TEK – Norwegian regulations on technical requirements for construction works

VAV – Variable Air Volume

WHO – World Health Organization

ZEB – Zero Emission Building

1. Introduction

CO2 emissions and climate change have been an ever-increasingly important topic as global warming has already shown observable effects on the environment. More extreme weather, rising sea levels, and more frequent droughts and floods are some of the many implications [1]. It is essential to implement measures to minimize the implications of climate change, and the most significant measure is to release less CO2 into the atmosphere. However, when global energy consumption is steadily rising and is forecasted to be rising for most parts of the globe, a study by Ahmad et al. [2] estimated a 23% increase in primary energy consumption when comparing the year 2020 to 2040. Therefore, if consuming less energy is not a viable option, producing cleaner energy from renewable sources and phasing out fossil fuels is likely the solution while improving energy efficiency. Figure 1 shows forecasted global electricity consumption and CO2 emissions, and it is evident that measures have a promising effect as electricity consumption rises at a higher rate than CO2 emissions.
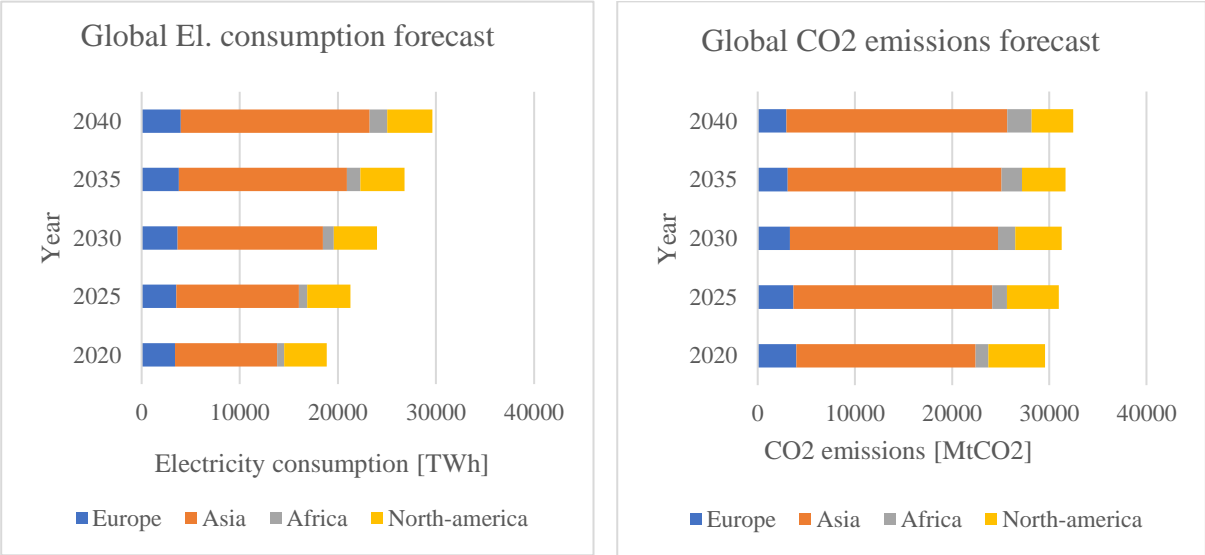
Figure 1: Forecast for global electricity consumption and CO2 emissions by Ahmad et.al [2].

To motivate and promote decarbonization and green energy, international organizations and numerous countries have made a global effort to develop strategies, policies, arrangements, and roadmaps to try to keep global warming at a minimum. The EU has established a long-term climate-neutral strategy by 2050, and the Paris Agreement sets out a global framework to pursue the 2°C goal.

Norway's part of the Paris Agreement is to reduce greenhouse gas emissions by 40 percent by 2030 compared to 1990 levels [1]. Although the nation sets an ambitious goal, the Norwegian Environment Agency [3] only reports a reduction in greenhouse gases of 4,2% from 1990 to 2020. Norway's actual greenhouse gas emissions have mostly been stable since 1990, as shown in Figure 2. 2020 was affected by COVID19, so it does not accurately represent Norway's normal GHG emissions.
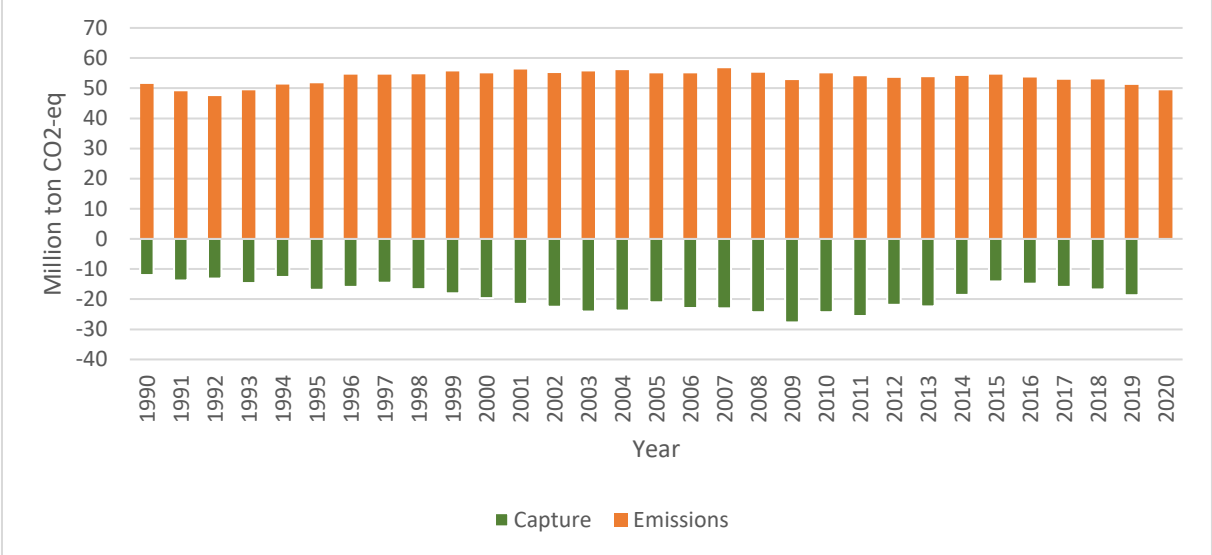
Figure 2: Capture (by trees and land-use) and emissions of GHG in Norway [3]

Therefore, every energy-demanding sector in Norway needs to contribute to reducing the national GHG emissions. As seen in Figure 3, the building sector in Norway accounts for 5% of these CO_2 emissions.
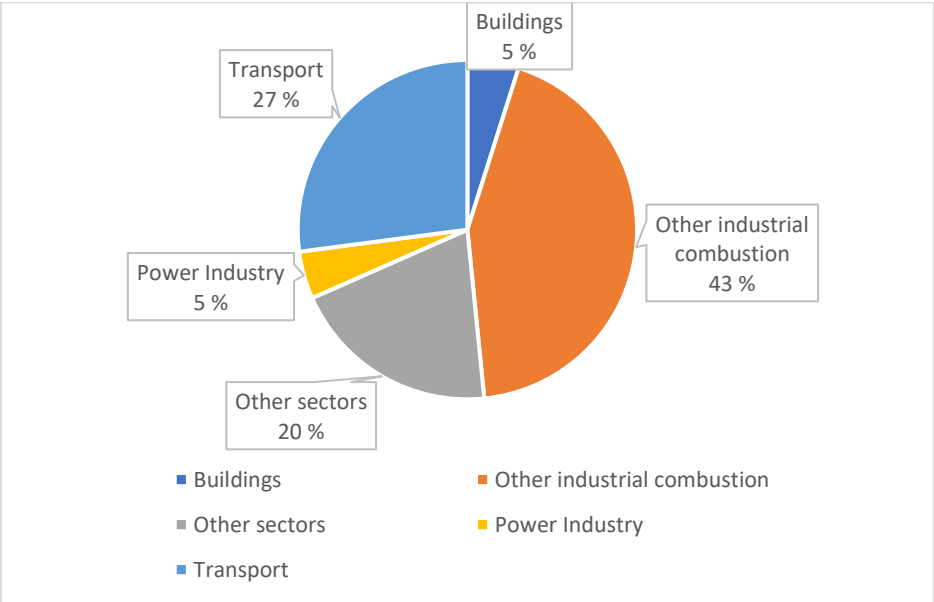
Figure 3: Fossil CO_2 emission by sector in Norway 2020 [4]

1.1.Background

The research center on zero-emission buildings (ZEB) started as a project supported and funded by Norway's research council and was one of their FME projects from 2009 to 2017. Facilities such as Living Lab and Test Cell Laboratory [5], [6] were created and designed with the goal of developing knowledge, competitive products, and solutions for existing and new buildings whose production, operation, and demolition give zero emissions of greenhouse gases while also considering the users need for comfort and flexibility [7].

By applying the ZEB concept, the ZEB laboratory, located in Trondheim at NTNU Gløshaugen, was built and opened for use in March 2021. The vision of the ZEB lab is to be an arena where new and innovative components and solutions are developed, investigated, tested, and demonstrated in mutual interaction with the building's occupants [8]. This project is a collaboration between NTNU and SINTEF and will be:

- A laboratory for the development of competitive international industry
- A laboratory for knowledge generation at a high international level
- A research arena for the development of zero-emission buildings
- An arena for reducing risk when implementing solutions for zero-emission buildings
- A national resource for all research organizations in the field

The building is designed with the ambition level of ZEB-COM and should achieve this over 60 years.

Thermal comfort in buildings in TEK17 [9] requires that operative temperature in buildings where occupants do "light work" shall be in the range of 19-26°C. Though, for hot summer days, it is accepted that 50 hours/year surpasses this upper limit. However, the ZEB lab is very well insulated and has no mechanical cooling installed, so some other means for cooling are needed to be within the acceptable temperature range. The planned solution for the building is to utilize natural ventilation as it will also provide a cooling effect and is controlled and regulated by automatically controlled windows. Such a solution will reduce energy consumption for ventilation; however, more importantly, it removes the energy needed for mechanical cooling. The building is packed with 1500 sensors and 150 controlled objects and generates 17000 data points [10]. This makes the building highly capable of having a sophisticated building energy management system that can be utilized to control the windows for cooling purposes. The windows with actuators are currently not in operation and only opened manually or via an app, so control algorithms need to be produced, tested, and implemented into BMS so that the building can meet the requirements for operative temperature during the summer.

Additional note. This master thesis is a continuation of my previous work last semester. The previous project assignment consisted of on-site airflow measurements at ZEB-lab and proved to be very helpful in preparing this thesis. Therefore, some parts of this thesis's literature study and theory are copied from the previous project assignment. Both assignments are based on much of the same information and were thus deemed acceptable to use again.

1.2. Objective and scope

The objective of this master thesis is to develop window control algorithms that can be utilized for ventilative cooling during the summertime for ZEB-lab building. The work will not be a final product that can be directly implemented into the Building Energy Management System (BEMS) but rather a window control algorithm modeled in IDA-ICE. A great deal of time dedicated to this thesis is used to evaluate wind pressure coefficients for the ZEB lab, as the wind pressure coefficients provided by the BEM are imprecise and not specific to ZEB lab. Hence, on-site measurements and calculations for wind pressure coefficients specifically for the ZEB lab are completed.

If wished, the ideas and work from this thesis can be implemented and tested at ZEB-lab, but this will require the algorithms to be programmed from IDA-ICE's user interface over to the BEMS. The work can also provide some guidelines if later master students or employees at ZEB-lab wishes to continue to work on this problem.

The thesis work mainly consists of these three parts:

1. Develop a detailed and accurate Building Energy Model (BEM) to address the cooling efficiency of window cooling of the ZEB lab.
2. Obtain sufficiently accurate pressure coefficients for the BEM, which will be done by on-site measurements and calculations, which must be evaluated for accuracy.
3. Test and develop four window control algorithms for the BEM, to address how each model performs and the optimal strategy for ventilative cooling in the ZEB lab.

To answer the two research questions, *"How do the wind pressure coefficients from databases compare to the on-site measured and calculated wind pressure coefficients for ZEB lab, and what is the optimal window cooling strategy for ZEB lab?"*

The report is built up by first presenting relevant theory for the thesis work, including theory regarding the thermal environment, building ventilation, fluid mechanics, and window cooling. Furthermore, the methodology chapter presents the on-site measurement setup and wind pressure calculations, the BEM, and a description of the proposed window control algorithms. The result chapter is divided into on-site measurement results + pressure coefficient calculations, a comparison of the provided pressure coefficients in the BEM with the new measured ones, and an assessment of the proposed window control algorithms.

2. Indoor environment

Inhabitants living in the Nordic climate spend, on average, 90 percent of their time indoors; thus, the indoor environment has great importance to our health, well-being, and productivity [11]. According to World Health Organization (WHO), the indoor climate is defined by five categories: thermal, atmospheric, acoustic, actinic, and mechanical environment. In addition to the five climate parameters, the indoor environment is also affected by the esthetic and psychosocial environment. A short description of the climate parameters can be found in Table 1.

Table 1:Description of Indoor climate parameters [12]

Indoor climate parameter	Description
Thermal environment	The body's heat balance and everything that affects it. Such as air temperature, heat radiation and draught.
Atmospheric environment	Quality and contents of indoor air. Such as gases, smells, chemical substances, and particles.
Acoustic environment	Sound levels, noises, and frequencies.
Actinic environment	All types of radiation. Such as lighting, daylight, reflections, electrical fields, and radioactive radiation.
Mechanical environment	Such as ergonomics, sitting position, devices and helping aids in the building (e.g., handrail, anti-slip)

This thesis aims to study how the thermal environment is affected by natural ventilation (NV) cooling. Therefore, it is only necessary to present this indoor climate parameter in detail in this chapter. The atmospheric, acoustic, and actinic environment will also be impacted by NV-cooling and will be considered in the result/discussion chapter.

2.1. Thermal environment

The thermal environment entails the relationship between the environment and the body's heat balance and includes every factor influencing it. The human body tries to maintain a core temperature of roughly 37°C (some variation from person to person), and this core temperature is maintained within narrow limits. This balancing act of the body is a continuous battle between heat loss and gain and is greatly affected by external conditions, such as temperature and clothing. The heat balance of the body can be expressed with the following equation 2.1 and can be used to calculate the heat gain (or loss) of the body.

$$S = M - W - (C_{res} + E_{res} \pm C \pm R + E)$$

2.1

Where S is the heat storage of the body, M is the metabolic rate, W is external work rate, C_{res} is the respiratory convective heat loss, E_{res} is the respiratory evaporative heat loss, C is the convection, R is the radiation and E is the evaporation of sweat.

Thermal comfort

Thermal comfort is a condition of the mind which expresses satisfaction with the thermal environment [13]. Every individual will experience the thermal environment differently because of the variations of their bodies, both psychologically and physiologically. Therefore, it is impossible to ensure thermal comfort for everybody, and a building should be designed to provide a thermal environment that satisfies most people.

Undeniably, thermal comfort depends on environmental factors, clothing factors, and physiological factors [14]. There are currently two common approaches to evaluating how these elements affect thermal comfort: Fanger's model of thermal comfort and the adaptive model for thermal comfort.

2.2. Fanger's model of thermal comfort

Fanger's thermal comfort model [15] is based on empirical studies where he analyzed the thermal comfort of 1396 subjects in a climate chamber with steady-state conditions. The models he developed are the PMV- and PPD-indices which are now the standard go-to-method used to evaluate thermal comfort in Norway today by the standard NS-EN 16798 [16]. These indices are based on the six fundamental factors that define thermal comfort for humans. Four of these are affected by the surrounding environment, and two are affected by each individually, i.e., behavioral factors. These factors are described in Table 2.

Table 2: Fanger's thermal comfort factors

Environmental	
	1. Dry bulb temperature (T_a)
	2. Black-globe temperature (MRT)
	3. Air velocity (v)
	4. Relative humidity (RH)
Behavioral	5. Clothing (Clo)
	6. Metabolic rate (M)

The environmental factors are mostly the same for everybody in that specific environment and must therefore be aimed to suit the masses. These factors can be calculated and measured with well-defined and proven equations, elaborated by Ingebrigtsen [12]. The last two factors, clothing and activity level, can vary between individuals to suit their psychology and physiology. I.e., if an occupant is cold, then put on more clothes.

2.2.1. Clothing

When evaluating the thermal comfort, it is essential to assess how much clothing the occupants are using and how much thermal resistance the clothes create between the skin surface and the outside of the clothes surface. This resistance is referred to as isolation and has the unit (m2K)/W or Clo, where 1 Clo is equal to 0.155 (m2K)/W. Table 3 includes some examples of typical clothing outfits and their representative Clo values.

Table 3: Clo-values for different outfits [12]

Clothing	Clo	$(m^2K)/W$
Naked	0.0	0.000
Typical tropic outfit (shorts, t-shirt, and sandals)	0.3	0.050
Summer outfit (light dress, tights, panties)	0.45	0.070
Summer outfit (light pants, shirt with short sleeves, light socks, and shoes)	0.5	0.080
Light work attire (long-sleeved shirt, work trousers, wool socks, and shoes)	0.7	0.110
Ordinary winter outfit (long-sleeved shirt, pants, jacket or sweater, thick socks, and shoes)	1	0.155
Outdoor attire (coat, jacket, west, pants etc)	1.5	0.230

Table 3 shows typical Clo values for standing humans; however, it does not include factors such as a typical office chair that would increase Clo by 0.15. Estimations for summer clothing outfits are expected to be around 0.5 and, in the winter, around 1. This is merely an estimate as clothing varies from person to person. Nevertheless, this approach is considered sufficiently accurate when addressing a group of people that occupies a zone.

2.2.2. Metabolic rate

The human body uses energy to perform mechanical work and internal heat production. This oxidation process is referred to as metabolic rate, and it influences the thermal comfort of humans and what temperature range is acceptable. I.e., warehouse workers and office workers should have a different thermal environment in their workspace because of the difference in activity level. Furthermore, energy related to mechanical work can be assumed to be zero in most buildings, such as offices and schools. Therefore, the metabolic rate equals the internal heat production, which is directly correlated to the activity level. A generalization can then be made by distinguishing between different activities and their correlated heat production. The standard unit for this is 1 met and is equal to 58W/m2 skin surface area and correlates to sitting still at a relaxed activity level. Other everyday activities and their correlating met and W/m2 can be found in Table 4.

Table 4: Met-values for different activities [12]

Activity	[W/m^2]	[met]
Lying still	46	0.8
Sitting, relaxed	58	1.0
Standing, relaxed	70	1.2
Sitting, calm activity (office, residential, school)	70	1.2
Standing activity (laboratory, light industry)	93	1.6
Standing activity (housework, work by machines)	118	2.0
Medium activity (heavy work by machines, workshop work)	165	2.8
Elite sport activity	870	15.0

2.2.3. PMV- and PPD-model

Predicted mean vote (PPD) is an index used to predict the mean values of thermal votes when a group of people is exposed to the same thermal environment. The PMV index is a 7-point scale developed by Fanger [15] and is based on experimental studies and goes as follows:

+3 very hot
+2 hot
+1 slightly hot
0 neutral (comfortable)
-1 slightly cold
-2 cold
-3 very cold

Where the ideal PMV = 0.

The PMV index can be used qualitatively by questionnaires or quantitative by calculations and measurements. For calculations, one must gather data for all environmental and behavioral comfort factors and use tables and equations from NS-ISO 7730 [17] to calculate the corresponding PMV value.

Predicted people dissatisfied (PPD) is a function of PMV and predicts the percentage of dissatisfied people in the group experiencing the same thermal environment. Some people will always be dissatisfied with the thermal environment because of psychological and physiological factors, so the minimum PPD value is 5%. The following equation 2.2 and Figure 4 describes the relation between PMV and PPD.

$$PPD = 100 - 95 \cdot e^{(-0.03353 \cdot PMV^4 - 0.2179 \cdot PMV^2)}$$
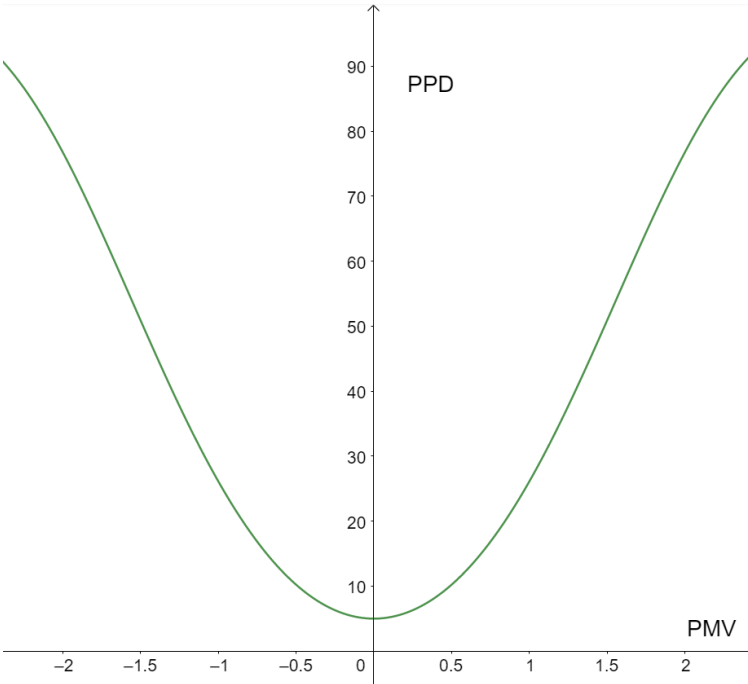
Figure 4: PPD as a function of PMV

The PMV and PPD-model have been accepted as the go-to-model for many years by standardizations and regulatory organs. As the model has undergone more scrutinization over the years [18], [19], other thermal comfort models have been developed to address the issues by implementing other approaches for evaluation.

The PMV model is based on experiments performed in 1970 with a relatively small dataset and was measured in a steady-state thermal environment. Hence, it does not include all aspects that affect human thermal comfort. New technology and data logging over long timespans have shown that the model may not be as complete as previously believed and has therefore been under investigation for its accuracy. Cheung et al. [22] did a thorough analysis by comparing the ASHRAE Global Thermal Comfort Database II with the PMV/PPD-model and concluded that the overall accuracy was only 34%; when comparing the PMV versus the observed thermal sensation. It was also demonstrated that a simple thermal comfort model that only utilized temperature as comfort criteria would have had an accuracy of 43%. Additionally, a study performed by Hoof et al. saw a low correlation between the percentage of dissatisfied (PD) and PPD [20], which caused ASHRAE Standard 55-2017 [21] to remove the PPD model due to low prediction accuracy.

2.3. Adaptive thermal comfort model

The adaptive models do not accurately predict people's thermal comfort, but models under what operative temperature range people will experience satisfactory thermal comfort. Generally, people will adjust themselves or their surroundings to reduce thermal discomfort and physiological stress. Factors such as thermal adaptation, climatic, cultural, and social aspects affect thermal comfort [23]. Hence when occupants can control their environment by adaptive measures, such as a change in clothing, cooling by fans, and control of window opening, it has been observed that a broader temperature range of 17 to 31°C can still achieve an acceptable level of thermal comfort [24]. Following Figure 5 shows the acceptable temperature range by building category accepted by the standard EN 16798-1:2019 for buildings without mechanical cooling systems.
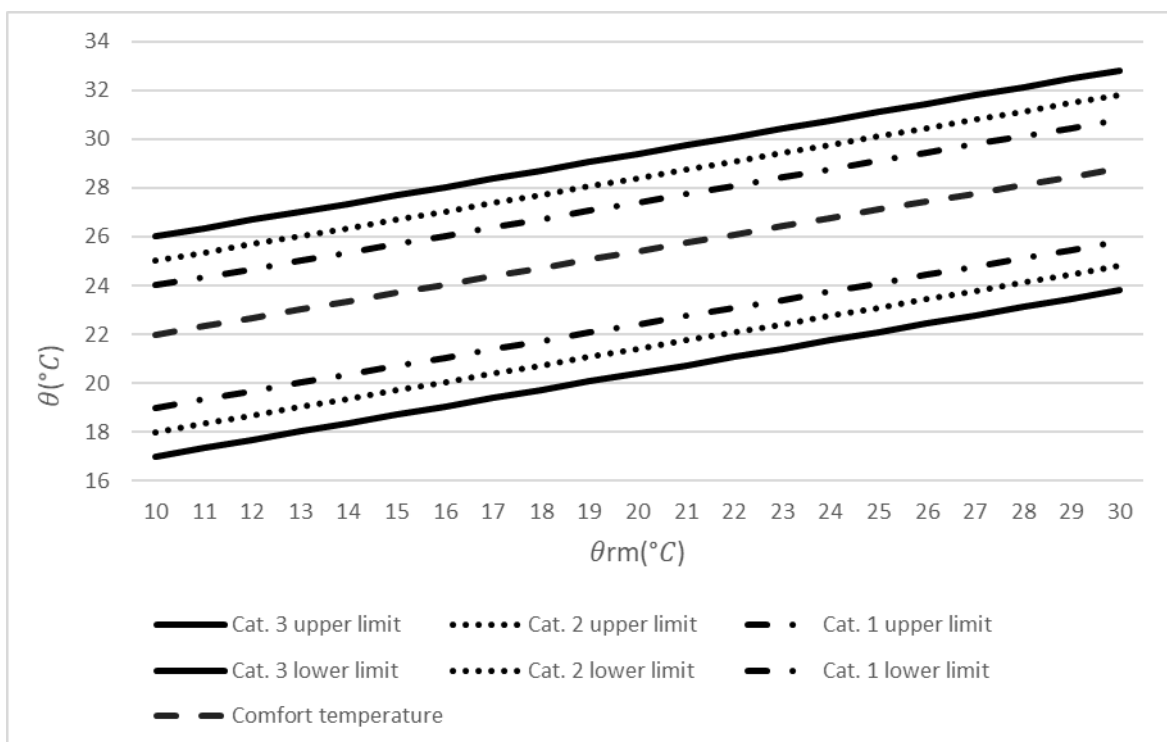
Figure 5: Acceptable indoor operative temperature range for Adaptive Models, recreated from NS-EN 16798-1:2019 [16]

Where $\theta(°C)$ is the indoor operative temperature, and θrm$(°C)$ is the running mean outdoor temperature.

Building category 1 has a high level of expectation of thermal comfort, 2 is medium, and 3 is low. Hospitals and buildings where occupants have special needs are in category 1. Most offices and schools require a medium level of comfort, meaning category 2, and buildings with a low level of requirement for thermal comfort are category 3. ZEB-laboratory falls under category 2.

3. Building ventilation

The process of supplying fresh air to the building while extracting the used contaminated air is referred to as building ventilation. This can be accomplished in a few different ways: either mechanically, naturally, or a combination of both (hybrid). Mechanical ventilation utilizes fans to create pressure differences to move air around the building by ductwork and other components. Natural ventilation relies on the naturally generated forces by buoyancy and wind to create pressure differences in the air, and hybrid ventilation utilizes some aspects of both approaches.

3.1. Mechanical ventilation

Mechanical ventilation is usually driven by air handling units (AHU) connected to the building's ductwork that supplies and extracts air. The air handling unit typically consists of components such as fans, dampers, filters, heat exchangers, heating/cooling batteries, and humidifies/dehumidifiers - all after the specific requirements of the building. After AHU has processed the air, it is distributed through the duct network with the help of dampers to regulate pressure and then supplied to the zone/room with diffusers and air terminal devices. The old and contaminated air is then afterward extracted and exhausted outside of the building.

With the utilization of fans to distribute air, mechanical ventilation is considered a reliable solution with many advantages. A well-designed system can control air rates, temperature, moisture, and air contamination, which is necessary for buildings with strict requirements for air quality like hospitals. Due to its many advantages, it is commonly utilized in many other building categories, like commercial and municipal buildings. Another advantage of mechanical ventilation is that it can save energy by utilizing heat recovery in the AHU, which can recover up to 85% heat of the extracted air [25]. Furthermore, in many cases, mechanical ventilation systems are operated by a complex Building Energy Management System (BEMS), which will regulate the ventilation system and optimize the indoor climate for the occupants while minimizing energy consumption.

Control strategies for mechanical ventilation
There are three common control strategies for mechanical ventilation: constant air volume (CAV), variable air volume (VAV), and demand-controlled ventilation (DCV). These control strategies suit different requirements, and therefore the choice of the control strategy is essential when designing energy and cost-efficient mechanical ventilation systems. It is also common to use a combination of all three strategies.

Constant air volume – CAV

A mechanical ventilation system with CAV control will supply the connected zones with constant airflow following a predefined schedule, and this is regardless of what the actual need of the zone is at the time. The CAV system operates by having an *On* and *Off-mode* where the *on-mode* is the design criteria for the zone (the maximum load of the zone), and the *off-mode* is the minimum requirement of the zone (usually only airflow needed to counteract the material pollution).CAV systems can easily over-ventilate zones, which will result in unnecessary energy usage, which can also have unwanted effects on the indoor climate, such as unwanted cooling. On the other side, CAV systems have low investment costs and more easily be maintained and controlled. This makes CAV-control best suited for zones with minor variations in pollution and heat load, where the ventilation requirement is usually continuous [26]. Such rooms can be printing rooms, hallways, storage, or WC.

Variable air volume – VAV

VAV ventilation variates the airflow in response to changes in air pollution or sensible heat/cooling load in the zone. Thermal comfort in the conditioned space is maintained by having a constant temperature and varying the quantities of supply air [27]. This control schedule regulates the air volumes by utilizing zone dampers that will regulate after a set of predefined variables. The input from sensors (usually CO_2, temperature, and motion detection) will give an input value, and the dampers regulate airflow afterward. The advantages of VAV are considerably lower energy usage than CAV and more control, but more complex and expensive to install.

Demand controlled ventilation – DCV

Demand-controlled ventilation is a feedback or feedforward control method that automatically regulates the airflow to meet the specific demand based on the air quality indicator. DCV is considered an advanced demand management system that can variate both airflow and temperature and is useful in buildings with high requirements for indoor air quality and thermal comfort. DCV can be regulated after occupancy, air quality, humidity, or temperature and can be highly customizable to meet specific needs in different zones and for different occupants. Studies have shown that DCV compared to CAV and VAV indeed results in drastically lower energy usage related to fans, heating, and cooling. Ahmed et al. found a decrease of up to 41% reduction in energy consumption by fans, heating, and cooling when compared DCV to CAV [28], and Wachenfeldt et al. saw an energy reduction of 87% in fan energy and 21% in heating energy [29].

13

3.2. Natural ventilation

Natural ventilation can be driven by either buoyancy, wind, or a combination of both. Buildings can be designed to take advantage of these forces by utilizing openings in the facades and floor dividers to circulate airflow throughout the building. A well-designed natural ventilation system can therefore result in close to zero operating costs and can also provide considerable savings in space cooling. With also low investment cost and low carbon emissions, the advantages of utilizing natural ventilation can be favorable in many circumstances, and it is widely used and considered one of the most common passive energy-saving technologies [30].

Depending on what natural force is generating the most dominant pressure difference in the air at the time, it will be the main driving force for airflow. If it is particularly windy, the thermal buoyancy force will have minimal impact on airflow and vice versa. A more detailed description of the fluid mechanics for natural ventilation will be explained in chapter 4.

The problem with natural ventilation is its ability to maintain adequate temperature for good thermal comfort and sufficient IAQ, especially in climates with high outdoor air temperature and relative humidity. One is very much dependent on external conditions, and this can cause unwanted draught, over/under ventilating the building, or undesirable temperatures. Outside noise can also annoy the occupants if windows must be kept open for ventilation and cooling purposes. However, many challenges to overcome it is feasible to design adequate natural ventilation systems, and studies have even shown that occupants are generally more satisfied and report higher thermal comfort in buildings with natural ventilation [31].

Natural ventilation is commonly categorized into four different strategies. Namely cross ventilation (CV), stack ventilation (SV), single-sided ventilation (SSV) and corner ventilation (CRV) [32]. Depiction of the strategies can be seen in Figure 6.

(a) CV

(b) SV

(c) SSV

(d) CRV
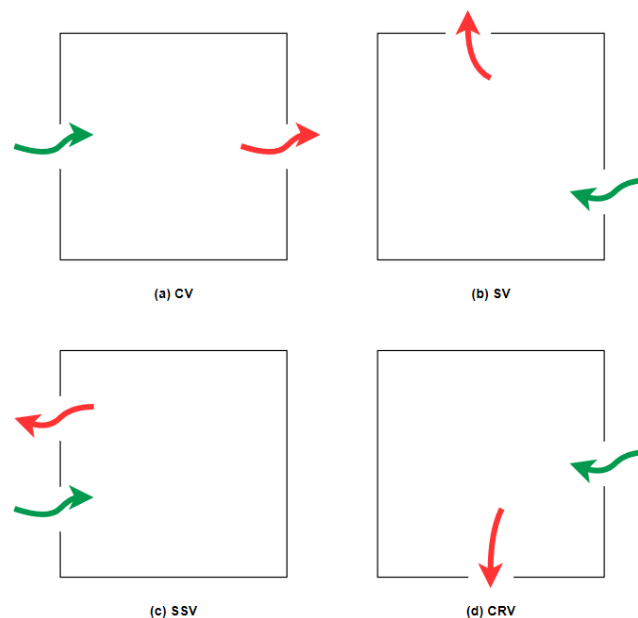
Figure 6: Classification of natural ventilation strategies revised from [32]: (a) cross ventilation (horizontal plane), (b) stack ventilation (vertical plane), (c) single sided ventilation (vertical or horizontal plane) and (d) corner ventilation (horizontal plane).

CV occurs when there are two openings on different facades, where there is a flow path between the facades. Air will then enter the building via an opening on the windward side, then flow through the building and exit on the leeward side. Wind-generated pressure differences usually dominate CV, and the occurring pressure gradient through the building will create significant ventilation rates when compared to the other strategies [32].

CRV shares many similarities with CV, as airflow also enters on one façade and exits on another façade; in CRV's case, the airflow exits on the adjacent façade, which implies that wind-generated pressure differences also dominate CRV. Airflow rates for CRV will usually be lower than CV since the pressure gradient between the facades will be lower; there is a tendency for CRV to have a short circuit between the inflow and outflow openings [33].

SV relies mainly on buoyancy to be the main driving force. As colder air enters through an opening on a façade, the hotter, less dense, and contaminated air flows upwards and exits through an opening on the roof. The effect of buoyancy increases the more significant the vertical height is between the openings, and the higher the driving force and ventilation rate will be [34]. However, even though buoyancy is the dominant driving force, wind can still create much higher pressure differences than buoyancy under moderate air temperatures. Hence under windy conditions, SV may also be wind-driven. If the wind opposes buoyancy, the ventilation flow may tend to zero or, in the worst case, reverse the flow path Thus, stagnation in airflow may occur, but this will never be a stable configuration due to the variations in wind direction and intensity. In a case study performed by Gladyszewska-Fiedoruk et al. [36] on the effect of wind in a building with SV, it was found that under windy conditions, the ventilation rate can change by up to 350%.

Much like SV, SSV does only have openings on one façade. However, due to the many configurations of opening setups for SSV, the dominant driving force may be different. SSV can utilize only a single opening where air enters and leaves the zone through the same opening. The airflow is usually small and is attributed to pressure variations across the opening, primarily due to wind fluctuations. Alternatively, multiple openings at different geometries and heights can induce pressure differences by buoyancy or local pressure variations in the zone to induce higher airflow. Multiple-opening SSV systems were found to be creating higher airflow quantities than single-opening even though the same opening area [37].

3.3. Hybrid ventilation

Hybrid ventilation combines both mechanical and natural ventilation, aiming to utilize the advantages of both ventilation methods while avoiding the negative attributes. The benefits of implementing a hybrid ventilation system should be (in the ideal case) low energy consumption because of the natural ventilation aspect and better reliability from the mechanical ventilation. The control strategy and implementation of a hybrid ventilation system can lead to less-than-optimal efficiencies of the HVAC systems if not thoroughly planned and tested. Haein et al. [38] studied occupants' behavior concerning hybrid ventilation systems and their efficiency. They discovered some implications related to occupants' adaptive behavior that resulted in overheating and over-ventilation that occurred regularly. Especially when occupants have window control, they saw that windows were used to cool while the heating system was heating, which was caused by wrong adjustments of the heating curve. Nevertheless, even though less-than-optimal efficiency, it was concluded that the hybrid ventilation system that they studied consumed less electricity than a high-energy efficient mechanical ventilation system would consume.

There are a few common approaches to design and methods of hybrid ventilation. The principle of *Natural and mechanical ventilation* is based on two entirely separate systems in which the control strategy is to switch between the two systems or use either of the systems in a room/zone. For example, the control strategy can be to use natural ventilation in the summer and mechanical in the winter, or mechanical in the hallway and natural in an office. The second common principle for hybrid ventilation is *fan-assisted natural ventilation,* where the idea is to utilize fans to drive airflow when the natural forces do not create sufficient airflow. The last principle is *stack- and wind-assisted mechanical ventilation,* where one utilizes the natural driving forces for airflow inside the building instead of fans and ducts. An example of this principle is to have the AHU in the attic and have the old and contaminated air rise through the building, which will eliminate the need for return ducts, as the air will travel from the zones directly to the AHU.

Mixed-mode ventilation

Lastly, for hybrid ventilation, there is the possibility to mix both natural ventilation by electrically controlled openings (windows/doors/louvers) and mechanical ventilation in one zone at the same time – this is referred to as mixed-mode ventilation. While there is no standard way to apply such a system, there are some common approaches in practice today [39]. Some of the principles from hybrid ventilation can also be applied here; there is *concurrent mixed-mode (same space, same time)* operation which entails a combination of HVAC and natural ventilation by operable openings in a zone. Here the mechanical ventilation is mostly for supplementing the natural ventilation where the occupants can regulate windows freely. Furthermore, the two other approaches are *change-over (same space, different times)* and *zoned (different space, same time)*. A change-over system determines what mode of ventilation shall be applied based on outdoor/indoor climates, occupancy sensors, or any form of predefined modes. The zoned system has different strategies and combinations in different zones throughout the building. Mixed-mode ventilation must have a reliable control system that can handle different scenarios and outdoor/indoor climates and conditions. Typical examples of such a system are VAV-dampers, sensors for air/temperature/movement, louvers, and window-control actuators that can regulate the indoor climate after occupant behavior and predefined modes in the ventilation system.

16

4. Fluid mechanics for ventilation

Due to the complexity of airflow patterns and the forces that are involved, an accurate estimation of natural ventilation efficiency can quickly become a complicated task. Although it is possible to calculate airflows with high accuracy with conventional fluid dynamics with well-defined boundary conditions, it is not a practical method in most scenarios. With the turbulent nature of wind and ever-changing outdoor conditions, it is considered an impractical problem to solve with this approach. However, there are a few other viable methods that can be utilized to address this issue. Depending on the complexity of the model and the required input data, all with various levels of accuracy. For example, detailed empirical algorithms can give a valuable overview of single-zoned buildings but are limited in their accuracy. When higher accuracy is needed, then: network, zonal, or CFD models are required. In this chapter, these commonly utilized approaches for estimating airflows for a natural ventilation system will be elaborated further.

4.1. Fluid mechanics equations

The fundamental equations for fluid mechanics are presented in this subchapter, with the focus on equations that are necessary for natural ventilation calculations.

Mass conservation equation

Under steady-state conditions, the mass going into a zone must equal what is going out. This is expressed by the following equation 4.1, where airflow enters/exits the zone via ventilation ducts and by various leaks.

$$m'_{vent} + \sum_{k=1}^{N_k} m'_k = 0$$

4.1

Where the total mass flow through ventilation m'_{vent} [kg/s] added with all distinctive leaks N_k and their corresponding mass flow m'_k [kg/s] is equal to zero.

Continuity equation

From the equation 4.2 of mass conservation one can derive the relationship between the density, area that the fluid is flowing through, and velocity. This results in the following equation for steady, one-dimensional flow.

$$\rho_1 A_1 u_1 = \rho_2 A_2 u_2$$

4.2

Where $\rho_{1,2}$ is the fluid density [kg/m^3], A_{1-2} is the opening area [m^2] and u_{1-2} is the velocity of the liquid [m/s].

In many applications, the difference in fluid density can be neglected if there is close to zero difference in temperature and pressure. When applied to multiple inlets and outlets, always ensure that the net mas flow is equal to zero and with a positive/negative sign with respect to flow direction.

Conservation of energy (Bernoulli equation)

Bernoulli principle is used to describe a fluid's state along its flow direction, as shown in equation 4.3. It describes the relationship between the fluid's pressure, speed, and height and is regarded as the energy-equation of fluids in motion.

$$P + \frac{1}{2}\rho u^2 + \rho g h = constant$$

4.3

Where P is the fluids pressure [Pa], g is the gravity constant of 9.81 [m/s²], and h is the height [m].

And by following a volume of fluid along its path, some of the variables may change but the total remains the same. One can then describe the relationship between two points along the fluids path with the following equation 4.4.

$$P_1 + \frac{1}{2}\rho u_1^2 + \rho g h_1 = P_2 + \frac{1}{2}\rho u_2^2 + \rho g h_2$$

4.4

Where P_1, u_1, h_1 refers to the static pressure, velocity, and height of the fluid at point 1, and P_2, u, h_2 at point 2. To utilize Bernoulli's equations, it is also considered that the fluid has constant density, the flow is steady, and there is no friction.

Stagnation pressure

When fluids in motion strike a surface perpendicular to its flow, some of the fluid is forced to change direction. In this process, some of the dynamic pressure of the fluid will be converted into static pressure. The new pressure occurring at the surface is referred to as stagnation pressure. This effect can be seen in Figure 7.
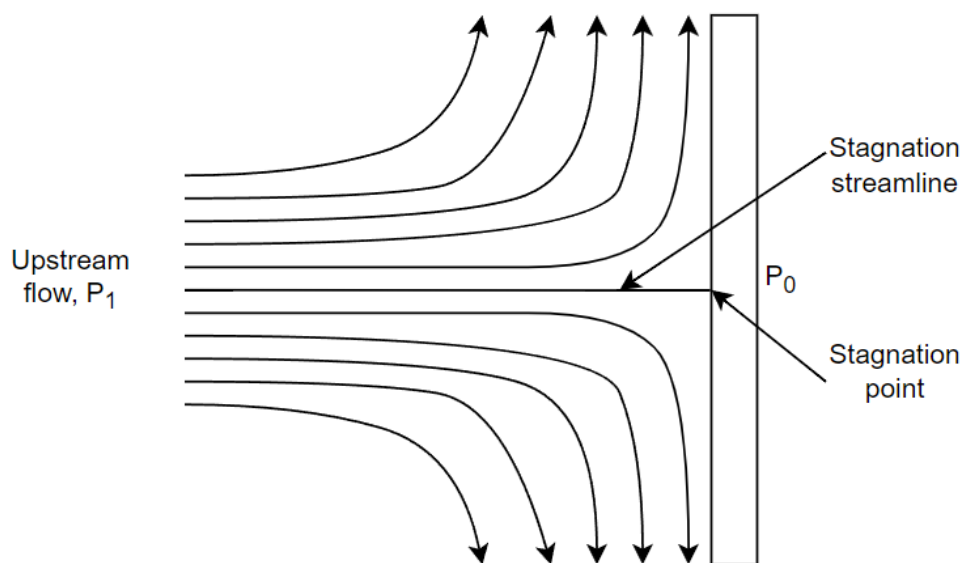
Figure 7: Visualization of stagnation streamline and point

In this example of stagnation pressure, half of the streamline flows upwards and half downwards. However, there is a point where the streamlines are dividing, and the fluid comes to complete rest. This point is referred to as the *stagnation point, a*nd at this point, the following equation 4.5 can be derived from Bernoulli's equation.

$$P_1 + \frac{1}{2}\rho v_1^2 = P_0$$

<div align="right">*4.5*</div>

The occurring pressure P_0 is called total pressure or stagnation pressure. It is the highest pressure found anywhere in the flow field and is the sum of the static and dynamic pressure upstream, where the perpendicular plate does not affect the pressure of the fluid.

4.2. Stack-effect

Temperature variations in the air can be a driving force for airflow, known as buoyancy-driven ventilation or the stack-effect. The air temperature in a zone is usually not homogenous, which results in a temperature gradient throughout the zone. The heavier and colder air will flow towards the floor, and the hotter and lighter air will flow upwards towards the ceiling. This effect is enhanced by the greater temperature and heigh difference between the upper and lower apertures in the zone. Not only does the pressure difference between the apertures induce airflow, but the airstream in motion will have a higher speed than stationary air. By applying Bernoulli's principle to the air in motion, it is apparent that the air in motion will have lower pressure [40], further inducing more airflow. Therefore, the occurring pressure differences on which buoyancy ventilation is based are a combination of temperature differences and Bernoulli's principle's effect. Visualization of airflow due to the stack-effect can be seen in Figure 8.
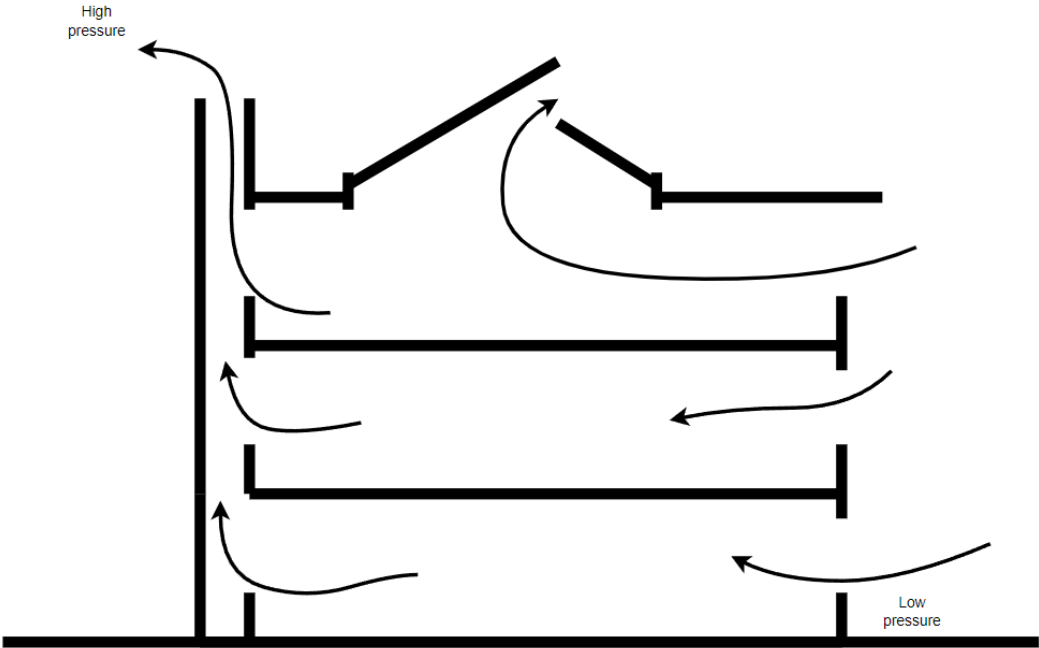
Figure 8: Airflow due to stack ventilation and Bernoulli's principle

The difference in air density ρ with relation to the air temperature T, can be calculated from equation 4.6.

$$\rho = \rho_{ref} \cdot \frac{273.15}{T}$$

Where ρ_{ref} is the air density at 0°C and is equal to 1.29 kg/m³, and T is the air temperature [K]. This equation is only viable if the air is considered an ideal gas.

To study the effects of thermal buoyancy and calculate the airflow that occurs due to the pressure differences, one first needs to describe the pressure profile of the zone being considered. The following Figure 9 shows an example of a pressure profile for a zone with airflow into the zone at a low height and outflow at a higher height in the zone, excluding potential wind-induced pressure variations.
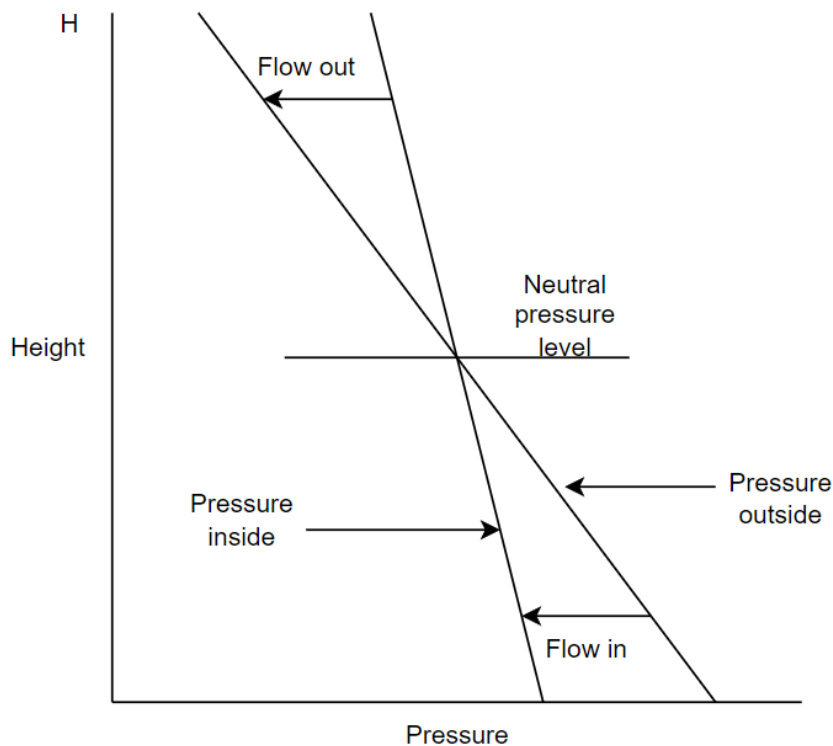
Figure 9: Pressure profile due to stack-effect and excluding the effect of wind

By excluding the effects of wind-induced forces and only evaluating the pressure differences caused by buoyancy, equation 4.7, describes *static pressure P_1 at a given height h_1.*

$$P_1 = P_0 - \rho_1 \cdot g \cdot h_1$$

Where P_0 is static pressure at reference level and ρ_1 is the air density at height h_1.

By combining equations 4.6 and 4.7, one can calculate the pressure difference between two interconnected isothermal zones connected by a component such as a window or a door. At the height of *z*, the following pressure difference, only due to variations in density, can be calculated by equation 4.8.

$$\Delta P_s = P_1 - P_2 + \rho_{ref} \cdot \left(\frac{273.15}{T_1} - \frac{273.15}{T_2} \right) \cdot g \cdot h$$

4.3. Wind-effect

Air pressure outside of building facades affects several aspects relating to the building's performance, processes, equipment operation, pollution protection, and the ability to control the indoor climate. Usually, the wind is the culprit of these variations in air pressure because when the wind strikes a façade, a region of higher air pressure is created on the façade the wind hits (the windward side), and a lower air pressure region at the opposite side of the building, called leeward side. A visualization of this effect can be seen in Figure 10. Wind's effect on a building is based on three different parameters: climatic, environmental, and the building body. Climatic parameters are wind velocity and incident angle; environmental parameters are related to plan area density, relative building height, and building parameters such as frontal aspect ratio and relative vertical position [43]. Furthermore, the wind will create a pressure gradient inside the building that encourages airflow from one side to another due to infiltration by openings and cracks in the building envelope. Therefore, when utilizing window openings for ventilation and cooling, it is preferred to understand how the wind will affect airflow through the building envelope and internally through the building.
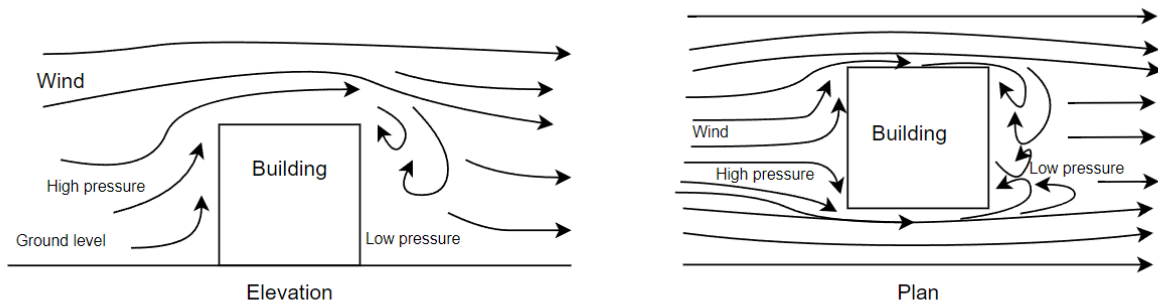
Figure 10: Pressure regions created by wind force hitting a building's facade

Components and the geometry of the building can also be utilized to harvest the energy of wind. Wing walls can improve the air change per hour while also having a shading effect from the sun [44]. Exhaust cowls can convert wind energy into negative pressure and reduce the power needed for exhaust fans [45]. Other methods, such as one of the oldest natural ventilation techniques, wind catchers, can provide an adequate level of ventilation while also achieving a satisfactory level of thermal IAQ [46] .

The pressure profile of a building for a building/zone only affected by wind is illustrated in Figure 11. It demonstrates that airflow will flow in at the windward façade and exit at the leeward façade; this implies that other forces do not counteract the pressure profile induced by the wind.
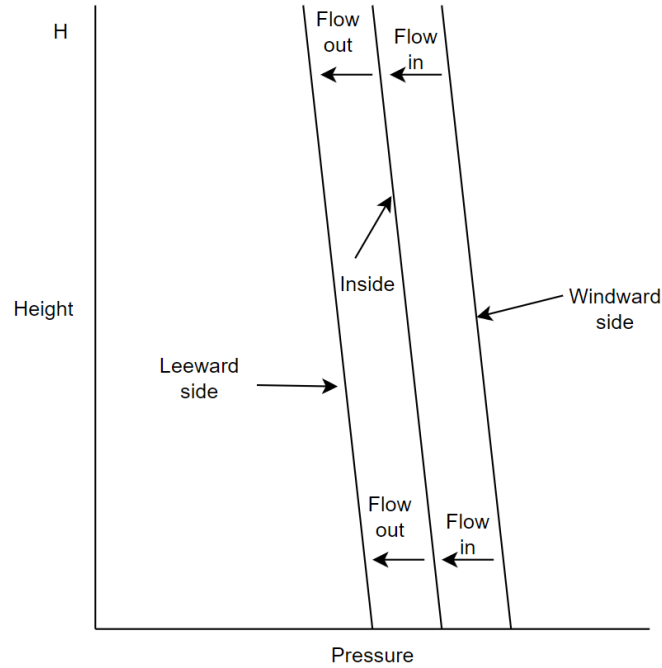
Figure 11: Pressure profile of a building when only accounting for the effects of wind

The following equation 4.9 expresses the air pressure variations caused by the wind.

$$P_{wind} = C_p \frac{1}{2} \rho_e u_{ref}^2$$

<div align="right">

4.9

</div>

Where P_{wind} is the air pressure, C_p the wind pressure coefficient [-], ρ_e is the external air density, and U_{ref} is the wind velocity at a reference freestream point.

From this expression, one can derive the pressure difference between internal and external air pressure by:

$$\Delta P_{wind} = C_p \frac{1}{2} \rho_e u_{ref}^2 - P_i$$

<div align="right">

4.10

</div>

Where P_i is the internal air pressure, and now the pressure difference between the internal and external part of the façade ΔP_{wind}, can be used to calculate the air infiltration induced by the wind.

4.3.1. Pressure coefficients

The wind is highly turbulent and somewhat unpredictable and will cause variations in air pressure around the building that needs to be addressed. This can often be a challenge for engineers and building designers due to the lack of information in the planning stages of a project. Since every building is different (or in a different location), it will always be problems when relying on data from another building. The challenge when estimating the effect of wind on the building body comes down to the *pressure coefficients* C_p. This non-dimensional coefficient determines the wind-induced local air pressure at a given point on the building's façade relative to the freestream wind pressure. Pressure coefficients can be calculated by equation 4.11.

$$C_p = \frac{P - P_\infty}{\frac{1}{2}\rho u_\infty^2}$$

<div align="right">*4.11*</div>

Where P is the pressure at a point of interest on the building's façade, P_∞ is the static pressure in freestream, ρ is the freestream air density, and u_∞ is the freestream wind velocity at the building height [47].

The C_p-coefficients are determined by the shape of the building, the wind direction, and the surrounding terrain. This implies that every building will have somewhat different C_p-coefficients because of each building's specific geometry and variations in geographical location. Therefore pressure coefficients found in current codes and standards will suffer from deficiencies and render them unusable if high accuracy is required [48]. If high accuracy is required, there are a few options for estimating C_p-coefficients, and it can be done by: analytical models, wind-tunnel experiments, or on-site measurements. Although these methods have their challenges to overcome and varying accuracy, full-scale on-site measurements usually provide the most representative description of pressure coefficients [49].

The usage of surface averaged wind pressure coefficients has been demonstrated to be highly uncertain, so the higher the resolution of pressure coefficient nodes on the building facades, the better description of the microclimate of the building [50]. This is especially necessary for high-rise and medium-rise buildings, as the variation in C_p-coefficients becomes more significant the higher the building structure is.

Pressure coefficients accuracy and building energy modeling (BEM)

Building energy modeling (BEM) commonly provides a set of standardized pressure coefficients [49]. However, the accuracy and reliability are not the best, as is demonstrated by Charisi et.al [51] in a recent study. They conclude that using predefined pressure coefficients can lead to significant errors in air infiltration and energy usage, and this error can be reduced by utilizing building-specific pressure coefficients. Furthermore, they concluded that BEM with integrated CFD modules could provide much higher accuracy than BEM that uses predefined coefficients. Nevertheless, the best accuracy was by using their CFD software to add the pressure coefficients into the BEM software.

4.4. Combined effect of wind and buoyancy

Both wind and stack-effect influence air pressure simultaneously, which will create changes in airflow rates and patterns depending on what force is dominant. In some cases, the driving forces may reinforce and increase the total pressure difference and airflow, or they might clash and reduce airflow. In some cases, even stagnate airflow or reverse airflow patterns in contrast to its design. Hence, a simple equation to describe the total air pressure difference ΔP_{tot} is created by combining the wind ΔP_w and buoyancy ΔP_b by adding them together [52].

$$\Delta P_{tot} = \Delta P_b \pm \Delta P_w$$

4.12

Following Figure 12 shows the pressure profile for an arbitrary zone/building affected by wind and buoyancy. Where in Figure 12 (a), both driving forces act similarly on the airflow, and wind induces higher airflow rates while the effect buoyancy is still distinct. In Figure 12 (b), the wind-induced pressure difference dominates over buoyancy, resulting in a change in airflow paths, such as inflow from the bottom to the top level at the windward side.
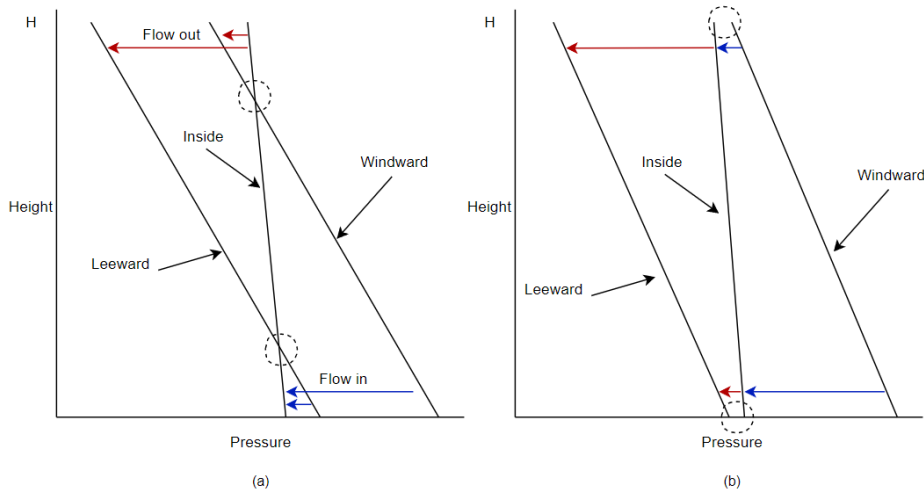
Figure 12: (a) pressure profile when the effect of wind and buoyancy are comparable, (b) pressure profile when wind effect is more substantial than buoyancy. Revised from [53].

Calculating the total pressure difference over an opening that is a result of both wind and buoyancy can be done by utilizing the same principle as in equation 4.12 by adding both pressure differences together. Hence, combining equations 4.8 and 4.9 will produce the following equation 4.13.

$$\Delta P_s = P_1 - P_2 + \rho_{ref} \cdot \left(\frac{273.15}{T_1} - \frac{273.15}{T_2} \right) \cdot g \cdot z + C_p \frac{1}{2} \rho_1 U_1^{\,2} - C_p \frac{1}{2} \rho_2 U_2^{\,2}$$

4.13

Where U_1, ρ_1 and U_2, ρ_2 are the respective wind speed and air pressure at both sides of the interconnected opening between the zones. However, if the opening of interest is exterior, then $U_2 = 0$, and $U_1 = U_{ref}$. The air density is then ρ_i for internal and ρ_e for external, P_0 is the reference pressure to the zone and z is the height of the opening. Thus, the equation 4.13 can be rewritten as equation 4.14 to include these differences.

$$\Delta P_{ext} = P_0 - C_p \frac{1}{2} \rho_i U_{ref}^2 + (\rho_i - \rho_e) \cdot g \cdot z$$

$$4.14$$

In the case of interior openings, both U_1 and $U_2 = 0$, hence the only pressure difference is by buoyancy, and equation 4.8 applies.

The airflow induced by the pressure difference across an opening depends on the size and geometry of this opening [54]. For large openings, such as windows and visible gaps, the airflow can be considered equivalent to flow through an orifice plate. The following equation 4.15 gives the orifice flow.

$$Q = C_d A \sqrt{\frac{2}{\rho} \Delta P}$$

$$4.15$$

Where Q is the air flow rate, C_d the discharge coefficient, A is the opening area and ΔP is the pressure difference across the opening. For smaller openings, such as airflow through gaps and cracks in the building material, the airflow is transitional between laminar and turbulent. The following Power Law, equation 4.16 is frequently used for this application [54].

$$Q = C \Delta P^n$$

$$4.16$$

Where the flow coefficient C is related to the size of the opening, and n is the flow exponent, which characterizes the flow regime. The flow exponent varies from 0.5 to 1.0, where 0.5 is fully turbulent, and 1.0 is fully laminar flow.

5. Cooling with natural ventilation

There are a few passive techniques for cooling, such as evaporative and radiative cooling, but in the case of natural ventilation, it is referred to as convective cooling. It is cooling where heat dissipation is done by exhausting excess heat by air with various natural ventilation methods [55]. Convective cooling by windows, Trombe-wall, or solar chimney are a few common approaches. However, all methods have in common that the airflow utilizes buoyancy or wind, or both, to be the driving forces. The cooling methods that are elaborated further are only the ones that are relevant to this thesis.

Window cooling potential

The cooling potential of windows directly correlates to how much heat the air can absorb by convection and how much air enters through the window and can be exhausted outside. Moreover, how much heat is absorbed is influenced by airflow patterns, air exchange per hour (ACH), the temperature difference between inside and outside, and relative humidity. Natural ventilation systems are greatly dependent on the external climatic parameters, which cannot be altered; hence the window cooling potential of a building is decided by building design and utilization of passive cooling techniques. Furthermore, since climatic parameters significantly influence the potential cooling effect, there is a varying degree of thermal comfort if the same methods are applied in different climates [56].

Cooling with night-time ventilation

A building's heat gain during the daytime may be discarded during the night by circulating cold, nocturnal air throughout the building. This process cools down the air and building structure, resulting in a colder building at the start of the day and reducing the heat gain rate during the day [55]. The efficiency of cooling by night-time ventilation is highly dependent on the building's thermal mass since it is utilized to store the coolness that is absorbed during the night. Hence, the materials and size of the construction is the limitation of what this cooling technique can achieve. Other factors that influence the efficiency are the ventilation air rates and temperature variations from night to daytime. The lower the night-time air temperature, the more efficient the night-time cooling [57]. Buildings such as office buildings may be unoccupied at night and can apply relatively high airflow rates to maximize the cooling effect. Moreover, in moderate climates, this may be enough to only rely on this method for cooling during the summertime [58]. In some cases, night-time ventilation might even have implications with overcooling [59]. However, it should be evaluated if the gain in thermal comfort outweighs the issues relating to ventilative night-time cooling. Issues regarding the external climate, such as heavy wind and rainfall, might happen during the night, and security-related issues need to be addressed if windows are open when no occupants are present.

Building design and airflow pathways for natural ventilation

As elaborated in chapter 3.2, natural ventilation can be divided into four types, all based on the airflow path throughout the building. These types provide varying airflow rates and then also varying cooling effects. The types that provide the most significant pressure difference also create the highest airflow rates. However, natural ventilation building design frequently applies more than one strategy. The resulting pressure profile may be a mix of strategies, such as cross-ventilation and stack-ventilation, as shown in Figure 13.

Furthermore, hybrid ventilation systems may also implement cooling by windows. In this case, one can influence the pressure gradient and airflow path by mechanical fans. Depending on the hybrid ventilation mode (concurrent, change-over, zoned), all the possible design choices make it necessary to simulate the airflows by Building Energy Model (BEM) to evaluate the efficiency and reliability of such cooling systems.
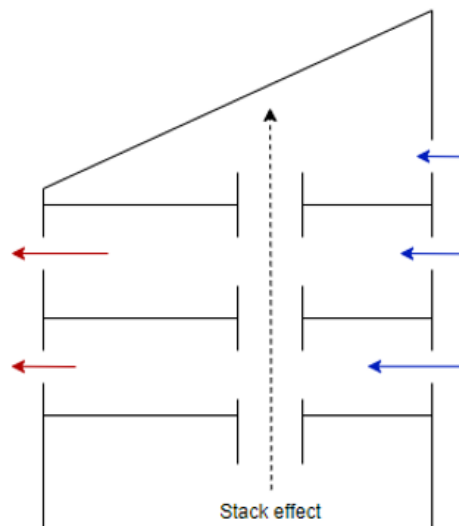
Figure 13: Building utilizing cross-ventilation and stack-ventilation as natural ventilation strategy. Where inflow through the facades is represented by blue arrows and outflow is red arrows

Some more concrete design choices for natural ventilation and the airflow pathways are by improving the efficiency of buoyancy as a driving force by utilizing shafts, which may be by using stairwells or atriums as "ducts" to extract hot and contaminated air [60]. However, for this to work, the zones connected must have some opening between them so that airflow can move freely from the window openings on the facades to the air extraction in the shaft.

5.1. Window opening control schemes

An important factor when utilizing windows for natural ventilation and cooling purposes is to consider how to control them. In practice, various levels of window control are used. They can be as simple as spontaneous control, where occupants control everything, to highly advanced and sophisticated, fully automatic control systems. This presents the following control schemes: spontaneous control, informed occupant control, heuristic control, and model predictive control, as proposed by Chen et al. [61] as the commonly utilized control strategies. Machine-learning techniques and artificial intelligence may also be utilized for BEMS and as a window control scheme but will not be presented in this thesis [62].

Spontaneous control

Spontaneous control is the simplest form of the window control scheme that lets the occupants freely control the window to their desire. This strategy may seem advantageous due to the low investment and maintenance cost, but in practice has shown to achieve sub-optimal energy savings and thermal comfort [61]. Chen et al. studied the cooling energy saved in different climates and compared it to other control strategies [63]. It was found that spontaneous control had 17.2-18.6% less cooling energy saved when compared to model predictive control and 1.6-12.4% less when compared to heuristic control. The reason is that occupants struggle to fully comprehend the dynamic behavior of the internal and external circumstances, leading to undesired window opening patterns. In addition to this, the unpredictability of occupant's window opening patterns may cause implications for other HVAC systems, e.g., hybrid ventilation systems or BEM's accuracy. However, window opening patterns for occupants are a commonly researched topic, and one may utilize stochastic models to address this issue [64], [65], [66].

Informed occupant control

A way to solve the unpredictability of occupants' window opening patterns is to inform the occupants whether the windows should be opened or closed. A control algorithm can evaluate what opening position is best and inform the occupants to open/close the windows, such that the occupants act as actuators. Signaling devices, like indicator lights, can inform what window position is best, and then the occupants shall change it accordingly.

Some of the implications of this approach are that occupants may act as they seem fit and might not act accordingly to the signaling device. These implications were demonstrated by Katie [67], as the paper's findings indicated that occupants were highly unpredictable in their response to the signaling device. Additionally, the willingness to disregard the signal was generally 40-60%. Therefore, it is not unexpected that studies have shown that informed occupant control has little to no improvement over spontaneous control [61].

Heuristic control

Conventional heuristic control models apply rule-based criteria and regulate the window opening accordingly. A fully automated control system utilizes mechanical window actuators to alter the window opening position and has been demonstrated to significantly reduce energy usage while maintaining adequate thermal comfort [61].

Heuristic control models utilize IF-THEN rules, where variables such as indoor and outdoor air temperature, wind, and relative humidity are used to decide if the windows should be open. Furthermore, the control method can be combined with controls for the BEMS and ensure satisfactory interactions between window openings and HVAC systems, such as, e.g., turning off mechanical ventilation if windows are open and vice versa. Additionally, in some scenarios, heuristic control may be advantageous to prediction-based models due to its ease of implementation and reliability.

Model predictive control

Advanced control schemes that apply a prediction-based modeling approach to evaluate the window opening position are called model predictive control. An algorithm is employed to solve an open-loop optimization problem over a finite sequence of control actions at each sampling instance [68]. Model predictive control (MPC) as a window control strategy will then run a series of parallel tests to minimize a predefined cost function by employing control measures. For example, control measures can be, e.g., open window 10/20/30/40%, turn on/off HVAC, close one window, and open another. The cost function may be based on optimization of thermal comfort or minimize energy consumption.

Window control comparison

Chen et al. compared the different window control schemes to a non-NV baseline in five different climates [61]. Heuristic control had an energy reduction of 10-66% and MPC 17-80%, all with zero thermal discomfort degree hours. However, MPC had a substantially higher total amount of window operations. It was annually operated between 3000-7000, while heuristic control was from 500-1700. Such a high frequency of window operations may annoy the occupants. If they both had the same amount of window operation, the real difference between MPC and heuristic control might result in a similar energy reduction.

In the same study by Chen et al., informed occupant control found no significant improvement over spontaneous control, with 10-19% lower energy savings than fully automatic cases. Spontaneous control was reduced by 1-12% and 16-18% when compared to the heuristic control and MPC case, respectively.

The fully automatic control schemes provided substantial energy savings over the non-NV baseline. They should both be considered to utilize the full potential of natural ventilation cooling, even though they have substantial investment and maintenance costs over spontaneous control.

6. Methodology

The methods that are utilized for this thesis are presented in this chapter. It consists of three parts: The on-site measurements, a BEM of ZEB lab developed in IDA ICE, and four proposed window control algorithms for assessing ventilative cooling performance.

6.1. On-site differential pressure measurements and wind pressure coefficients calculations

As elaborated in chapter 4.3.1, precise pressure coefficients are essential for a BEM to deliver accurate and reliable air infiltration results. Databases with wind pressure coefficients such as from AIVC are frequently used in BEM, but it does not describe the wind-induced loads with high accuracy on an arbitrary building. Sheltering effect of neighboring buildings, the geometry of the building, and local vegetation is just some of the parameters that are difficult to incorporate correctly in wind tunnel tests or CFD models of the building. Therefore, in this thesis, it is concluded that to get accurate air infiltration simulations, on-site measurements will be conducted to calculate accurate wind pressure coefficients well suited for the ZEB lab building.

General idea

The plan for the on-site measurements is to measure all necessary data to calculate wind pressure coefficients with equation 4.11. Data for four parameters are required: total pressure at various points on the facades, freestream static pressure, freestream air velocity, and freestream air temperature. The measurement data is collected from the facades with 15 differential pressure sensors (DP-sensors) and a freestream static pressure measurement is measured above the building body. A weather station on the roof of the ZEB lab measures the other external climatic parameters. Compensations for zone conditions, in regards to zone height, temperature, and pressure loss in the tubes, are made to find the pressure difference between the façade and freestream reference DP measurements.

6.1.1. On-site measurements setup

This subchapter will present the methodology for the on-site measurements. That includes everything from equipment, challenges, setup, and necessary simplifications.

Total pressure measurements for the basis of wind pressure calculations

The pressure difference over the facades is measured by DP-sensors, where one tip of the sensor measure inside air pressure, and the other measure outside air pressure. Figure 14 shows the measurement setup of one of the 14 sensors that measure DP across the facades. One sensor-tip measure the internal air pressure directly, and the other sensor tip is connected to a tube that goes through the window gasket and measures the pressure outside.
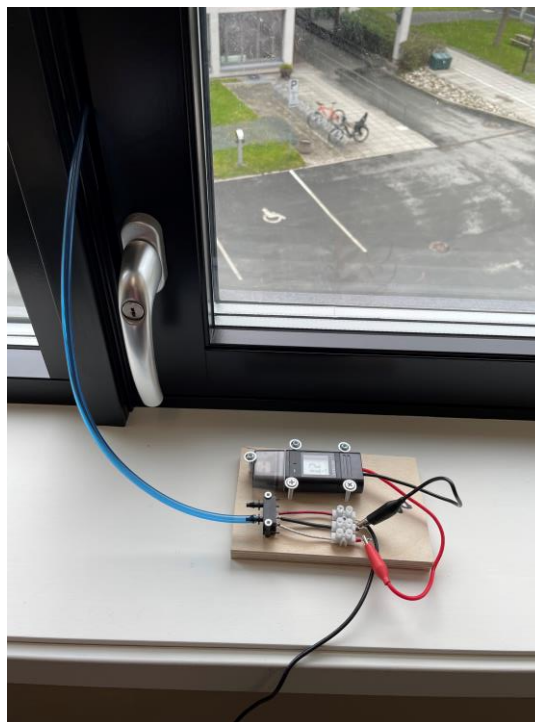
Figure 14:One of the 14 facade DP-sensor measurement setup, all DP-sensors have an identical setup.

A pneumatic tube connects the sensor to the external air pressure. The tube is relatively stiff, with an inner diameter of 4mm and a length of ~0.5m. This results in the tube only getting slightly deformed when closing the window, and sufficient airflow through the sensor is maintained. As shown in Figure 15, the tube only goes barely through the window gasket (from the inside to the outside).
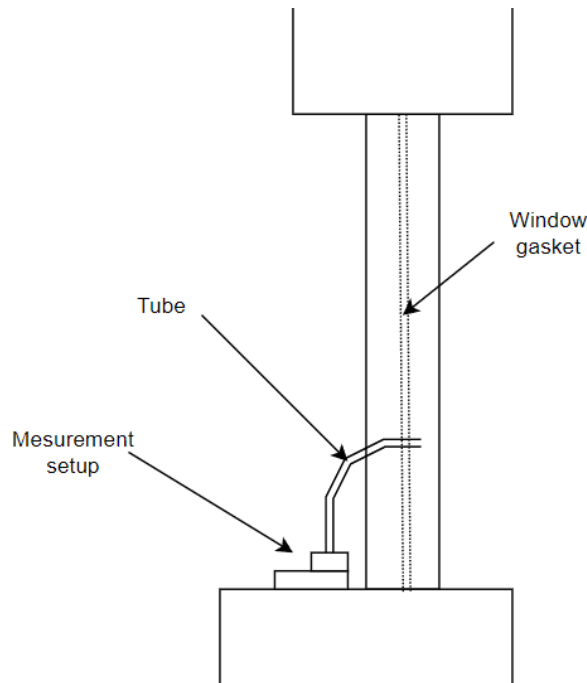
Figure 15: Illustration of the measurement setup and how far the tube goes through the window gasket

The tube tip ends at this location to reduce local turbulence around the tube tip and diminish pressure variations in the tube due to airflow perpendicular to the facades. Only pressure variations due to the stagnation pressure of the wind are desired. Hence, the simplification is made that by installing the tube this way, the sensor will only measure the stagnation pressure of the wind. However, this is a simplification, and one cannot guarantee that no local turbulence or perpendicular airflows might impact the measurements.

Placement of the DP-sensors

As mentioned, 14 DP-sensors measure pressure difference across the facades. Where two DP-sensors at both east and west facades and five on the south and north facades. These sensor placements and an assigned number for each sensor are found in Figure 16, Figure 17, and Figure 18 (figures are clipped from the BEM in IDA ICE).
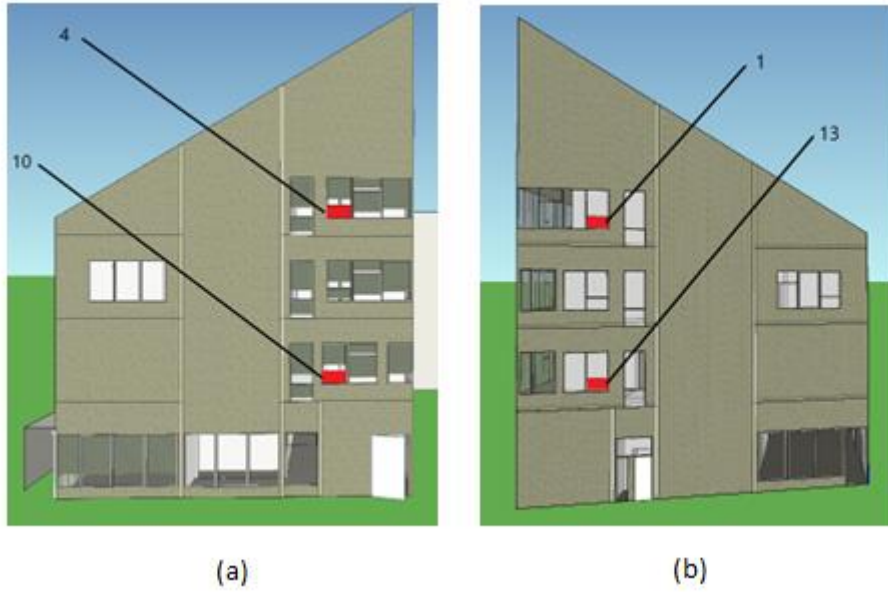
Figure 16: Points of differential pressure measurement at the ZEB lab., (a) east façade and (b) west façade

Figure 17: Points of differential pressure measurements on the north façade at the ZEB lab

Figure 18: Points of differential pressure measurements on the south facade at the ZEB lab

Freestream static pressure

The reference freestream pressure is measured by a tube of 4mm inner diameter connected to the weather station at the ZEB lab. This weather station is located on the northeast roof corner and in the middle of a 2.5m high pole, as illustrated in Figure 19.
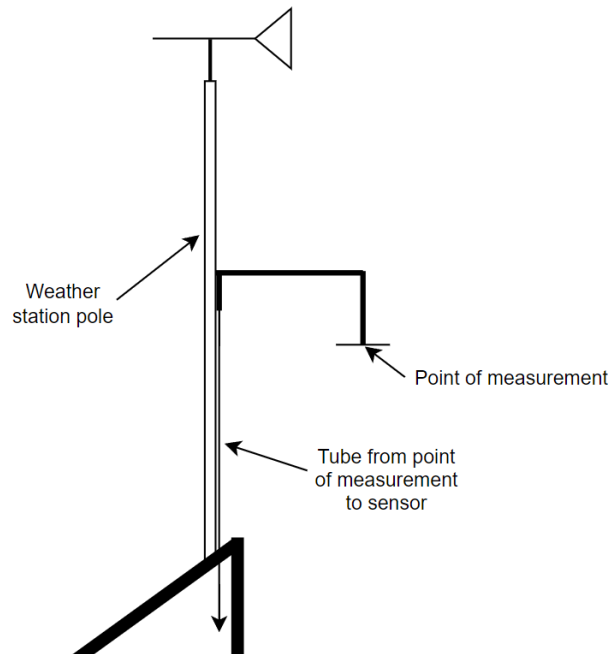
Figure 19: demonstrates the weather station pole and reference pressure measurement at the ZEB lab roof (northwest corner)

At this height, the assumption can be made that the wind only has a horizontal velocity vector. Thus, by mounting the tube tip end (at the weather station side) flush to the surface of a horizontal plate, the horizontal wind will not impact the pressure in the tube. Moreover, with no stagnation pressure from the wind, the simplification is made that the tube only measures static pressure. Additionally, it is also assumed that at this height, the measured pressure is in freestream and is undisturbed by the building body and the surroundings.

The tube goes from this point of measurement, enters zone 40 under the roof at approximately 10m above floor height, is lowered to floor level, and is connected to the sensor. The reference freestream sensor and logger are the same as those utilized for the facades, as seen in Figure 14. The total length of the tube from the sensor to the point of measurement is ~20m.

Air velocity and temperature

Data for wind speed, direction, and air temperature are collected at the weather station on top of the ZEB lab. The assumption is that at this height, it is in freestream and undisturbed by the building body and the surroundings.

6.1.2. Setup and equipment

The full-scale measurements lasted approximately ten days and were logged at one measurement/minute frequency. The setup consists of four components: sensor, data logger, power supply, and tube. An overview of the sensor and logger used can be found in Table 5.

Table 5: Equipment used for the full-scale measurements

Equipment	General info
SENSIRON SDP816-125PA	- Sensor measures by mass flow compensated differential pressure. - Analogue output and tube connection. - Temperature-compensated. - Measurement range of -125Pa to 125Pa - Zero-point accuracy: 0.08Pa - Span accuracy: 3% of reading Manufacturers datasheet: [69]
VOLTCRAFT DL250V	- Voltage data logger, unit of measurement: voltage 0.01-30V - Resolution 0.01 - Accuracy ±0.5% - Sampling rate 1min-24hours - At most, 31320 measuring values can be saved - USB port for data transfer Manufacturers documentation: [70]

The analog output signal of the sensor is based on the supply voltage it receives. Hence, a power supply with stable voltage is required. It was concluded that an AC/DC power adapter rated for 5V would produce acceptable accuracy. The selected model has a voltage set point accuracy of ±2% at 60% load [71]. However, considerably less load is utilized when measuring, so lower voltage accuracy is expected. The supply voltage was measured before and during the measurements, and it was observed that the supply voltage was steady with minimal variations. Observed variations in supply voltage were a maximum of 0.03V, and the average supply voltage was ~5.13V. All sensors are compensated for variations in the power supply voltage, which will be elaborated on further in the next chapter.

6.1.3. Compensations for the on-site measurements

Three transformations/compensations of the on-site measured data must be performed to get the actual differential pressure. This implies transforming the raw output voltage data to the differential pressure and compensating for the tube and height difference.

Voltage to differential pressure compensation

The output curve of the sensor is in the configuration "square root" which gives a fully bi-directional output. It was utilized because of more stable zero point and higher sensitivity at lower pressure, than the other configuration "linear". The compensation equation (equation 6.1) provided by manufacturer for the 125Pa model is as follows [69].

$$DP = sign\left(\frac{AOut}{VDD} - 0.5\right) \cdot \left(\frac{AOut}{VDD \cdot 0.4} - 1.25\right)^2 \cdot 133$$

<div align="right">6.1</div>

Where DP is differential pressure [Pa], $AOut$ is the ratiometric analog voltage output [V], and VDD is the voltage supply [V].

Compensation for pressure drop in the tube

As elaborated under the general info about the SDP816-125PA sensor, it utilizes a measurement technique of mass flow compensated differential pressure. This entails that some mass flow through the sensor is required to operate as expected, and the tube's diameter matters for the measurement results. However, the manufacturer of the sensors has anticipated this issue and developed compensation curves and guidelines to address this pressure drop [72] to calculate the effective differential pressure dp_{eff}.

$$dp_{eff} = \frac{dp_{sensor}}{1 + \epsilon}$$

<div align="right">6.2</div>

Where:

$$\varepsilon = -\frac{64}{\pi}\frac{L}{D^4}\frac{\eta_{air}}{\rho_{air}}\frac{m_C}{\Delta p_{sensor}}\left(\sqrt{1 + \frac{8\Delta p_{sensor}}{\Delta p_c}} - 1\right)$$

$$\eta_{air} = (18.205 + 0.0484 \cdot (T[°C] - 20)) \cdot 10^{-6}\frac{Pa}{s}$$

$$\rho_{air} = (1.1885 \cdot P_{abs}[bar] \cdot \frac{293.15}{273.15 + T[°C]}\frac{kg}{m^3}$$

$$m_c = 6.17 \cdot 10^{-7}\frac{kg}{s}$$

$$\Delta p_c = 62Pa$$

With
L = being the total length of the tube [m]
D = is the inner diameter of the tube [m]
η_{air} = the viscosity of air at a temperature T in Celsius [$°C$]
ρ_{air} density of air at a temperature T [$°C$]
Δp_{sensor} DP reading of the sensor in Pascal [Pa]
P_{abs} the absolute air pressure in the tube in bar

m_c and Δp_c is constants provided by the manufacturer.

Compensation for the height difference

For practical reasons, the DP-sensors measure the inside and outside of the facades and are not directly connected to the reference freestream pressure sensor. Hence, the DP-sensors have to be compensated for height and temperature differences.

The ZEB lab is an open building with mostly all zones having an airpath directly connected to the stairwells. Moreover, assuming all air paths will result in air pressure equilibrium between the zones/stairwells, the whole building can be considered a single zone. However, this is a simplification since the zones provide some inertia for the airflow, and the mechanical ventilation system may alter the pressure gradient in most zones. Nevertheless, this assumption was deemed sufficient for the on-site measurements' viability.

By this logic, the building can be considered a single isothermal zone, as shown in Figure 20, and the height difference between the reference freestream and façade sensors can be compensated.
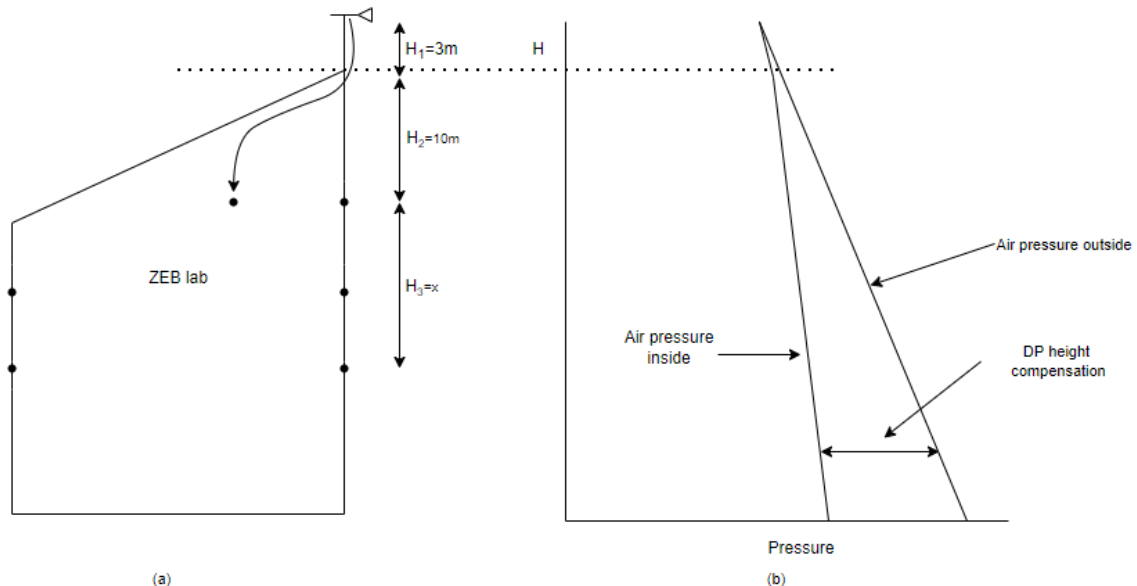
Figure 20: (a) Illustration of ZEB lab and height compensation for the DP-sensor, and (b) is the pressure profile of the building and external air that is used as a basis for further evaluation of height compensation.

Where H1 is the length of the tube from the point of measurement to the inside layer of the roof and H2 is the height difference between the reference freestream sensor and the inside layer of the roof. Lastly, H3 is the height difference between the façade and the reference sensors.

To perform compensation for temperature and height, one should consider the external and internal parts of the building separately. The outer part, i.e., the reference freestream point of measurement, is compensated for the outdoor temperature and the height of the sensor that is being evaluated. The internal part of the building, i.e., all façade sensors, must be compensated from the reference freestream sensor to the respective height of the façade sensors.

Firstly, the reference freestream sensor is evaluated and compensated separately for practical reasons. The freestream reference compensated differential pressure ($DP_{ref,comp}$) is adjusted after the density differences because of temperature variations between inside and outside, which is elaborated in equation 6.3.

$$DP_{ref,comp} = \rho_{ref} \cdot g \cdot \left(\frac{273.15}{T_{outside}} \cdot (H_1 + H_2) - \left(\frac{273.15}{T_{outside,tube}} \cdot H_1 + \frac{273.15}{T_{inside}} \cdot H_2 \right) \right) - dp_{eff}$$

$$6.3$$

By following the same principle as in equation 6.3, the compensated façade differential pressure ($DP_{facade,comp}$) by the following equation 6.4.

$$DP_{facade,comp} = \rho_{ref} \cdot g \cdot \left(\left(\frac{273.15}{T_{outside}} \cdot (H_1 + H_2 + H_3) \right) - \left(\frac{273.15}{T_{inside}} \cdot (H_2 + H_3) + \frac{273.15}{T_{outside,tube}} \cdot H_1 \right) \right) - dp_{eff}$$

$$6.4$$

Following these steps, the $DP_{ref,comp}$ and $DP_{facade,comp}$ is compensated for tube, height, and temperature variations and can be used for wind pressure coefficient calculations with equation 4.11.

6.2. Building Energy Model – IDA ICE

The ZEB lab building is modeled in IDA ICE to test wind pressure coefficients and the ventilative cooling performance of window control algorithms.

6.2.1. IDA ICE as a BEM tool

IDA-ICE is a dynamic modeling tool that analyzes building performance, such as energy consumption, indoor climate, and thermal comfort. The software offers flexibility through its multi-zonal design, where one can define specific parameters for a zone and how the zone interacts with the other zones. Global building parameters, technical systems, and control strategies are highly adjustable, making the software well suited to examine building and system designs that would otherwise require solving complex mathematical problems. Compared to measured data, the software has been demonstrated to be accurate by several studies [69], [70], and the developers show transparency by open-source all utilized equations. The user-friendly 3D interface, flexibility, demonstrated accuracy, and highly adjustable settings for both the zones and the systems, made IDA ICE the optimal choice of BEM for this thesis.

6.2.2. ZEB-lab implementation in IDA ICE

The ZEB-lab has been modeled into IDA ICE to evaluate the performance of the window control algorithms. This chapter will present ZEB-lab, including building body/structure, openings, usage, and ventilation, and document how it is implemented into IDA ICE. Floor and façade plans, including window and zone dimensions, are directly implemented into IDA ICE to create all the building zones. The model is created after earlier energy simulations and reports and *as-built* documentation of the building and its technical systems [73], [74], [75], [76]. Some currently utilized zone settings and systems are gathered from the operations employees at ZEB-lab.

6.2.3. ZEB-lab building body/structure

The ZEB laboratory is a four-story-high living lab at approximately $1800m^2$ and 23m in maximum height. The architects drew inspiration from silicon crystals for the building structure [77], which resulted in the building's northwest and northeast corners having an upward slope from the ground level. Furthermore, the south-facing roof has a 32-degree tilt, which is also because of its optimal angle for electricity production of the PV panels. The external walls are made from traditional half-timbering, supporting structures are made of laminated timber, and floor dividers, bracing walls, and elevator shafts are built from solid wood [77]. The external surfaces are primarily covered in dark wood panels or PV panels. PV panels cover the whole roof, most of the south facade, and partly the west and east facades. At the ground level on the south façade, an external structure consisting of partly wood and partly PV panels also act as a shade for ground-level windows. The building has a collective window area of roughly 28% of gross area, which results in 488 m^2 of windows. Figure 21 contains photos of the facades at ZEB-lab.

Figure 21: As-built photos of ZEB-lab facades. Photos taken in February 2022

For the implementation of the ZEB lab into IDA ICE, some simplifications and modifications had to be made. IDA ICE does not currently support an option to change the vertical surface angle, such that the northeast and northwest corners in the model do not have the same geometry as the building. Furthermore, this also makes it necessary to modify the windows placed in these corners. Additionally, due to limitations, the external ground level structure in front of the south facade does not have the same geometry as the real one. A CAD model of the external structure could have been implemented, but this was not deemed crucial for the model's accuracy. Following is a clipping of the IDA ICE model facing the southwest presented in Figure 22.
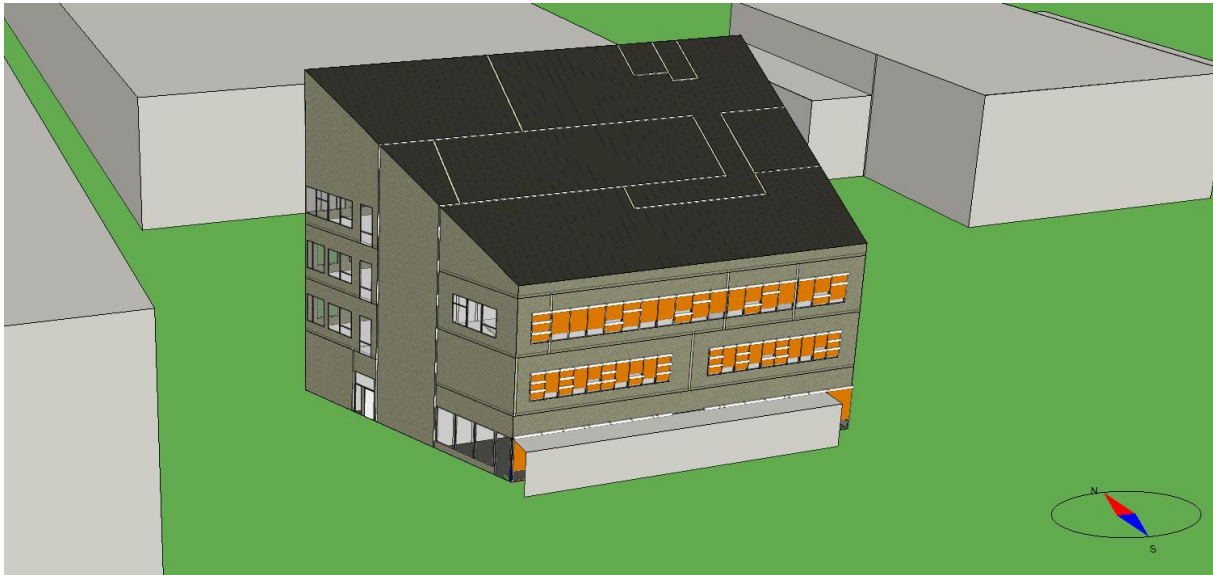
Figure 22: ZEB lab model in IDA ICE, facing the southwest

For the thermal transmittance values (*U-values*), an average value of the different building constructions is presented. Table 6 presents the U-values used for the building construction components and other vital prerequisites.

Table 6: Thermal transmittance for the building structure and other essential prerequisites used in the BEM

Construction component	Value and unit
Roof (average)	≤ 0.90 W/m^{2}K
External walls (average)	≤ 0.15 W/m^{2}K
Window	≤ 0.80 W/m^{2}K
Floor towards ground	≤ 0.10 W/m^{2}K
Normalized thermal bridges	≤ 0.03 W/m^{2}K
Infiltration, leakage rate, n50	≤ 0.30 h^{-1}

The external walls, floor dividers, and roof consist mainly of wood, with thermal conductivity of 0.14W/mK, a density of 650kg/m^3 and specific heat of 1200J/kgK, which results in significantly lower thermal mass than if the ZEB lab were a concrete based structure.

6.2.4. Floor plan

The BEM is divided into 44 zones over four floors, each consisting of approximately 440m^2 of surface area. Furthermore, to reduce the amount of total zones and computational time for the BEM, combining some rooms as one zone was deemed acceptable if it would not create any changes to the airflow pathways or cooling effect of the windows.

The first floor comprises a big cafeteria of 144m^2, an energy plant, wardrobes, toilets, and hallways/entrances. Most zones have a height of 4.45m, except for the elevator, technical shaft, and stairwells, which have a height of 22.8m, 12.2m, and 19.1m, respectively (both stairwells are the same height). Additionally, the white open space on the floor plan is a bike washing station. Following is Figure 23, is the 1st floor plan, clipped from IDA ICE.
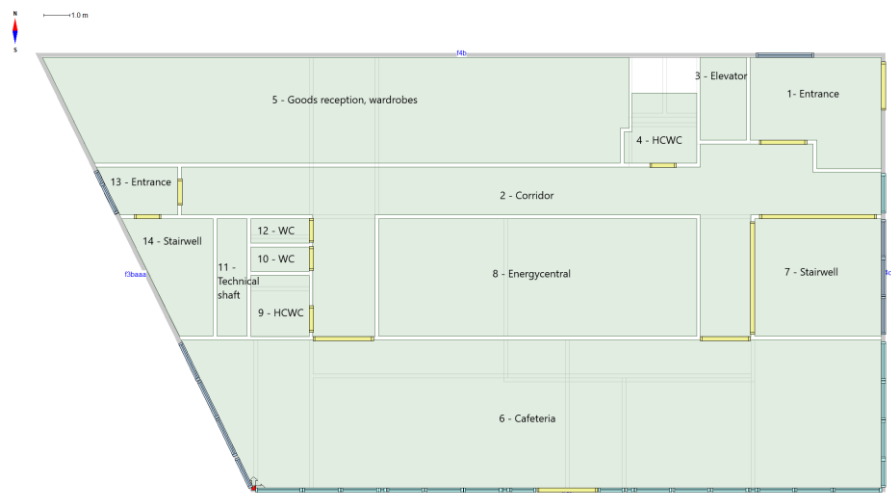
Figure 23: Floor plan of the 1st floor at ZEB lab, clipped for BEM in IDA ICE

The second floor contains office landscapes, team/meeting rooms, toilets, and two twin office landscapes utilized for research purposes (zone 16 and 17). All zones have a height of 3.85m, except those that go from the first to the top floor. Figure 24 is floor plan for the 2nd level at ZEB lab in IDA ICE.
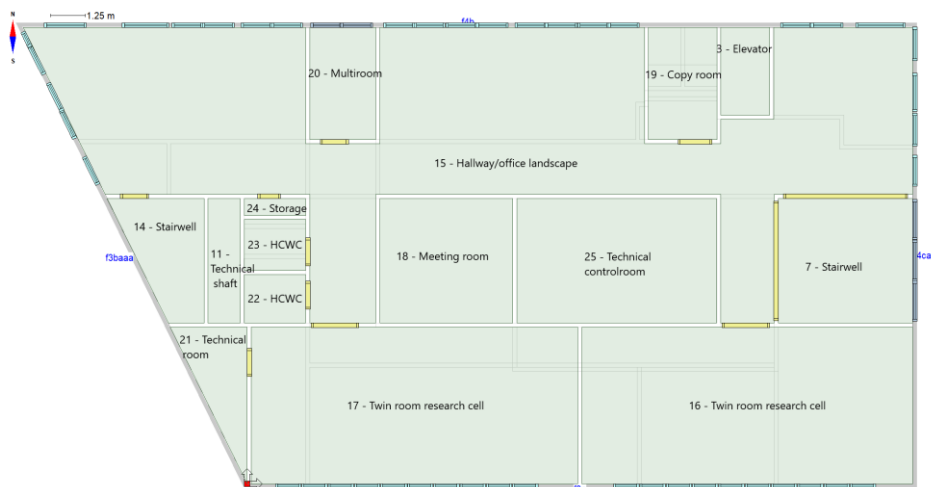
Figure 24: Floor plan of the 2nd floor at ZEB lab, clipped for BEM in IDA ICE

43

The third floor consists primarily of office landscapes, meeting rooms, and toilets. All zones have a height of 3.85m, except those that go from the first to the top floor. Figure 25 shows the IDA ICE model of the 3rd floor of the ZEB lab.
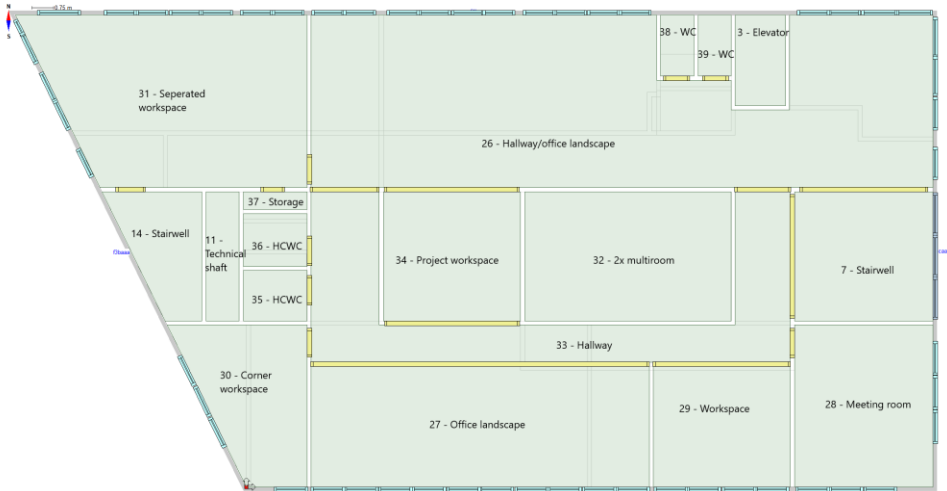
Figure 25: Floor plan of the 3ʳᵈ floor at ZEB lab, clipped for BEM in IDA ICE

The fourth floor consists of a classroom, knowledge center, storage, and a showcase room of the ventilation unit. All zones on the fourth floor have varying height levels due to the slanted roof of the building. Hence, the zones range from 2.6m to 10.6m in height. Figure 26 shows the floor plan of the 4th floor, implemented into IDA ICE.
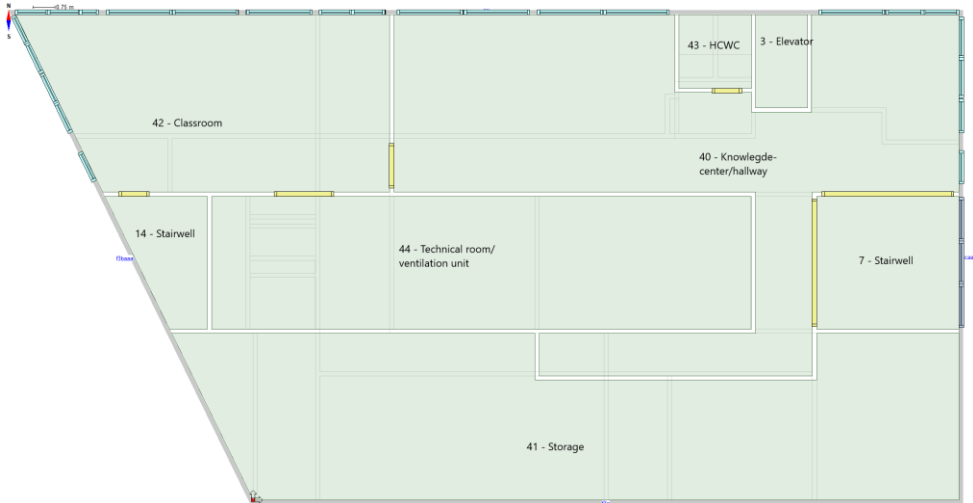
Figure 26: Floor plan of the 4th floor at ZEB lab, clipped for BEM in IDA ICE

Later in this thesis, all zones will be referred to as zone numbers and the names given, as shown in Figure 23, Figure 24, Figure 25, and Figure 26.

6.2.5. External and internal openings

The external openings of the ZEB laboratory consist of windows and doors. The doors are only manually opened, while windows can be manually or electrically opened. A total of 37 windows can be opened with window actuators, which can be seen in Appendix A. Furthermore, the windows are simulated to have a maximum opening of 60% of the geometric area of the windows. The manually operated windows will always remain closed, as the window opening patterns for occupants combined with automatic window control were not a part of this thesis.

The windows are constructed as three-pane windows, where each pane is 4mm thick and has a 17mm gap of argon gas. Which results in U-value of $0.80W/m^2K$, solar heat gain coefficient of 0.56, frame factor of 0.1 with $2.0W/m^2K$ U-value.

All windows on the south façade have an external ZIP screen as shading, and the east façade windows have internal blinds as shading. The external ZIP screens produce a reduction factor of 0.12, and the external produce a reduction factor of 0.4. Both internal and external blinds are solar radiation regulated, where the blinds close when solar radiation exceeds 100 W/m^2.

Other openings

Two of the three doors at the 1st floor are simulated as always closed. Only the main entrance has an opening schedule of 10% during 7:30-8:30 and 15:30-16:30, as it sees the most frequent usage. For the internal openings, i.e., internal doors, observations have been made during the many visits to the ZEB lab during this thesis work. It is noted which doors usually remain open and closed and are further implemented into the IDA ICE model.

6.2.6. Internal gains and schedules

The internal gains from occupancy, equipment, and lighting are based on standards, previous assessments by master students and internal documents regarding energy usage, and logical assumptions. Appendix B provides an overview of all schedules used for all zones.

Occupants

The assessment of how many occupants are staying in each zone is based on the number of chairs and the use-case of the room/zone. For office spaces, it is assumed that each chair represents one occupant. It is assumed that 80% of the seats are filled for meeting rooms, and for the rest, e.g., hallways, toilets, and stairwells, the total number of occupants is generally 1-3 people, based on logical assumptions of each zone. Figure 27, Figure 28, Figure 29, and Figure 30 shows the schedules used for the different types of zones. For the weekends and holidays, the load is set to zero. Additionally, some zones are also assumed to have zero occupancy.
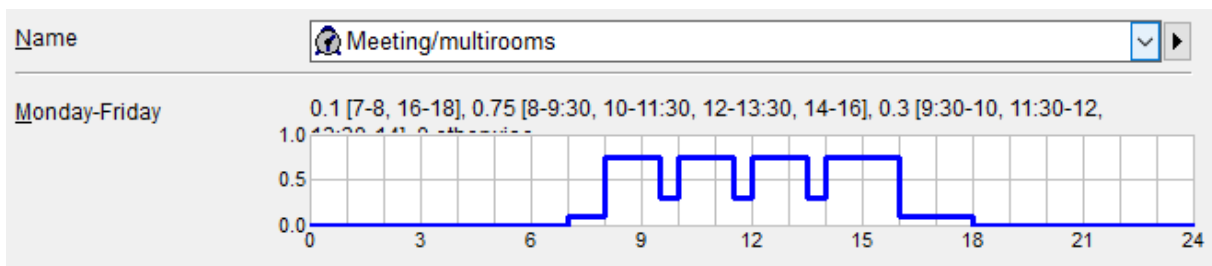
Figure 27:Meeting/multiroom type zones occupancy load schedule
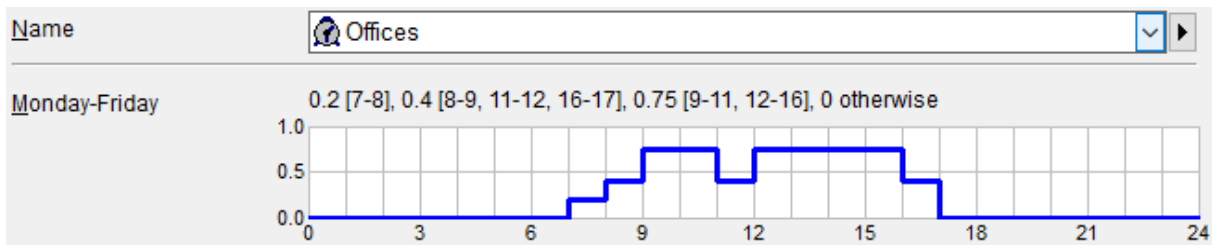
Figure 28: Office zones occupancy load schedule
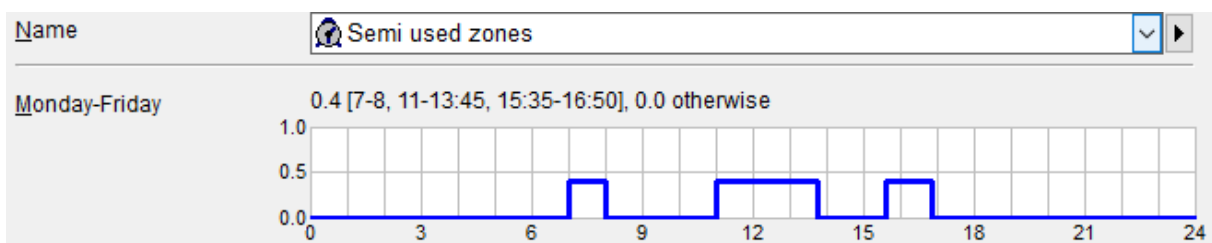
Figure 29:Semi-used zones (hallway, storage, toilets etc.), occupancy load schedule
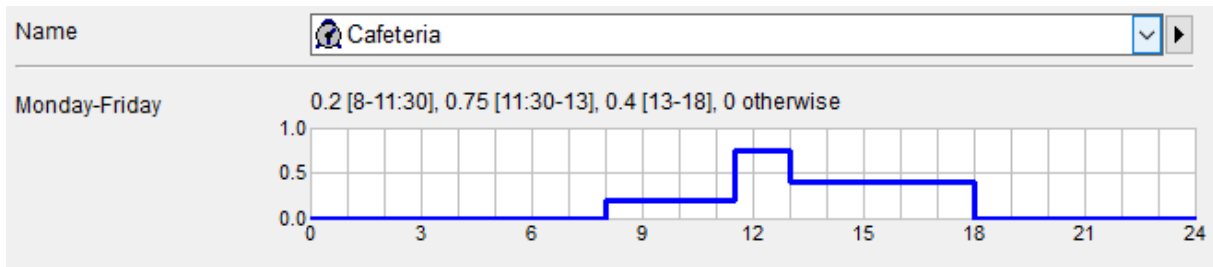
Figure 30: Cafeteria occupancy load schedule

Equipment

Internal loads from equipment vary from 3.2-17.5W/m^2 depending on room type. These values are collected from previous energy evaluations [76], as is stated at the start of the chapter. They also follow the identical schedules as Figure 27, Figure 28, and Figure 29, with some exceptions like the energy-central and zones with infrequent usage.

Lighting

3W/m^2 is used as a foundation for internal heat load from lighting. It is also based on documentation from previous work regarding the energy consumption of the ZEB lab [76]. Figure 31 and Figure 32 shows schedules used for different rooms and split into frequently used or infrequently used zones. The used rooms have a total energy consumption of ~10kwh/m2 annually, corresponding to previous LENI evaluations [76]. Moreover, the infrequently used rooms have about 5.5kwh/m^2 annually. Both schedules have 10% of maximum energy for lighting for the rest of the day and on weekends.
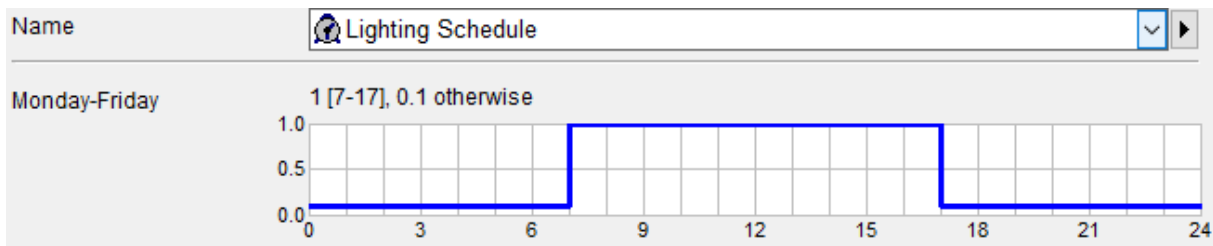
Figure 31:Lighting schedule for frequently used zones, e.g., offices and meeting zones.
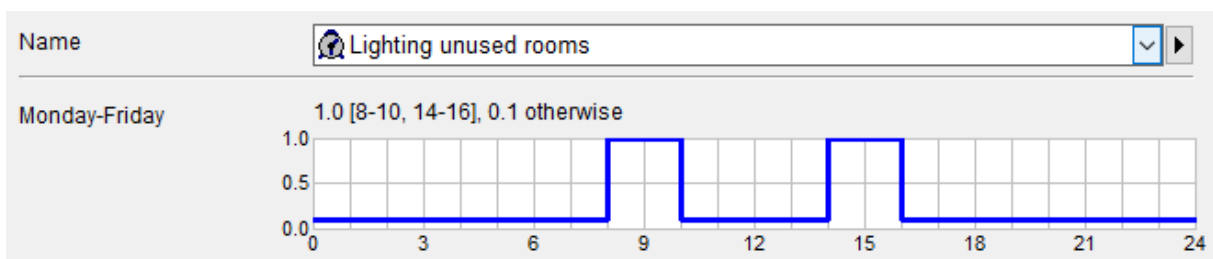
Figure 32: Lighting schedule for infrequent used zones, e.g., hallways and storage zones.

47

6.2.7. Ventilation at ZEB lab

THE ZEB labs ventilation system utilizes mechanical and natural ventilation. In this thesis and IDA ICE model, the mechanical ventilation system is modeled as-built and does not directly regulate or adjust after the window control algorithm. Some of the VAV-dampers do, however, respond to changes in CO2 levels and air temperature; therefore, natural ventilation will indirectly impact mechanical ventilation. The resulting hybrid ventilation system in the IDA ICE model will thus be *concurrent mixed-mode*.

General info on the mechanical ventilation system

ZEB lab has two ventilation units on the fourth floor, totaling $16000m^3/h$. It also has two air supply ventilation units for the research cells on the second floor, totaling $2400m^3/h$, which will not be considered during this thesis, as they are used for research purposes and not for regular building usage. The mechanical ventilation system is balanced, with displacement ventilation as its distribution strategy.

Zone setpoints are 21°C for heating, 22°C for cooling and min CO2 of 700ppm and max of 900ppm and are the regulatory setpoint of the zones with VAV-dampers.

In the IDA ICE model, the AHU is modeled as one ventilation unit. The fans have a Specific Fan Power of $1kW/(m^3/s)$ and operate at 100% capacity during office hours and 10% during non-office hours. The heat exchanger is at 85% efficiency, and the supply temperature is at a constant 19°C. However, the supply temperature may be higher if the outdoor temperature exceeds 19°C. Furthermore, the ZEB lab has no installed cooling coil, so the cooling coil is set to 0 to represent no installed mechanical cooling in the IDA ICE model. An overview of the AHU in the IDA ICE model can be seen in Figure 33.
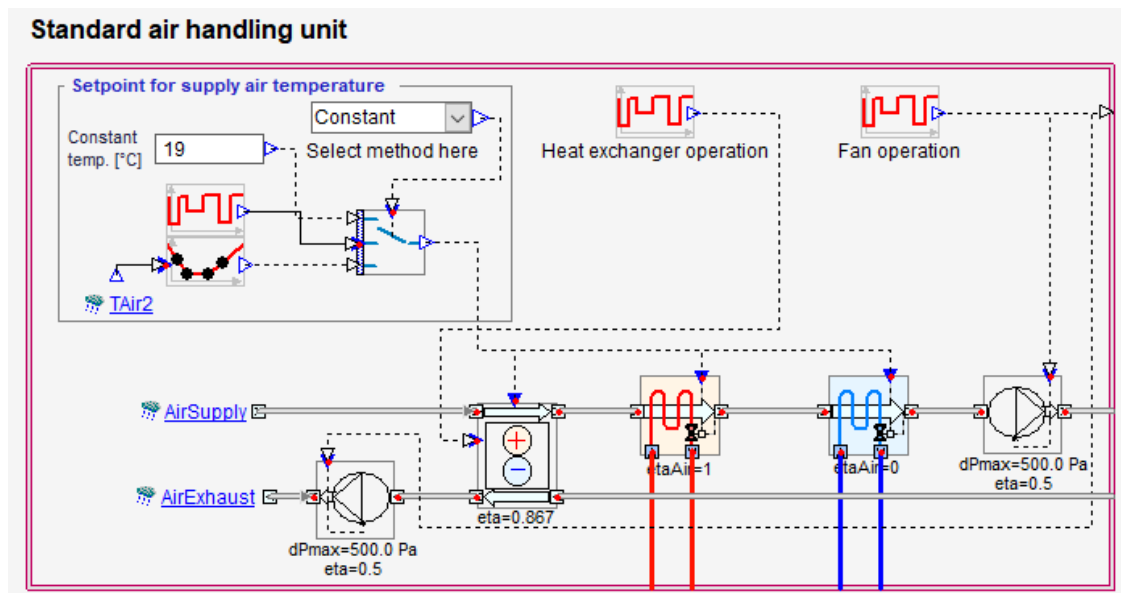
Figure 33:Overview of the ZEB labs AHU modeled in IDA ICE.

Supply and extraction of air

ZEB lab applies the principle of stack-ventilation, as it uses both stairwell shafts to extract old and contaminated air from the 1st, 2nd, and 3rd floors. Two exhaust grills at the top of the stairwell shafts on the fourth floor extract most of the supplied air at a rate of ~4600m^3/h at the east stairwell and ~5900m^3/h at the west stairwell. Some exceptions as, e.g., toilets, storage, and hallways, which have extraction by ductwork directly connected to the zones. A complete overview of the supply/extraction method and airflow rates can be found in Appendix B.

The overall air supply system is by branches coming from the central ductwork that the two technical shafts use. Each branch has a VAV-damper that regulates airflow from the central ductwork and the zones. As such, these airflow ratings determine the mechanical airflow supplied to the corresponding zones. The supply air ductwork is either directly connected to a diffuser or by supplying overpressure to the lowered ceiling. In addition, the total airflow for each zone is a product of the *as-built* ventilation ductwork.

Several zones do not have a direct opening between them and are therefore connected by overflow ductwork to create airflow. The overflow air comes from a neighboring zone that requires a higher quality of air to a zone with a lower air quality requirement. Toilets are usually supplied with overflow airflow. In addition, overflow is used so that zones like research cells can exhaust the air to the stairwells so that it can be extracted on the fourth floor. It should also be noted that overflow in IDA ICE is implemented as leakage between zones, and it is not implemented with dampers, such as some overflow ductworks at the ZEB lab. The overflow duct diameter in the as-built documentation corresponds to the leakage opening leakage area in the IDA ICE model.

6.2.8. Global data and additional settings

IDA ICE has a vast set of climate data files based on the ASHRAE IWEC 2 database, which contains weather files for 3012 locations. Moreover, this dataset's closest location to the ZEB lab is from Trondheim Værnes, and for this thesis, it is deemed acceptable to use for the BEM.

The closest buildings that provide the most shading are modeled into the IDA ICE model, which can be seen in Figure 22 . However, this does not cover all shading, such as the horizon and vegetation. Previous BEM and energy consumption evaluations concluded a sun-shading factor of 0.74/0.95/0.97/0.95 from the façade direction (N/E/S/W), respectively [73]. It is noted that the north façade is especially affected by shading, which is mainly from the neighboring buildings, which are included in the IDA ICE model. The other facades, especially south and east, are significantly more exposed to direct sunlight and only have 0.95 and 0.97 shading coefficients, respectively. Therefore, the external shading on the ZEB lab is considered acceptable in this IDA ICE model.

The wind pressure coefficients utilized for the BEM model are from the Air Infiltration and Ventilation Centre (AIVC) database. These wind pressure coefficients are provided by IDA ICE and come in three optional sets of Cp: exposed, semi-exposed, and open. In the base model (that is used to compare the new on-site measured Cp), the Cp set of semi-exposed. Further elaboration on this comparison is in chapter 7.2.1.

6.3. Window control algorithms

As elaborated in chapter 5.1, occupant control window control gives suboptimal cooling results. To fully utilize window cooling to its potential, the best results are from fully automatic control in the form of heuristic or MPC. It is decided that heuristic control will be tested in this thesis due to its relative ease of implementation in IDA ICE compared to MPC.

The proposed window control algorithms

Four different window control algorithms are evaluated. They are all simplistic, and the only objective is to provide cooling and accomplish adequate thermal comfort. The control model is mainly based on IF/THEN statements and does not involve complex calculations. In addition, the control model does not consider CO2, RH, and noise when controlling the window openings. The thesis aims to study the ventilative cooling potential, which could effortlessly be implemented into the control models by a few IF/THEN statements. However, this should not create any issues in the credibility of the control algorithms because the mechanical ventilation system will operate as usual and should provide adequate IAQ.

All four models of window control have several of the same criteria for control, which are summarized in the following Table 7. Furthermore, a fully open window is 60% of the geometric area of the window. The values for indoor/outdoor temperature, wind speed, and daytime schedule were demonstrated to provide a satisfactory indoor climate by previous master student Martin Sande [78], which is the basis for opting to utilize these values.

Table 7: Control criteria and values for the window control algorithms

Control criteria	Control criteria = 1
Outdoor temperature	IF outdoor air temperature > 12 °C
Indoor temperature	IF zone air temperature > 22 °C
Wind speed	IF wind speed < 10 m/s
Daytime schedule	IF time in range 07-18

In addition to these criteria, every model has a time constant of 0.5h, a sampling rate of 0.5h, and a required change of a minimum of 0.1. This entails that the model only changes the window opening position once every 30 minutes if the change is greater than 10%. A complete step-by-step explanation of how all four window control algorithms work can be found in Appendix C.

Control algorithm 1 – Typical ON/OFF cooling

The first control algorithm is a standard ON/OFF openings model, where the "ON" mode refers to fully open window (60% of window geometric area), and "OFF" is 0% opening. The ON/OFF state is evaluated after the outdoor temperature, indoor temperature, and wind speed and follows the daytime schedule as presented in Table 7. An illustrative flow diagram of control algorithm 1 from IDA ICE can be seen in Figure 34.
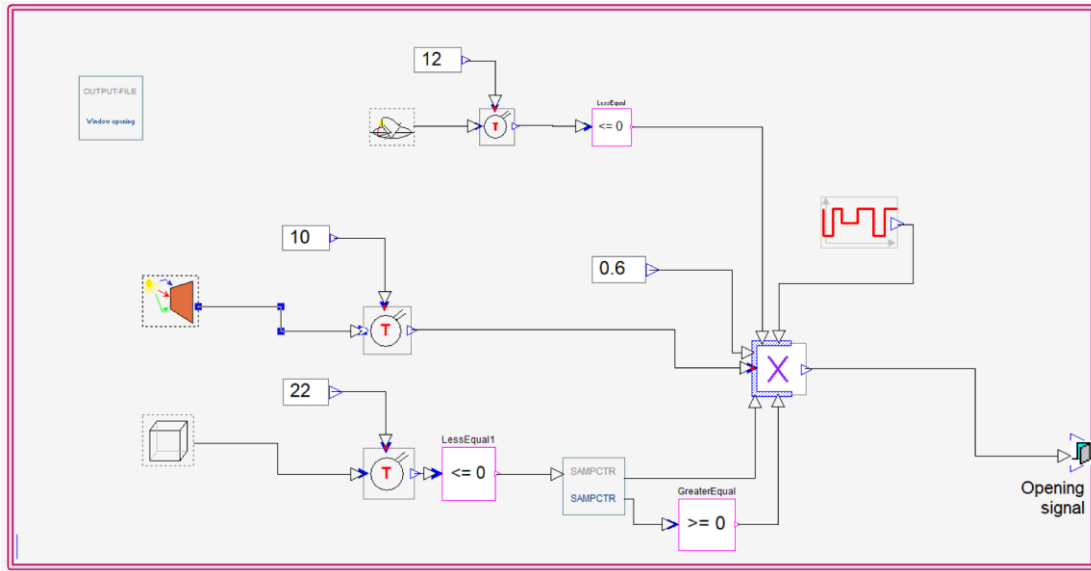
Figure 34: Typical ON/OFF window cooling control algorithm, cropped from IDA ICE

Control algorithm 2 – Typical ON/OFF cooling with night cooling

The key difference between control algorithm 1 and 2 is that control algorithm 2 includes night cooling. Night cooling has a different set of criteria than daytime and only requires the operative temperature to be above 21 °C. Control algorithm 2 can be found in Figure 35.
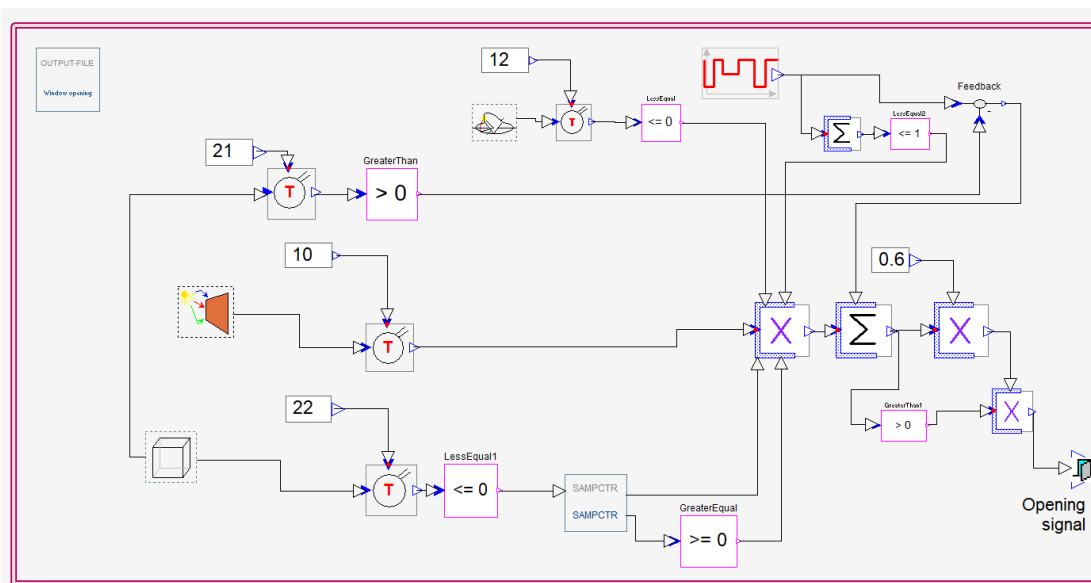
Figure 35: Typical ON/OFF window cooling control algorithm that includes night cooling, cropped from IDA ICE

52

Control algorithm 3 - Variable window opening

The third control algorithm uses a linear relationship to determine how much the window should be opened based on indoor air temperature, from zero opening at 21.9 °C to the maximum opening of 60% at 26°C. Otherwise, the algorithm is the same as with control algorithm 1. An illustrative flow diagram of control algorithm 3 from IDA ICE can be seen in Figure 36.
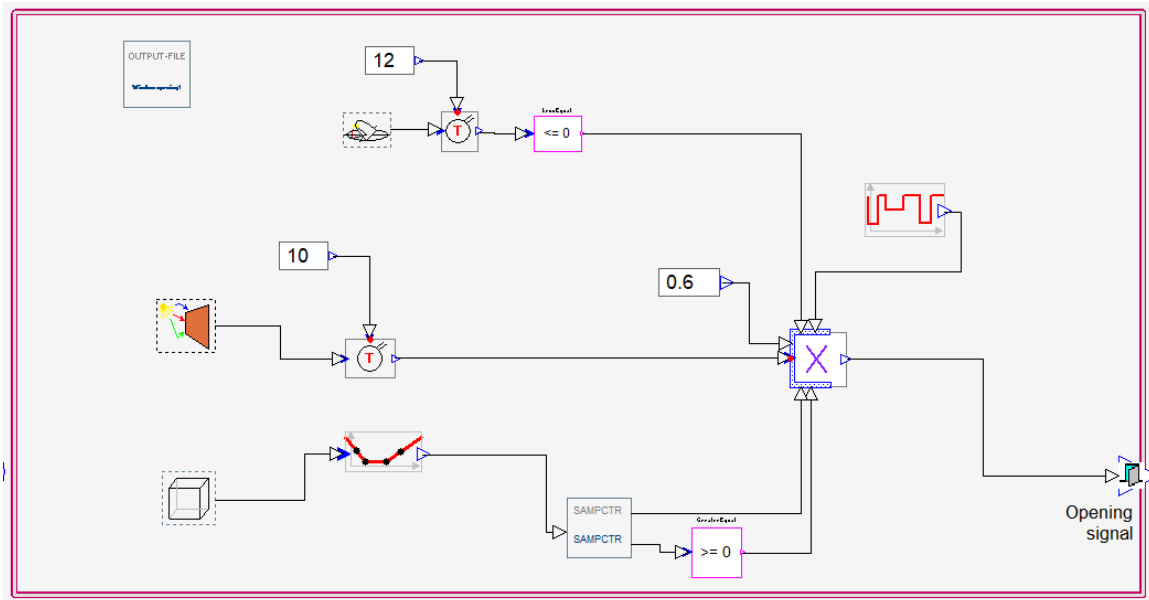
Figure 36: Variable window opening control algorithm, cropped from IDA ICE

Control algorithm 4 – Variable window opening with night cooling

The fourth control algorithm uses the same linear relationship as control algorithm 3 to determine how much the window shall be opened and has the same nighttime cooling functionality as control algorithm 2. An illustrative flow diagram of control algorithm 4 from IDA ICE can be seen in Figure 37.
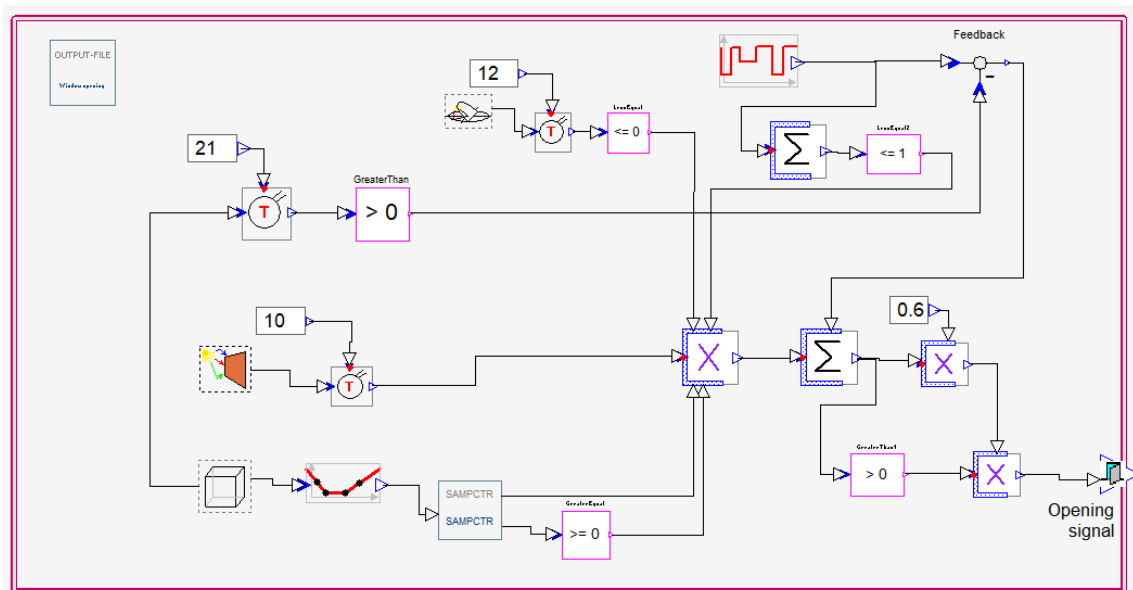
Figure 37: Variable window opening control algorithm with night cooling, cropped from IDA ICE

53

7. Results and discussion

The results are divided into three parts: the on-site measurements and wind pressure calculations, a comparison of the AIVC Cp's and measured/calculated Cp's, and an assessment of the performance of the four proposed window control algorithms.

7.1. On-site measurements

As elaborated in the method chapter, 15 on-site DP-sensor measurements have been performed over a period of ten days. Figure 38 shows the freestream reference sensor output differential pressure, and Figure 39, Figure 40, Figure 41, and Figure 42 shows differential pressure for all sensors on the west, east, south, and north façade, respectively. With 1min interval between each data point and x-axis of the figures represent each datapoint. All sensors are compensated for pressure drop in the tube with equation 6.2, except for the reference freestream sensor in Figure 38. The reasoning behind this is elaborated further in the latter part of this chapter. The raw data from the sensors can be found in Appendix D.
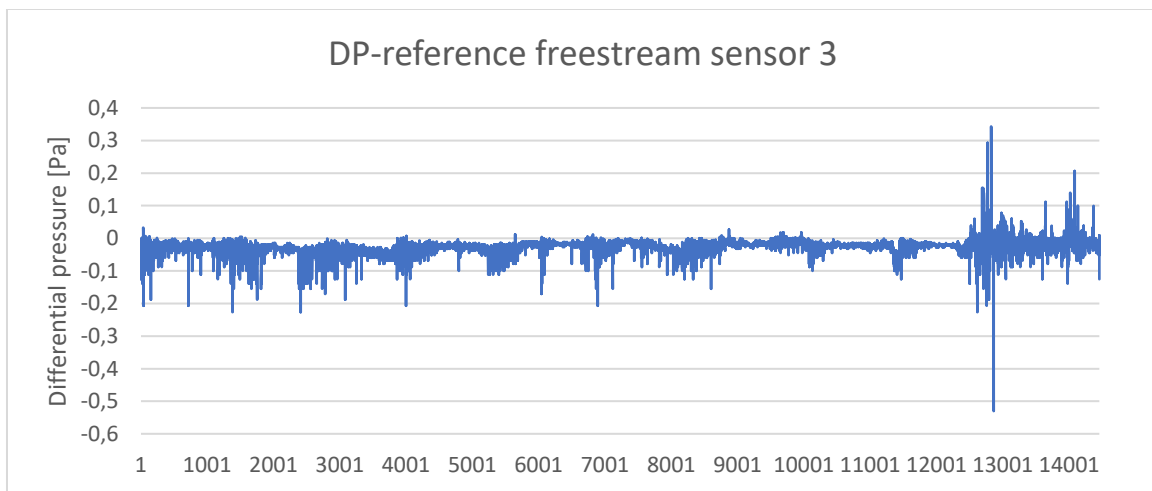
Figure 38: Reference freestream measured pressure sensor output in voltage, measurement interval of 5min. Measurement setup for sensor 3 is performed as illustrated in Figure 19 and Figure 20.
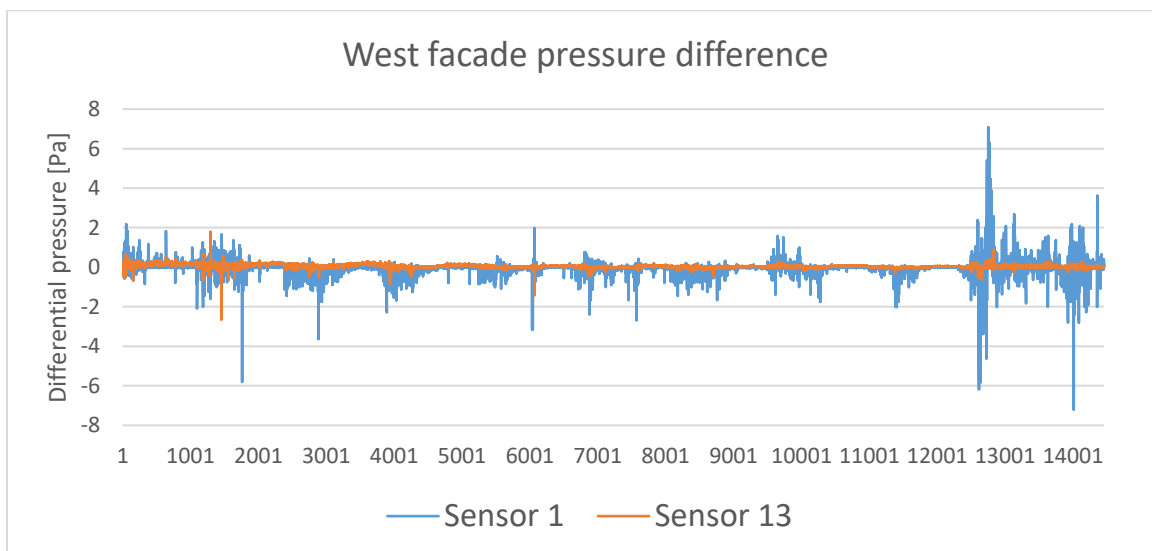
Figure 39: West facade measured pressure difference for sensors 1 and 13 with a measurement interval of 5min. The placement of sensors can be found in Figure 16 (b).

54
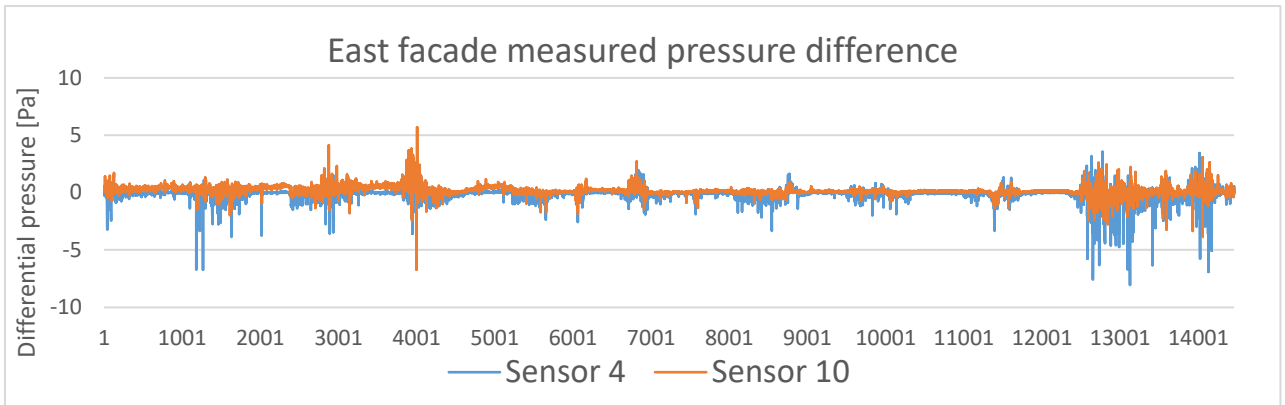
Figure 40: East facade measured pressure difference for sensors 4 and 10 with a measurement interval of 5min. The placement of sensors can be found in Figure 16 (a).
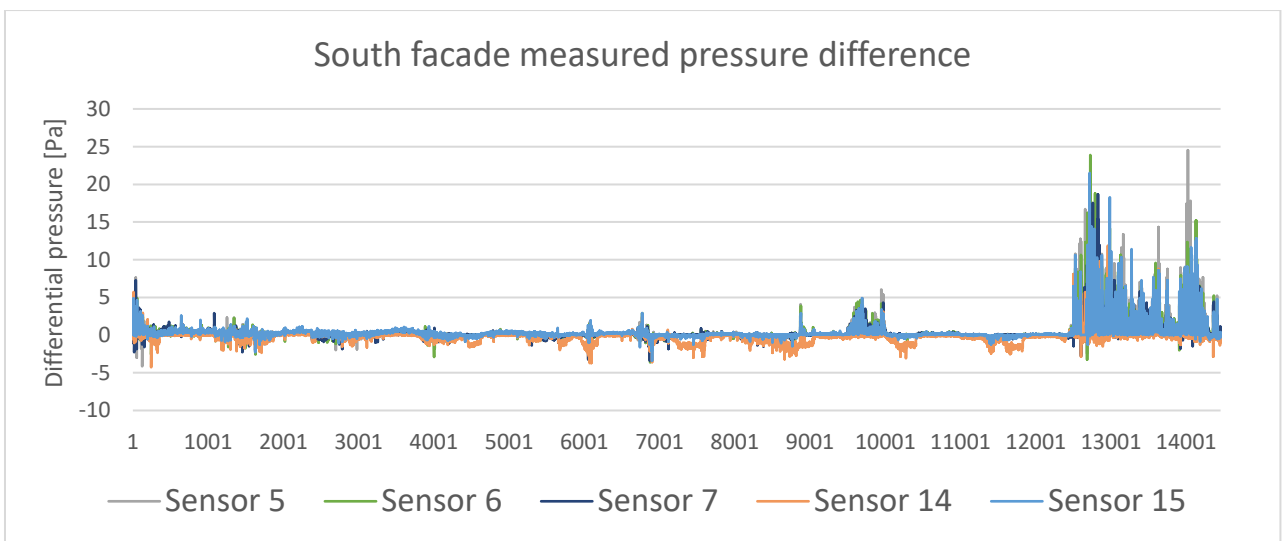
Figure 41: South facade measured pressure difference for sensors 5,6,7,14, and 15 with a measurement interval of 5min. The placement of sensors can be found in Figure 18.
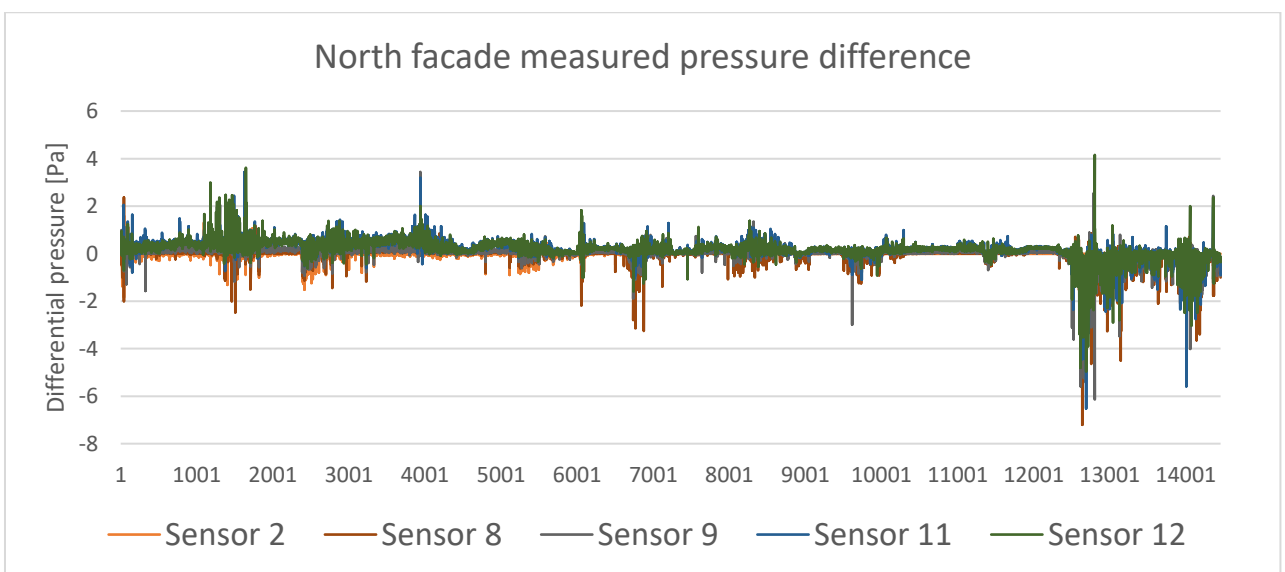
Figure 42: North facade measured pressure difference for sensors 2,8,9,11, and 12 with a measurement interval of 5min. The placement of sensors can be found in Figure 17.

Summarization of all DP-sensor measurements. Which includes minimum, maximum, mean differential pressure [Pa], and standard deviation in Table 8.

Table 8: Summarization of all on-site DP-sensor data

	Ref	West facade		East facade		South facade					North facade				
Sensor	3	1	13	4	10	5	6	7	14	15	2	8	9	11	12
Min [Pa]	-0,53	-7,20	-2,65	-8,06	-6,71	-4,14	-3,64	-3,38	-4,28	-3,38	-1,83	-7,20	-6,13	-6,52	-4,96
Max [Pa]	0,34	7,08	1,80	3,58	5,70	24,53	23,89	18,67	12,47	21,51	2,09	2,37	3,44	3,44	4,16
Mean[Pa]	-0,03	-0,04	0,05	-0,09	0,19	0,30	0,26	0,18	-0,24	0,33	0,00	-0,02	0,04	0,21	0,19
Standard deviation	0,02	0,34	0,08	0,41	0,31	1,06	0,91	0,71	0,66	0,86	0,11	0,28	0,29	0,34	0,32

The sensors located at the higher floor levels generally have lower DP readings than the lower levels. Sensors 1, 2, and 4 on the 4th floor have an average pascal reading of -0,04 Pa, -0,00 Pa, and -0.09 Pa, respectively. And the lowest level measured, 2nd floor has sensors 10, 11, 12, 13, 14 and 15 has mean DP readings of 0.19 Pa, 0.21 Pa, 0.19 Pa, 0.05 Pa, -0.24 Pa and 0.33 Pa respectively. This result is expected as the density of air outside increases at the lower altitude. Why sensor 14 is a discrepancy to this reasoning is elaborated in chapter 7.2.

The measurements' standard deviation describes how much the DP-sensors are affected by wind. A high standard deviation indicates higher fluctuations in the wind-induced air pressure variations. Other factors such as internal air pressure, for example, occupant opening/closing doors, and the mechanical ventilation system, can also create these variations. However, generally, it is considered that most of these variations are a product of wind-induced pressure differences. However, it is not seen a clear tendency in the dataset that higher-level floors experience greater wind-generated forces than the lower-level floors. The standard deviation for the east and west façade sensors is higher on the 4th floor than on the 2nd floor. On the south façade, there is no clear trend in wind load variation, as sensor 15 on the 2nd floor has an SD between sensor 6 and 7 on the 3rd floor SD (sensor 14 is excluded).

Moreover, on the north façade, the 2nd-floor sensors (11 and 12) have a higher SD than the 3rd-floor sensors (8 and 9). Sensor 2 is excluded from consideration as it did not measure the whole duration of the on-site measurements. Hence, the dataset does not show a clear trend in wind-induced air pressure variation compared to the floor heights' altitude. It should be noted that DP-sensors did not measure the 1st floor, where a noticeable drop in wind loads is expected. In addition, the maximum altitude difference between the sensors is only 7.5m (ZEB lab is a max height of 23m), and they are primarily placed in the middle of the facades.

7.1.1. Complications relating to the DP-sensor measurements

A few concerns regarding the raw data that from the DP-sensors were observed - and must be investigated before continuing to process the data.

Reference freestream sensor

The general idea behind the reference freestream pressure measurement is to establish local variations in air pressure unaffected by wind. However, as is evident in Figure 38, this is not precisely the case for the data received by the reference freestream sensor. The sensor is affected by wind to a relatively small degree, as seen when compared to all the other sensors by having a standard deviation of 0.08. Under windy conditions, the reference freestream sensor is also affected, but at a low degree, with a low measurement range of -1.98 Pa – 1.2 Pa. However, the problem that arose was the compensation of the tube, which proved invalid because of the long length of the tube. It was noticed that varying the tube length (15-25m) in equation 6.1 resulted in wildly unreliable and illogical differential pressure compensations, which is why it is concluded that this is way beyond the scope of the equation. Hence, the reference freestream measurements cannot be compensated for the pressure drop that the tube induces. However, the reference freestream measurement will be used for further calculations of wind pressure coefficients without any compensations. This is far from ideal, but it will give a rough estimate of wind pressure coefficients, which would otherwise be unattainable to estimate if this simplification were not made.

Sensor 14 – south façade

Sensors 14 and 15 are placed in each test cell on the same floor; they are expected to provide comparable readings under normal operational circumstances. However, this is not the case as sensor 14 provides significantly lower voltage outputs. This is particularly evident when all south façade sensors have a mean DP measured at 0.33 Pa, while sensor 14 has -0.24 Pa. It is also evident that the sensor is working as intended because it is affected by wind in the same way the other sensors on the south façade are, as is shown in Figure 41 and is displayed in the raw output data in Appendix D-3.

Therefore, the occurring DP measured from sensor 14 is affected differently by the mechanical ventilation than in the other zones. The test cells at the ZEB lab have their own dedicated VAV air supply, and the zone is likely experiencing higher air pressure than intended. Every zone, in theory, should have similar air pressure, but if the VAV-damper or the damper in the overflow ductwork is offset, it could create a higher/lower than the intended air pressure in the zone. Therefore, all measured data from sensor 14 is excluded in the upcoming results.

Sensor 2 – north façade

Sensor 2 faced an issue roughly halfway through the measurement timeframe. This resulted in the sensor readings going to zero for a few hours. After this event, the sensor was set up incorrectly, resulting in a stable voltage reading of 2.53V, representing the zero point of the sensor. Hence, after this event, the measurements from sensor 2 are invalid and will not be used further. However, before this event, the measurements are considered valid and will be used for validation where it is deemed acceptable, as it was the event that created issues. This incident is evident in Appendix D-4, which shows the voltage output from sensor 2.

57

7.1.2. Weather station data

The climate parameters required to evaluate pressure coefficients are inside and outside air temperature and wind velocity. The external climatic parameters are collected from the weather station on the rooftop of the ZEB lab at an interval of 1 measurement per minute.

Inside and outside air temperature

The following Figure 43 shows the outside temperature, measured at the weather station, and the inside air temperature, which is the average temperature of 6 climate sensors at various floor levels and room categories around the ZEB lab building.
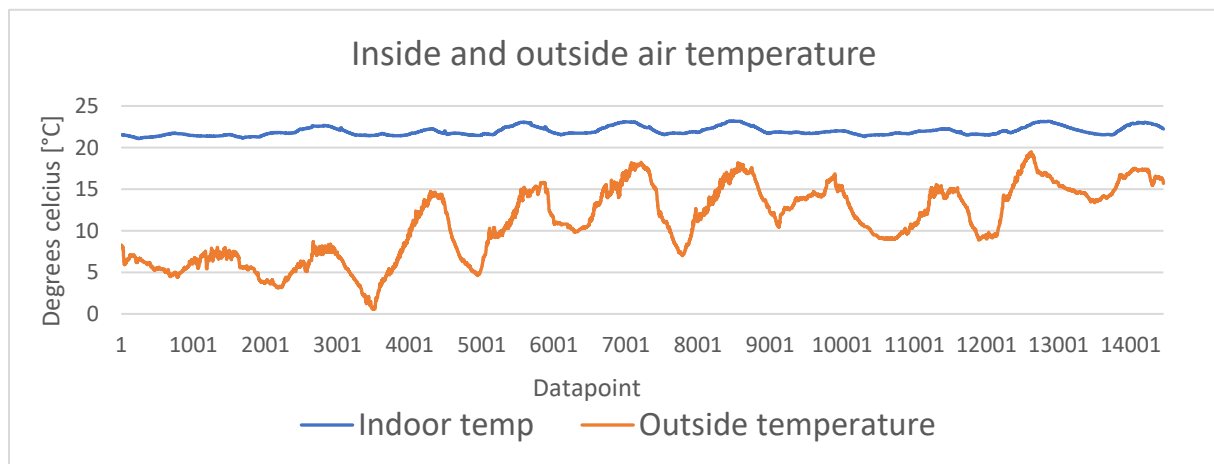
Figure 43: Inside and outside air temperature. Where inside is an average of multiple climate sensors located around the ZEB lab, and the outside is from the weather station.

The internal air temperature throughout the measurement period were measured in the range of 21.1 °C to 23.2 °C, and the external air temperature from 0.5 °C to 19.4 °C. The internal air temperature has minor variations in the measurement period, and the outside air generally saw a rise in temperature throughout the measurement period. It is prevalent that the lower difference between the internal and external air temperature results in a lower pressure difference measured by the sensors. However, this is not as prevalent in Figure 39, Figure 40, Figure 41, and Figure 42 as the range of these figures is too small to observe the minor variations in air pressure that the temperature variations create. However, it can be seen in the raw voltage data in Appendix D.

Wind velocity

Firstly, as the weather station was recently installed, it had a settings issue regarding the wind direction measurements that were not observed after its measurement period was over. This resulted in all measurements being capped at a maximum of 255 ° because data from the weather station was capped at 8-bit. Therefore, all wind direction data at 255 is excluded from the assessment, as it is unknown which wind direction it truly represents.

Data for wind speed and direction measured on the roof of the ZEB lab is summarized in Figure 44.
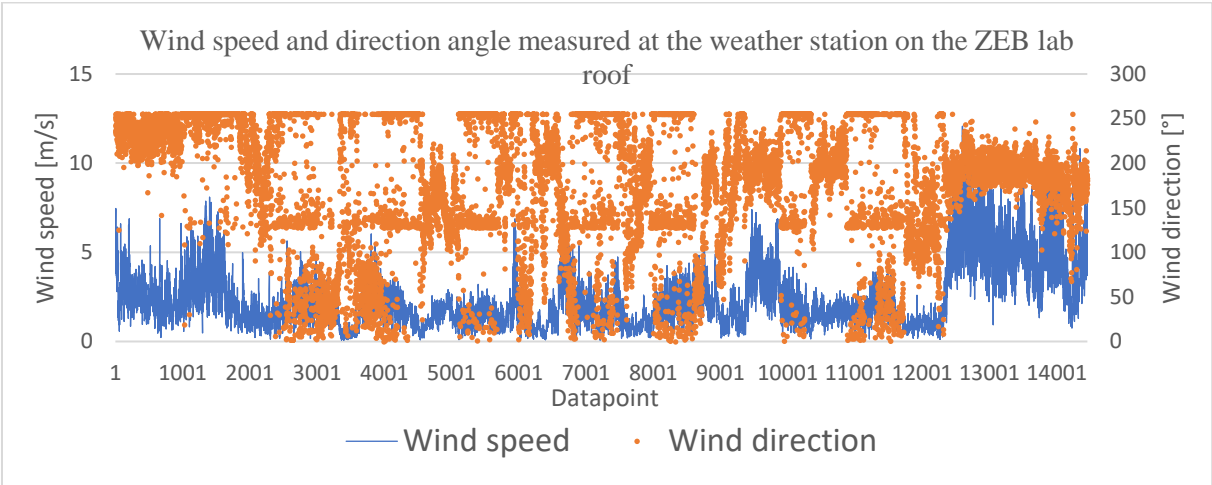
Figure 44: Wind speed and direction measured at the weather station on the rooftop of ZEB lab

The wind speed is measured in the range of 0-12 m/s and indicates especially windy conditions in the latter part of the measurement period (datapoint ~12500-14500). In this latter part, it is also observed that wind direction is mostly in the range of ~140 ° to 230 ° and does not fluctuate as much as normally when there is less wind. Furthermore, in the first part of the measurement period (datapoint ~0-1500), there are also observed somewhat more windy conditions than normal, with wind direction > 200 °. Moreover, under low wind conditions (datapoint ~1500-12500), the wind direction varies greatly and is not as clearly from a single direction but somewhat from all directions.

For further evaluation of wind direction and pressure coefficients, the wind direction is split into north-east, east, south-east, south, and south-west (NE, E, SE, S, SW). North, west, and north-west wind directions are excluded because of the issues with a maximum wind direction of 255 °. Each wind direction (NE, E, SE, S, SW) includes all datapoints in the range of ± 22.5 ° of the cardinal direction angle. The quantity of data points in each cardinal direction is found in Figure 45.
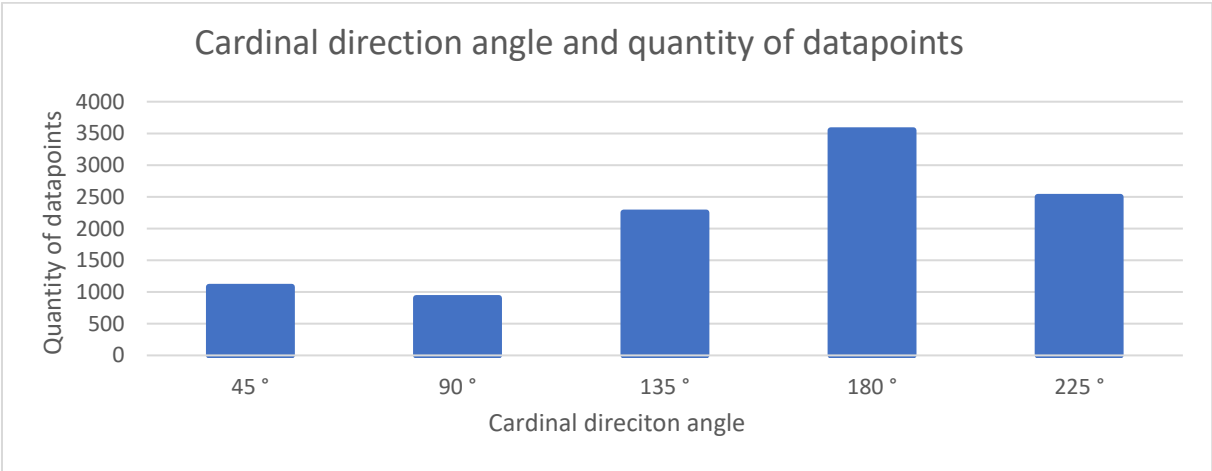
Figure 45: Quantity of data points in each cardinal direction angle, by including all datapoints in the range of ± 22.5 ° of each cardinal direction angle (-22.5 ° < $\theta_{direction}$ < 22.5°)

7.1.3. Pressure coefficients

Firstly, a summary of all the simplifications and limitations that the following calculations are based on. Sensors 2 and 14 are excluded, and the reference sensor 3 is not compensated for the tube's pressure drop, as elaborated in chapter 7.1.1. Furthermore, the cardinal directions are split into five directions (NE, E, SE, SE, SW), as is reasoned in chapter 7.1.2.

The following Table 9 gives an overview of wind pressure coefficients calculated from equation 4.11 and includes compensation for the height difference between the sensor altitude, as described in equation 6.3 and 6.4.

Table 9: Wind pressure coefficients for all eligible sensors and all eligible cardinal directions. Based on all data points and are compensated for height variations.

Wind pressure coefficients (Cp) including all datapoints (including height compensation)											
West facade		East facade		South facade				North facade			
Sensor 1	13	4	10	5	6	7	15	8	9	11	12
North-east wind direction 0,02	5,76	-0,01	5,41	3,13	3,13	3,13	5,50	3,13	3,08	5,35	5,38
East wind direction 0,01	10,38	0,03	9,85	5,61	5,62	5,63	9,99	5,65	5,56	9,72	9,71
South-east wind direction 0,04	6,20	0,03	5,92	3,33	3,34	3,36	5,98	3,41	3,32	5,80	5,83
South wind direction -0,01	3,61	0,01	3,45	1,88	1,89	1,92	3,43	2,00	1,96	3,40	3,42
South-west wind direction -0,01	5,90	0,04	5,63	3,13	3,12	3,14	5,63	3,25	3,17	5,52	5,55

These results show flaws in the methodology used, or the data used are inaccurate. The values in Table 9 are not in the same range as wind pressure coefficients are expected to be, which are usually in the range of 0 - 1. It is deemed that this is because the height correction from equation 6.3 and 6.4, based on equation 4.7 makes the height corrected DP discrepancy between the floor levels even higher than simply using measured and non-corrected for height DP. The average of median DP readings for each floor level separately is illustrated in Figure 46.
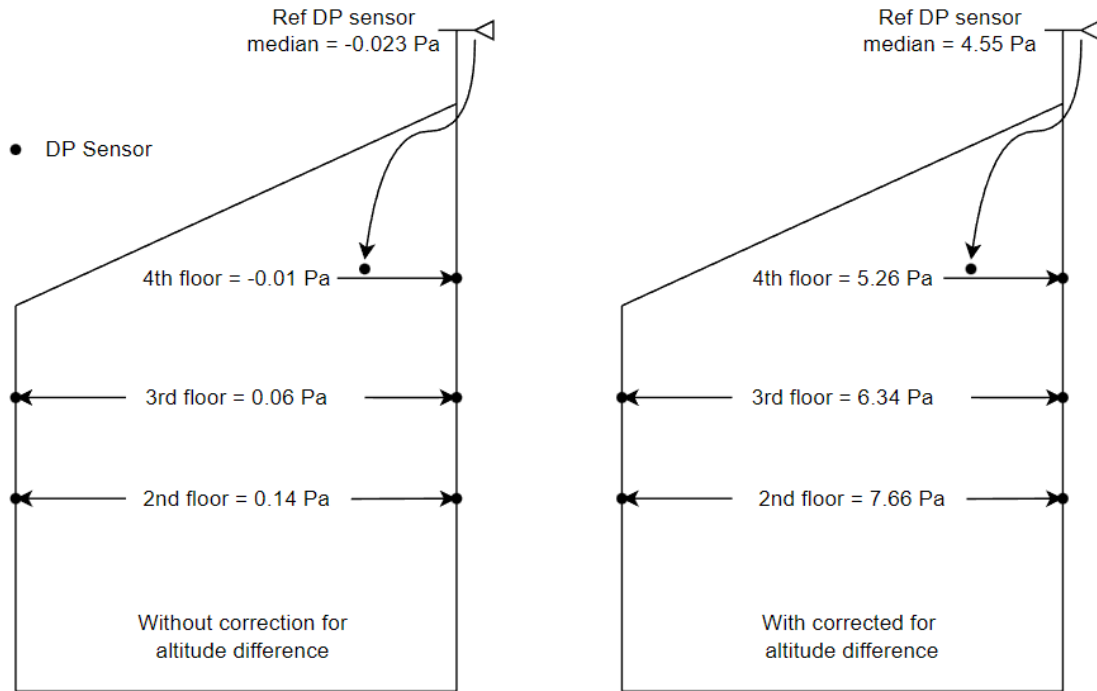
Figure 46: Average of all median DP readings from each sensor at each floor level separately. Without and with compensation for altitude difference.

Before height correction, the difference between the reference freestream pressure and each floor level's average median pressure is more stable. When comparing the average median DP for each floor level to the reference freestream sensor DP, both for the non-height compensated and height compensated, the results are drastically different, as shown in Table 10.

Table 10: Difference in average median DP from each floor when compared to reference freestream median DP

ΔP = Floor average median DP – Ref median DP		
	Without altitude correction	With altitude correction
4th floor	0.163	3.11
3rd floor	0.083	1.79
2nd floor	0.013	0.71

This essentially shows that when utilizing equation 4.11 to calculate Cp, the culprit for these out of expected range results is the increased ΔP between the façade sensors and the reference freestream sensor that the correction creates. The difference between each floor level's average median DP has increased, making the Cp highly inaccurate in low wind conditions. The explanation for why this correction is flawed is uncertain, but it is deemed that the altered internal pressure by the mechanical ventilation system is the problem. The internal air pressure is not only affected by air density variations due to temperature differences but also air pressure variations induced by the fans in the AHU and the various dampers in the ventilation ductwork.

Therefore, for further evaluation, it is considered that the most accurate way to assess Cp further is to exclude any corrections for altitude variations between the sensors, which results in Cp values found in Table 11.

61

Table 11: Wind pressure coefficients for all eligible sensors and all eligible cardinal directions. Based on all data points and are not compensated for altitude variations.

Wind pressure coefficients (Cp) including all datapoints (excluding height compensation)											
	West facade		East facade		South facade				North facade			
Sensor	1	13	4	10	5	6	7	15	8	9	11	12
North-east wind direction	-0,02	0,16	0,01	0,52	0,16	0,17	0,16	0,42	0,16	0,21	0,58	0,55
East wind direction	-0,01	0,26	-0,03	0,80	0,31	0,29	0,29	0,66	0,27	0,36	0,92	0,94
South-east wind direction	-0,04	0,16	-0,03	0,44	0,20	0,20	0,17	0,38	0,13	0,21	0,56	0,53
South wind direction	0,01	0,09	-0,01	0,25	0,18	0,17	0,14	0,27	0,05	0,10	0,29	0,28
South-west wind direction	0,01	0,17	-0,04	0,43	0,24	0,25	0,22	0,43	0,11	0,20	0,55	0,52

These Cp values in Table 11 are in the range of what is expected but not necessarily reasonable because, e.g., the north and south façade has somewhat similar Cp values for the same wind direction. It is anticipated that wind directions, for instance, south (190 °), will create a windward side at the south facade and higher than zero Cp, and the lower pressure region at the leeward side (north) will have lower than zero Cp, as is elaborated in chapter 4.3. These trends are not apparent in Table 11. Hence some further assessment is required.

Low wind speed conditions can create issues for the reliability of the calculation of wind pressure coefficients with equation 4.11. With Cp in the range of -263 to 277, the average of all sensor's median Cp values is only 0.037. Due to local wind gusts and the distance between all sensors and the weather station, it is challenging to evaluate Cp under non-windy conditions. Furthermore, since the wind speed parameter in equation is raised to the second power, it can be the culprit for these significant fluctuations of Cp when it is close to 0 m/s wind speed. Thus, if a slight wind gust at one façade creates a relatively big pressure difference (in comparison to the wind conditions) and the weather station does not encounter the same wind gust, the Cp values are far off what is expected. Hence, it is considered that under non-windy conditions, the Cp equation produces unreliable wind pressure coefficients due to limitations with the measurement setup. Moreover, excluding all DP data points with low wind speed is necessary to eliminate this inaccuracy.

Datapoint 12500-14500 are, however, under steady windy conditions, and the wind direction is generally stable in the cardinal direction of ~50-200 °, as shown in Figure 44 This gives reliable data points for east, southeast, south, and south-west. However, it is necessary to exclude the north-west due to a small number of data points in this cardinal direction from these 2000 data points, which gives the following Table 12, including wind pressure coefficients for the data points 12500-14500.

Table 12: Wind pressure coefficients for all eligible sensors and all eligible cardinal directions. Based on data, points 12500-14500. DP is not compensated for height variations.

Wind pressure coefficients (Cp) including all datapoints (excluding height compensation)											
West facade		East facade		South facade				North facade			
Sensor 1	13	4	10	5	6	7	15	8	9	11	12
East wind direction 0,05	0,01	0,03	0,03	0,27	0,26	0,10	0,19	-0,19	-0,24	-0,16	-0,08
South-east wind direction -0,02	0,01	-0,03	0,03	0,42	0,33	0,13	0,31	-0,13	-0,12	-0,09	-0,07
South wind direction 0,01	0,00	-0,02	0,01	0,13	0,10	0,07	0,11	-0,02	-0,02	-0,02	-0,01
South-west wind direction 0,01	0,00	-0,03	0,01	0,14	0,14	0,09	0,13	-0,03	-0,03	-0,02	-0,02

Calculating the average Cp values for each façade separately gives the following wind pressure coefficients, as shown in Table 13.

Table 13: Average Cp values for all sensors at each façade separately.

Average Cp for the facades				
Facade	West	East	South	North
East wind direction	0,03	0,03	0,21	-0,17
South-east wind direction	-0,01	0,00	0,30	-0,10
South wind direction	0,01	-0,01	0,10	-0,02
South-west wind direction	0,01	-0,01	0,13	-0,03

Pressure coefficient values from Table 12 and the summarization in Table 13 show that the west and east façades are not significantly affected by either of the included wind directions. The south façade has positive wind coefficients; the highest is from the southeast of 0.3 average, and the lowest is south of 0.1 average. North façade always has negative wind coefficients, with the highest average for the south wind direction of 0.02 and lowest at the east wind direction of -0.17.

It should be noted that only four of eight cardinal directions are considered, and these results do not provide all information required to assess how wind influences the building body thoroughly. However, it is observed that the south-facing wind does not produce the highest Cp for the south façade and does not create the lowest Cp for the north façade, which is expected if the surroundings do not influence the wind velocity. However, since buildings, vegetation, and other constructions are nearby, the expected Cp values will not be perfectly aligned with the wind direction and façade. Meaning that the south wind produces the highest Cp for the south façade, the east wind direction produces the highest Cp east façade, and so on. The building body of the ZEB lab itself also massively impacts how the wind-generated forces create air pressure variations around the building. With these points in mind, it is considered that the wind pressure coefficients in Table 13 are close to what is expected and can therefore be considered acceptable for further use in the IDA ICE model.

These results should be taken as is, and are far from accurate, when considering how many simplifications are made and the uncertainties surrounding the methodology, measurement setup, and calculations. The accuracy of the sensor, resolution of the data logger, and the input voltage from the power adapter is neglectable when compared to the simplification that are made, and therefore will not be elaborated on further.

7.2. AIVC vs new on-site wind pressure coefficients

In this chapter, the measured wind pressure coefficients are compared to the Cp set provided by IDA ICE from AIVC. The difference between the AIVC supplied wind pressure coefficients and the final on-site measured wind pressure coefficients from Table 13 is tested by inserting both Cp sets into the BEM presented in chapter 6.2, and the difference in the results is presented and elaborated. For this assessment, the model with AIVC wind pressure coefficients is referred to as the AIVC model, and the model with on-site measured wind pressure coefficients is referred to as the on-site model. Lastly, all BEM simulations are simulated in timeframe 01. May – 29. August.

7.2.1. AIVC wind pressure coefficients and on-site measured wind pressure coefficients

Two different simulations of the IDA ICE model are performed to compare the AIVC database Cp set and the measured and calculated Cp coefficients. Where the only difference between the models are the wind pressure coefficients used. The results are evaluated after the thermal environment and comfort performance and the difference in inflow/outflow for the internal and external walls for a few zones. Finally, window control algorithm 1 is used for this comparison. The wind pressure coefficients from the AIVC database, which are included in IDA ICE, are displayed in Table 14.

Table 14: AIVC wind pressure coefficients in IDA ICE for the "semi-exposed" setting

Building body	Cardinal direction (N, NE, E, SE, S, SW, W, NW)								Face azimuth
	0	45	90	135	180	225	270	315	
North facade	0.4	0.1	-0.3	-0.35	-0.2	-0.35	-0.3	0.1	0
East facade	0.4	0.2	-0.6	-0.5	-0.3	-0.5	-0.6	0.2	90
South facade	0.4	0.1	-0.3	-0.35	-0.2	-0.35	-0.3	0.1	180
West facade	0.4	0.2	-0.6	-0.5	-0.3	-0.5	-0.6	0.2	240
Roof	0.3	-0.5	-0.6	-0.5	-0.5	-0.5	-0.6	-0.5	180

This set of wind pressure coefficients is somewhat limited in its accuracy. It is used the same Cp values for building bodies facing north and south as with the building bodies facing east and west. This means that the BEM model will evaluate the wind-induced air pressure as the same for facades facing the opposite cardinal direction, which is not what theory implies will be the case, as elaborated in chapter 4.3.

The following Cp values in Table 15 are used for the on-site measured wind pressure coefficient model. They are a combination of AIVC and on-site measurement Cp values, as only Cp values from carinal direction 45-, 90-, 135- and 180-degree were deemed acceptable from the on-site measurements. The rest of the Cp values are from AIVC semi-exposed database.

Table 15: On-site measured wind pressure coefficients for 45-, 90-, 135- and 180-degree cardinal directions. The rest of the Cp coefficients are from the semi-exposed AIVC database (roof is all AIVC database).

Building body	Cardinal direction (N, NE, E, SE, S, SW, W, NW)								Face azimuth
	0	45	90	135	180	225	270	315	
North facade	0.4	0.1	-0.17	-0.1	-0.02	-0.03	-0.3	0.1	0
East facade	0.4	0.2	0.03	0.0	-0.01	-0.01	-0.6	0.2	90
South facade	0.4	0.1	0.21	0.3	0.1	0.13	-0.3	0.1	180
West facade	0.4	0.2	0.03	-0.01	0.01	0.01	-0.6	0.2	240
Roof	0.3	-0.5	-0.6	-0.5	-0.5	-0.5	-0.6	-0.5	180

7.2.2. Thermal environment assessment

Only 10 of the total 44 zones in the BEM are compared to evaluate the thermal environment and comfort. These zones should give an overall representation of all room categories, and zones with high occupancies, such as meeting rooms and office landscapes, are chosen over storage/WC zones. The full spreadsheet that includes all thermal environment parameters for all zones (except zones with no occupants) is found in Appendix E.

The ten zones' indoor operative temperature for both the AIVC and the on-site model is presented in Table 16, which includes minimum and maximum operative temperature, in addition to the difference between the min and max operative temperature between the models.

Table 16: Min and max operative temperature for ten zones for AIVC and on-site model + delta min and max operative temperature between each BEM

	AIVC Pc		On-site Pc			
Zone	Min [°C]	Max [°C]	Min [°C]	Max [°C]	Delta min [°C]	Delta max [°C]
6 - Cafeteria	21,62	26,12	21,62	26,07	0	0,05
15 - Hallway/office landscape	20,63	25,69	21	25,62	0,37	0,07
16 - Twin room reserach cell	21,22	26,33	21,22	26,07	0	0,26
17 - Twin room reserach cell	21,27	26,46	21,27	26,31	0	0,15
18 - Meeting room	21,61	25,31	21,68	25,23	0,07	0,08
20 - Multiroom	21,25	25,72	21,25	25,7	0	0,02
26 - Hallway/office landscape	20,59	26,2	21,05	26	0,46	0,2
27 - Office landscape	21,16	27,28	21,16	26,97	0	0,31
32 - 2x multiroom	21,51	24,5	21,57	24,43	0,06	0,07
40 - Knowledgecenter/hallway	21,19	25,63	21,19	25,61	0	0,02

The greatest difference in minimum air temperature between the zones is zone 26 at 0.46 °C, and the greatest maximum temperature between the zones is zone 27 at 0.31 °C. However, generally, the AIVC model has a bit lower minimum air temperature and a bit higher maximum air temperature, but the difference is neglectable since the difference is so minimal.

Thermal comfort assessment also supports the same pattern found in the max and min air temperatures, which are little to zero difference between the two models that are compared. Both models' thermal comfort parameters are found in Table 17 and Table 18.

Table 17: Adaptive thermal comfort model for ten zones for AIVC and on-site model. Three categories: 1,2, and 3, which are best, good, and acceptable, respectively.

Adaptive thermal comfort model						
	Cp from on-site			Cp from AIVC		
Total hours in each category [%]	Best	Good	Acceptable	Best	Good	Acceptable
6 - Cafeteria	0,948	0,998	1,000	0,946	0,998	1,000
15 - Hallway/office landscape	0,874	0,999	1,000	0,872	0,999	1,000
16 - Twin room reserach cell	0,860	1,000	1,000	0,856	1,000	1,000
17 - Twin room reserach cell	0,874	1,000	1,000	0,870	1,000	1,000
18 - Meeting room	0,999	1,000	1,000	0,999	1,000	1,000
20 - Multiroom	0,981	1,000	1,000	0,980	1,000	1,000
26 - Hallway/office landscape	0,913	1,000	1,000	0,897	0,999	1,000
27 - Office landscape	0,883	0,999	1,000	0,916	0,998	1,000
32 - 2x multiroom	0,937	1,000	1,000	0,940	1,000	1,000
40 - Knowledgecenter/hallway	0,900	1,000	1,000	0,908	1,000	1,000

Table 18: Evaluation of PPD and operative temperature of over 26 °C (TEK17 requirement).

	AIVC Pc		On-site Pc			
	PPD	Hours>26 °C	PPD	Hours>26 °C	Delta PPD	Delta hours>26 °C
6 - Cafeteria	13,77	14,6	13,3	13,8	0,47	0,8
15 - Hallway/office landscape	14,99	0	14,95	0	0,04	0
16 - Twin room research cell	13,54	4	13,56	2,5	0,02	1,5
17 - Twin room research cell	13,51	5	13,53	4,4	0,02	0,6
18 - Meeting room	12,94	0	12,81	0	0,13	0
20 - Multiroom	13,57	0	13,57	0	0	0
26 - Hallway/office landscape	14,27	1,6	14,25	1,1	0,02	0,5
27 - Office landscape	14,2	6,4	14,21	5,7	0,01	0,7
32 - 2x multiroom	12,99	0	12,9	0	0,09	0
40 - Knowledge-center/hallway	15,13	0	15,09	0	0,04	0

As seen in Table 17, all hours for both models are in the acceptable category, which is the requirement for the ZEB lab. No zones meet the requirement for all hours in the best category for both models, and it is mixed for the good category. The difference is neglectable between the models, as there are only a few hours of variance between the zones in each model. Table 18 also shows little to no difference, as the maximum difference in PPD is only 0.47, and the maximum difference in hours over 26 °C is 1.5h. All zones are well within the TEK17 requirement of a maximum of 50 hours above 26 °C.

Overall, the thermal environment assessment indicated that the difference between the two sets of wind pressure coefficients is subtle and close to zero. The culprit for why the difference is so small is from many sources, such as a minimal change in the quantity of airflow through the external facades, the window control algorithm that was used, or simply just a small change in cooling performance of window cooling. However, it is observed that changing the Cp values did not make a significant difference in the thermal environment, and the difference observed is so small that uncertainty with the BEM overshadows it.

7.2.3. Difference in airflow quantity through the facades assessment

To study the change in airflow quantity, an evaluation of in and outflow is performed through the external facades for a few chosen zones. An extensive evaluation of a few zones at the north and south façade, where most electric operable windows are placed, is considered to give a reasonable overview of the change in airflow quantity. Average inflow/outflow through the external facades for the four evaluated zones, including both AIVC and the on-site model, is found in Table 19.

Table 19: In and outflow through the external facades for AIVC and on-site BEM. There are two zones on the south façade (zone 16 and 17) and two on the north façade (zone 26 and 42).

Average inflow and outflow through external walls for each zone [L/s]	Cp from AIVC		Cp from on-site		Delta inflow	Delta outflow
	Inflow	Outflow	Inflow	Outflow		
16 - Twin room reserach cell	65,5	44,9	65,38	49,60	0,07	4,66
17 - Twin room reserach cell	65,4	48,6	64,78	52,92	0,65	4,34
26 - Hallway/office landscape	95,8	73,1	122,58	44,99	26,79	28,09
42 - Classroom	167,8	66,8	166,57	45,06	1,24	21,72

The values in Table 19 show the average inflow/outflow through the facades for all electrically controlled windows and are generally much lower than the peak airflow quantities. However, it is assumed that the differences between the Cp sets should be prevalent in these average values.

The south façade zones (16 and 17) have little change in average inflow through the facades but have a slightly higher outflow for the on-site Cp model. However, the north façade zones (26 and 42) significantly change the average inflow/outflow air quantity. Zone 26 has, on average, 26.79 l/s more inflow in the on-site model and 28.09 l/s higher outflow in the AIVC model. Zone 42 has a neglectable Difference in inflow but 21.72 l/s higher outflow in the AIVC model. The differences between the models using a different set of CPs are prevalent. However, to determine how they affect the inflow/outflow, it is needed to study wind directions separately.

One zone with a façade facing south and one with a façade facing north are used to evaluate the differences between the model's wind pressure coefficients when evaluating north and south wind direction. Datapoints with wind direction in the range of ± 22.5 ° for north and south cardinal directions are divided into inflow and outflow for these two zones with both AIVC and on-site Cp and are summarized in Table 20.

Table 20: Inflow and outflow through external facade for zone 16 and 26 from north and south wind directions. For both the AIVC and on-site Cp model.

Wind direction (north = in range 180 ° ± 22.5 °: south = 337.5 °- 360 ° and 0 ° - 22.5 °)	North wind direciton	South wind direction
Cp from AIVC: Zone 16 - Twin room research cell, average inflow through external facade [L/s].	45,9	90,6
Cp from on-site: Zone 16 - Twin room research cell, average inflow through external facade [L/s].	42,9	92,8
Cp from AIVC: Zone 26 - Hallway/office landscape, average inflow through external facade [L/s].	98,0	171,0
Cp from on-site: Zone 26 - Hallway/office landscape, average inflow through external facade [L/s].	96,8	116,2
Cp from AIVC: Zone 16 - Twin room research cell, average ouitflow through external facade [L/s].	33,6	75,0
Cp from on-site: Zone 16 - Twin room research cell, average outflow through external facade [L/s].	29,9	64,9
Cp from AIVC: Zone 26 - Hallway/office landscape, average outflow through external facade [L/s].	15,4	22,0
Cp from on-site: Zone 26 - Hallway/office landscape, average outflow through external facade [L/s].	17,9	110,3

By separating the inflow/outflow after wind direction, the differences between the wind pressure coefficients become more evident. For the south wind direction, the AIVC set of Cp's has higher inflow than outflow for both zones, as the north façade zone has 171 l/s inflow and 22 l/s outflows, and the south façade has 90.6 l/s inflow and 75 l/s outflows. The inflow and outflow pattern for the AIVC CPs does not support the theory of how the wind-induced pressure differences should act on a building body. It is projected that with the south facing wind direction, the south façade will have more inflow than outflow, and the north façade will have more outflow than inflow.

69

To assess the differences between the set of Cp's, the delta between each zone for the respective model, wind direction and quantity of airflow are calculated, as seen in Table 21 using values from Table 20.

Table 21: Differences between inflow and outflow for the AIVC and on-site model. Delta is the difference between the zones with the same setup. I.e., the on-site model vs. AIVC for each zone, inflow/outflow, and wind direction.

	Delta north wind direction	Delta south wind direction
Zone 16: difference in inflow between the models [L/s]	3,0	2,2
Zone 16: difference in outflow between the models [L/s]	-3,7	-10,1
Zone 26: difference in inflow between the models [L/s]	1,2	-54,9
Zone 26: difference in outflow between the models [L/s]	2,5	88,2

As the new set of wind pressure coefficients in Table 15 only has changes to the coefficients for the cardinal direction of 90 °– 225 °, the change in inflow/outflow quantity of air should be noticeable for the south wind directions but not significantly for the north. This is evident in Table 21, as airflow quantity regarding the north wind direction only has relatively minor changes (most significant difference of 14%). However, the quantity of airflow is heavily influenced by the new set of CPs when considering the south wind direction. The changes are most significant for zone 26 (zone at the north façade), which has a reduction of inflow through the facades from 171 l/s to 116.2 l/s. That is a reduction of -32% and an increase in the outflow from 22 l/s to 110.3 l/s, an increase of 401%. Furthermore, the south façade zone 16 sees a modest increase in inflow and reduction in outflow through the façade, with the change in inflow at 12% and outflow of -16%.

It is expected that higher Cp should increase inflow, as is shown in equation 4.10. This effect is evident when considering the south façade, with increased inflow and decreased outflow for the new set of CPs. However, the opposite effect can be seen in the north façade zone. Where the inflow is reduced, but the outflow is increased with an increase in Cp from -0.3 to -0.02. The reason for this effect is because the south façade has a higher increase in Cp (from -0.3 to 0.1) than the north façade, so the increased internal air pressure that comes from the south façade will ensure higher outflow for the north façade. Because all zones have internally connected airflow pathways, the increased internal air pressure will go from the internal south façade to the internal north facade. This effect is illustrated in Figure 12.

7.3. Comparison of the suggested window control algorithms

In chapter 6.3, four window control algorithms that utilize different window opening strategies were introduced. And to assess their performance, these four algorithms are simulated in the BEM with the new set of CPs from the on-site measurements and evaluated after standard performance parameters. Since this thesis aims to study the ventilative cooling potential, all models are compared based on thermal environment parameters. Additionally, other factors such as the window opening pattern for the windows are also considered. Lastly, all BEM simulations are simulated in timeframe 01. May – 29. August.

7.3.1. Evaluation of key thermal environment parameters

An overview of the minimum and maximum indoor operative temperature for ten zones is found in Table 22. An overview of all zones is found in Appendix F.

Table 22: Min and max operative temperature for ten zones for all four window control algorithms.

	Algorithm 1		Algorithm 2		Algorithm 3		Algorithm 4	
Zone	Min [°C]	Max [°]	Min [°C]	Max [°]	Min [°C]	Max [°]	Min [°C]	Max [°]
6 - Cafeteria	21,62	26,07	21,63	26,06	21,67	26,24	21,64	26,06
15 - Hallway/office landscape	21	25,62	21,12	25,58	21,07	25,74	21,13	25,53
16 - Twin room reserach cell	21,22	26,07	21,34	26,15	21,34	26,45	21,1	26,24
17 - Twin room reserach cell	21,27	26,31	21,25	26,37	21,3	26,6	21,08	26,45
18 - Meeting room	21,68	25,23	21,33	25,02	21,35	25,43	21,68	25,05
20 - Multiroom	21,25	25,7	21,19	25,53	21,27	25,73	21,25	25,5
26 - Hallway/office landscape	21,05	26	21,2	25,98	21,22	26,08	21,21	25,95
27 - Office landscape	21,16	26,97	21,02	26,99	21,21	27	21,09	27
32 - 2x multiroom	21,57	24,43	21,31	24,4	21,31	24,54	21,55	24,4
40 - Knowledgecenter/hallway	21,19	25,61	21,19	25,48	21,14	25,54	21,09	25,43
Average of these ten zones	21,30	25,80	21,26	25,76	21,29	25,94	21,28	25,76
Average of all zones	21,55	24,15	21,31	23,90	21,63	24,31	21,40	23,93

The difference in operative temperature between the models with different window control algorithms is insignificant, with only slight variations of less than one degree centigrade of the maximum and minimum average operative temperature between the models. Therefore, since no significant difference between the models is observed, there is no advantage to either of the window control algorithms regarding min and maximum operative temperature.

PPD and operative temperature hours over 26 °C show much of the same pattern as with the max and min operative temperature. However, it should be noted that since ZEB lab is utilizing cooling by windows, there is no requirement for PPD, and the models need to meet the thermal comfort requirement after the adaptive thermal comfort model from the standard EN-16798. However, PPD describes thermal comfort with parameters other than the adaptive model, which is helpful in this comparison of thermal comfort performance. An overview for the same 10 zones and their corresponding PPD and hours > 26 °C are found in Table 23.

Table 23: Evaluation of PPD and operative temperature of over 26 °C (TEK17 requirement) for all four window control algorithm models

	Algorithm 1		Algorithm 2		Algorithm 3		Algorithm 4	
Zone	PPD	hours>26°C	PPD	hours>26 °C	PPD	hours>26 °C	PPD	hours>26 °C
6 - Cafeteria	13,3	13,8	13,23	10,7	14,25	17,4	13,34	10,8
15 - Hallway/office landscape	14,95	0	14,71	0	14,76	0	14,58	0
16 - Twin room reserach cell	13,56	2,5	16,3	1,9	13,89	4,6	16,17	2,3
17 - Twin room reserach cell	13,53	4,4	16,28	2,6	13,94	5,4	16,28	4
18 - Meeting room	12,81	0	13,16	0	13,22	0	12,88	0
20 - Multiroom	13,57	0	14,35	0	14,13	0	13,93	0
26 - Hallway/office landscape	14,25	1,1	14,27	0,7	14,27	1,5	15,09	0,5
27 - Office landscape	14,21	5,7	14,33	4,9	14,37	6	14,39	5,5
32 - 2x multiroom	12,9	0	13,18	0	13,32	0	12,87	0
40 - Knowledgecenter/hallway	15,09	0	15,88	0	15,14	0	15,13	0
Average of these 10 zones	13,82	2,75	14,57	2,08	14,13	3,49	14,47	2,31
Average of all zones	15,21	2,09	15,33	1,51	15,24	2,66	15,12	1,58

All window control algorithms have less than 50 hours above 26 °C and therefore have no problem fulfilling the recommendations from TEK17 §13-4 (1). Furthermore, the models with night cooling, i.e., algorithms 2 and 4, have the lowest amount of hours > 26 °C with 1.51 hours and 1.58 hours, respectively. Algorithms 1 and 3 without the night cooling have a bit higher of 2.09 hours and 2.66 hours above 26 °C, respectively. However, the differences are considered insignificant since the quantity of hours above 26 °C is so low for all models compared to the requirement of TEK17.

Some variations in PPD between some zones are observed, such as zone 6 with 13.23 in algorithm 2 and 14.25 in algorithm 3. However, when considering the average PPD for all zones in each window control algorithm model, the range is only from 15.12 to 15.33. This is above the required maximum of 15% PPD in EN-16798. However, as previously stated, the ZEB lab does not follow the PMV requirement since it utilizes cooling by natural ventilation, so it is considered acceptable. Furthermore, IDA ICE does not calculate air velocity in the zones and only utilizes a fixed air velocity of 0.1 m/s for the PPD calculation. This makes the accuracy of the PPD low, and since the most significant difference between the models is only 0.21, it should be considered negligible. More regarding air velocity in the zones in chapter 7.3.2.

ZEB lab shall meet the requirement of category 3 for the adaptive thermal comfort model to ensure acceptable thermal comfort for the occupants. The assessment of the adaptive thermal comfort for all four window control algorithms is presented in Table 24.

Table 24: Adaptive thermal comfort for ten zones for each window control algorithm. They are measured in the percentage of all hours where the zone is occupied in each of the three categories. Categories 1, 2, and 3 represent best, good, and acceptable (from IDA ICE), respectively.

Adaptive thermal comfort												
	Algorithm 1			Algorithm 2			Algorithm 3			Algorithm 4		
Percent in each category [%]	1	2	3	1	2	3	1	2	3	1	2	3
6 - Cafeteria	0,95	1,00	1,00	0,94	1,00	1,00	0,95	1,00	1,00	0,94	1,00	1,00
15 - Hallway/office landscape	0,99	1,00	1,00	0,85	0,99	1,00	0,91	1,00	1,00	0,79	0,99	1,00
16 - Twin room reserach cell	0,86	1,00	1,00	0,84	1,00	1,00	0,93	1,00	1,00	0,91	1,00	1,00
17 - Twin room reserach cell	0,87	1,00	1,00	0,87	1,00	1,00	0,94	1,00	1,00	0,92	1,00	1,00
18 - Meeting room	1,00	1,00	1,00	0,98	1,00	1,00	1,00	1,00	1,00	0,99	1,00	1,00
20 - Multiroom	0,98	1,00	1,00	0,95	1,00	1,00	0,98	1,00	1,00	0,95	1,00	1,00
26 - Hallway/office landscape	0,91	1,00	1,00	0,87	1,00	1,00	0,93	1,00	1,00	0,81	1,00	1,00
27 - Office landscape	0,88	1,00	1,00	0,84	1,00	1,00	0,89	1,00	1,00	0,81	1,00	1,00
32 - 2x multiroom	0,94	1,00	1,00	0,88	1,00	1,00	0,96	1,00	1,00	0,89	1,00	1,00
40 - Knowledgecenter/hallway	0,90	1,00	1,00	0,82	0,99	1,00	0,93	1,00	1,00	0,78	0,98	1,00
Average of these 10 zones	0,93	1,00	1,00	0,88	1,00	1,00	0,94	1,00	1,00	0,88	1,00	1,00

All the ten zones in Table 24 for all four window control algorithms meet the requirement for adaptive thermal comfort category 3. However, the night ventilation models (algorithms 2 and 3) have significantly fewer hours in category 1. With only 88% of all occupied hours in this simulation, compared to the non-night ventilation models algorithm 1 and 3, with 93% and 94% of hours in category 1 respectively.

The decrease in performance for the night cooling algorithms is evident when comparing algorithms 3 and 4 for July of the simulation, as seen in Figure 47.
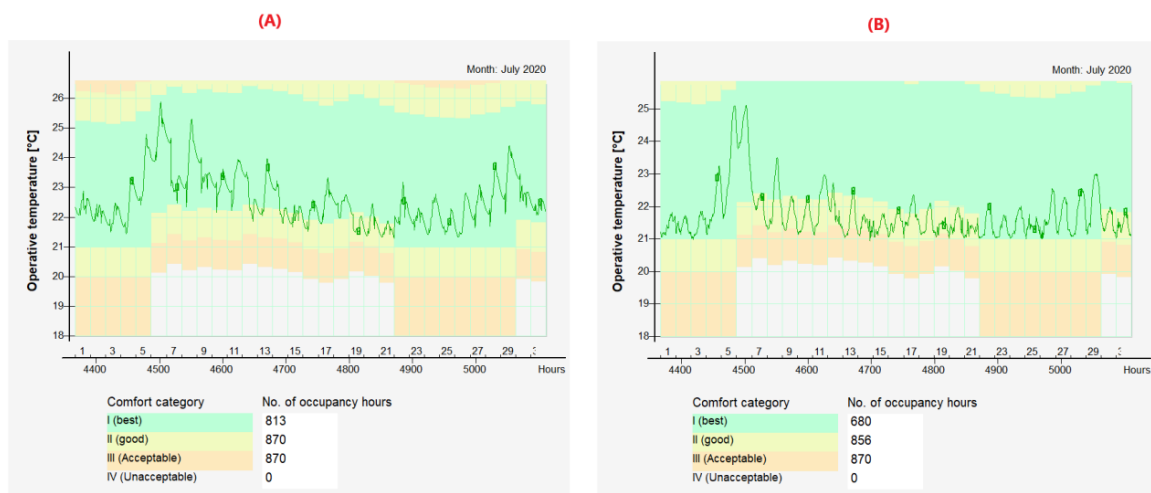
Figure 47: Adaptive thermal comfort for zone 40 during July of the BEM simulation in IDA ICE. Where (A) is with window control algorithm 3 and (B) is with window control algorithm 4.

The non-night cooling algorithm 3 has a higher temperature overall and much more variance than the model with window control algorithm 4. However, the hours outside of category 1 for algorithm 4 are because the adaptive thermal comfort model considers it too cold. The issue regarding night cooling then becomes apparent. If night cooling is set to be regulated to 22 °C during the night, it will not have cooled down the building as significantly and will experience hotter days than with 21 °C as it is the setpoint. The optimal temperature setpoint for night cooling with an automatic window control must therefore be variable. It must be determined after the building's thermal mass, the cooling efficiency of the windows, and the upcoming day's expected daytime outside air temperature. This assessment uses a fixed setpoint temperature for night cooling. It is why window control algorithms 2 and 4 have a high number of hours outside adaptive thermal comfort category 1 relative to the models without night cooling.

Adaptive thermal comfort assessment for July of the BEM simulation period with all four window control algorithms is presented in Figure 48.
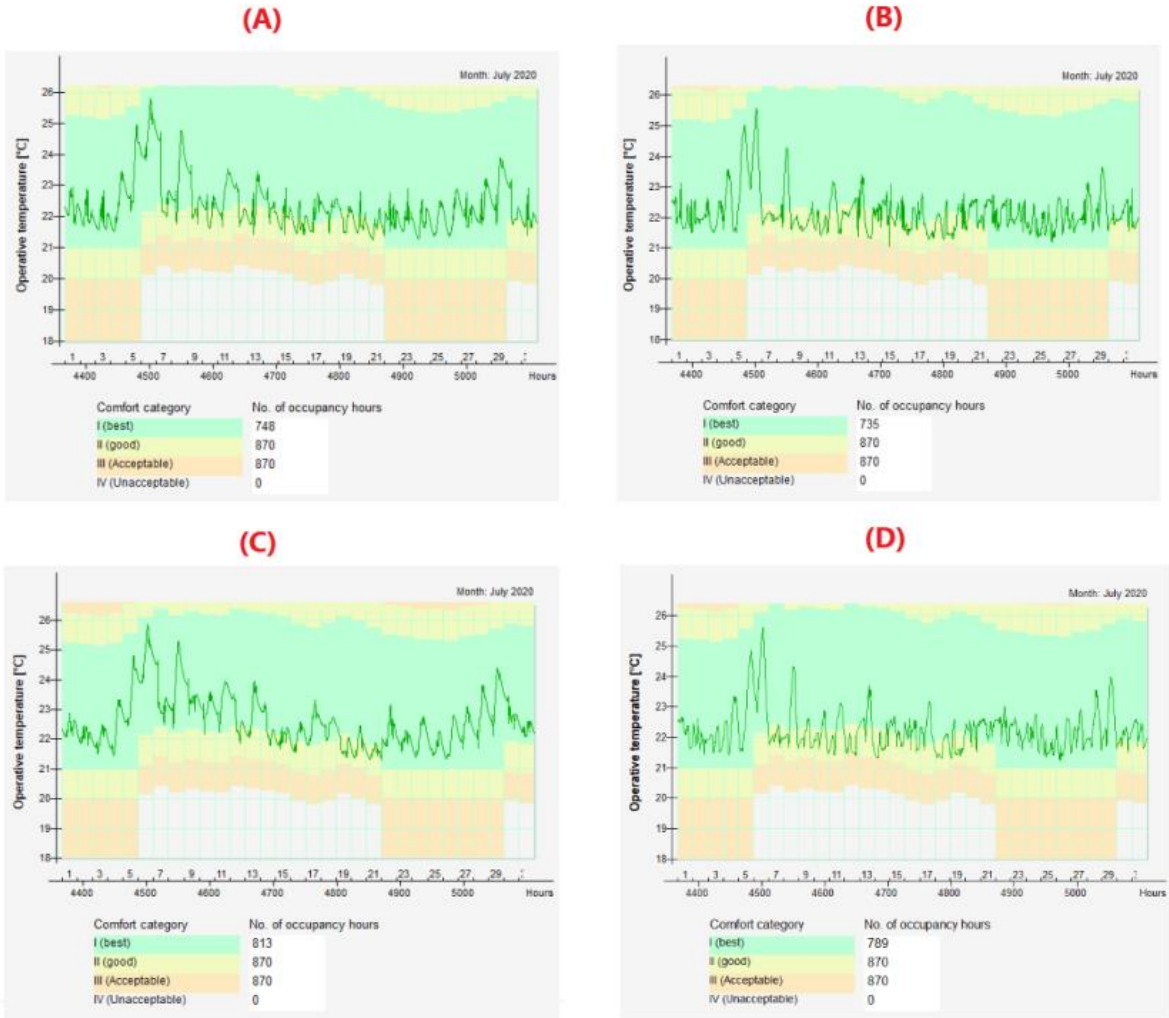
Figure 48: Adaptive thermal comfort for zone 16 during the month of July of the BEM simulation in IDA ICE. Where (A) is with window control algorithm 1, (B) is with window control algorithm 2, (C) is window control algorithm 3 and (D) is window control algorithm 4.

It is evident from Figure 48 that the same pattern as is seen in Figure 47 is prevalent in the night cooling models when compared to the non-night cooling models. Model B and D have a lower operative temperature, and A and C generally have higher ones. Additionally, model A has more hours in adaptive comfort category 1 compared to model B, which is based on the same principle of ON/OFF control. The same trend is seen with the models with variable opening percentages, as model C has more hours in adaptive comfort category 1 compared to model D.

As shown in Figure 48, the night cooling models (B and D) do not gain much of an advantage when considering the peak maximum temperature during the daytime. The peak temperature around hour 4500 in Figure 48 is approximately the same for all four models. This is most likely to the small thermal mass of the ZEB lab, as it gets heated up too quickly during the daytime for the hottest days. However, during the days with moderate outside air temperature, the positive effects of night cooling are observed. As the operative temperature range during the day is generally lower for the night cooling models.

7.3.2. Window opening patterns and occupant comfort

Draught, change in airflow quantity, and windows constantly changing their opening can be bothersome for the occupants. Therefore, this chapter evaluates each window opening control algorithm separately to assess which algorithm is occupant friendly when not considering thermal comfort.

Figure 49, Figure 50, Figure 51, and Figure 52 show each of the four window control algorithms 1,2,3 and 4, respectively, where the (A) part of each figure includes the window opening area (% of total window area) for a single-window in zone 16. And the (B) part of the figures is the corresponding mean air temperature and operative temperature in zone 16. The graphs are clipped from IDA ICE for a single day (31. June) from the BEM simulation, as this specific day shows multiple key attributes from each algorithm.

Window control algorithm 1
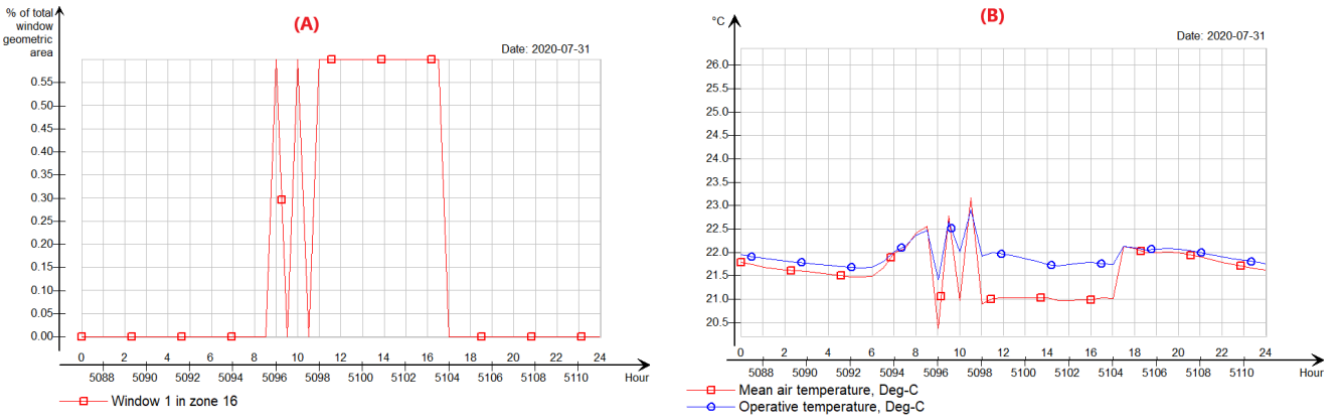
Figure 49: (A) window opening (% of the geometric area of the window) for zone 16 (date 31. June). (B) mean air temperature and operative temperature for zone 16 (date 31. June). Retrieved from IDA ICE with window control algorithm 1.

Window control algorithm 2
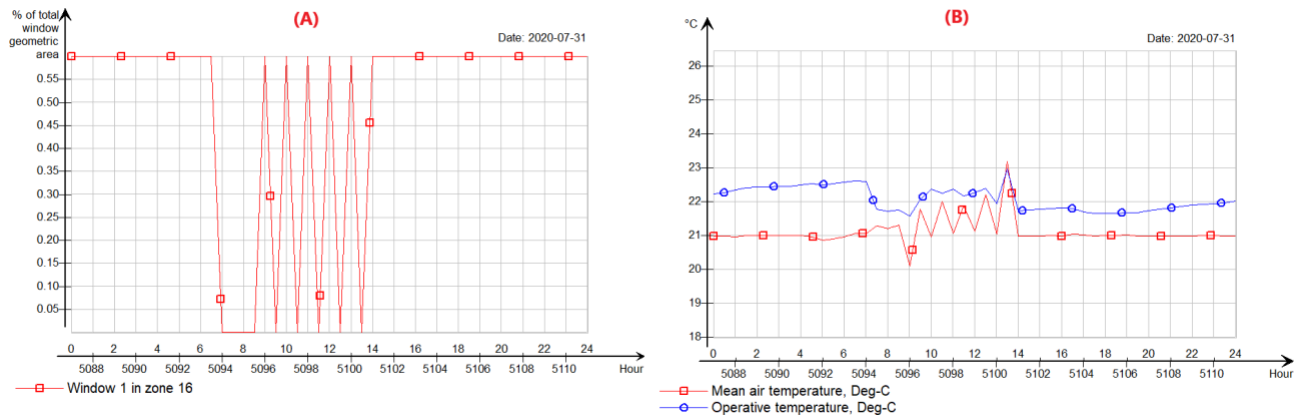
Figure 50: (A) window opening (% of the geometric area of the window) for zone 16 (date 31. June). (B) mean air temperature and operative temperature for zone 16 (date 31. June). Retrieved from IDA ICE with window control algorithm 2.

Window control algorithm 3
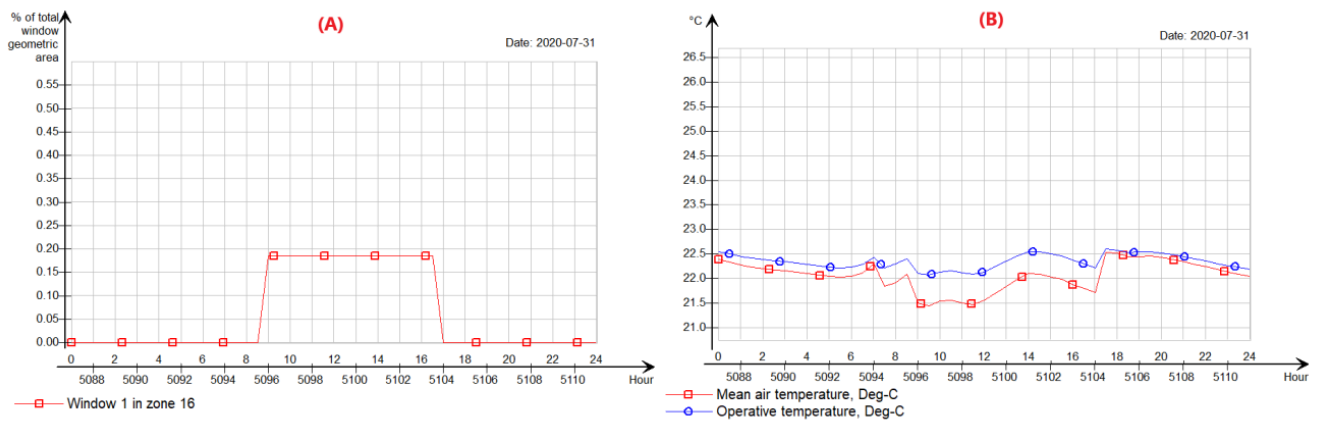
Figure 51: (A) window opening (% of the geometric area of the window) for zone 16 (date 31. June). (B) mean air temperature and operative temperature for zone 16 (date 31. June). Retrieved from IDA ICE with window control algorithm 3.

Window control algorithm 4
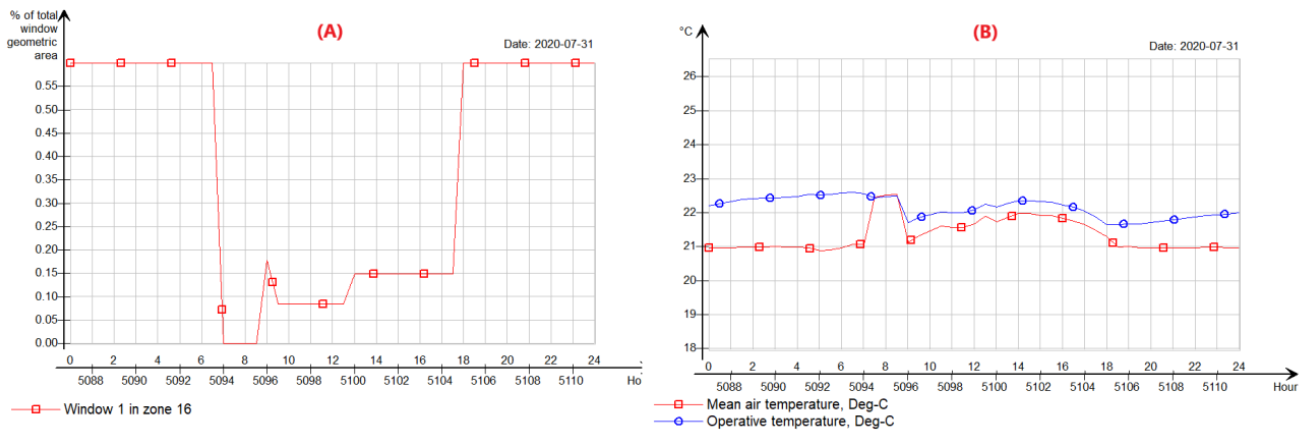
Figure 52: (A) window opening (% of the geometric area of the window) for zone 16 (date 31. June). (B) mean air temperature and operative temperature for zone 16 (date 31. June). Retrieved from IDA ICE with window control algorithm 4.

The issue with the ON/OFF models (algorithm 1 and 2) is days like 31. June, which is presented in the previous figures, the operative temperature is about the same as the operative temperature set-point for opening the windows, such that the windows oscillate between fully open and close during the day. The result of this opening pattern is that operative temperature then changes frequently during the day. The draught risk is very high since fully opening the windows induces high variations in air pressure, and occupants may experience the window actuator opening/closing event as annoying. There also seems to be no prevalent advantage for utilizing night cooling, as the operative temperature for algorithms 1 and 2 are in the same range. However, the night cooling model (algorithm 2) has a bit lower thermal mass and therefore sees the oscillating opening/closing pattern for longer until the operative temperature never goes under the set point of 22 °C. However, this pattern could be the opposite if a different day than 31. June was presented, where algorithm 1 experienced the periodically open/closing pattern more. Additionally, it should be noted that these oscillations for either model 1 and 2 algorithms only happen during specific climatic circumstances and are not seen for most of the simulated days.

Considering the variable window opening models (algorithm 3 and 4), there are no oscillations and a much more stable indoor operative temperature than the ON/OFF models (algorithm 1 and 2). With algorithm 3 without night cooling, the window opening is unchanged during the day and is ~20% of the total geometric area. And for algorithm 4 with night cooling, the window opening is more variable and changes three times during the daytime. The window opening for window algorithm 4 is in the range of ~8 % to ~17 % of the geometric area of the window. However, it stays mostly at ~10% and ~15% for most of the daytime.

Window control algorithms 3 and 4 provide acceptable indoor operative temperature, with few changes in window actuator position. If some positives/negatives sides are taken from algorithms 3 and 4. It is that algorithm 3 has zero changes during the daytime, and algorithm 4 has an overall smaller geometric area of the window opening (i.e., less airflow and draught risk). However, from the four algorithms, there are undoubtedly extensive advantages of utilizing variable window opening instead of ON/OFF control. Moreover, only small advantages are generally seen with night cooling.

Figure 53 shows all airflows through the facades, internal walls, and the mechanical ventilation system for zone 16. Retrieved for all four window control algorithms and same the timespan as in Figure 49, Figure 50, Figure 51, and Figure 52,
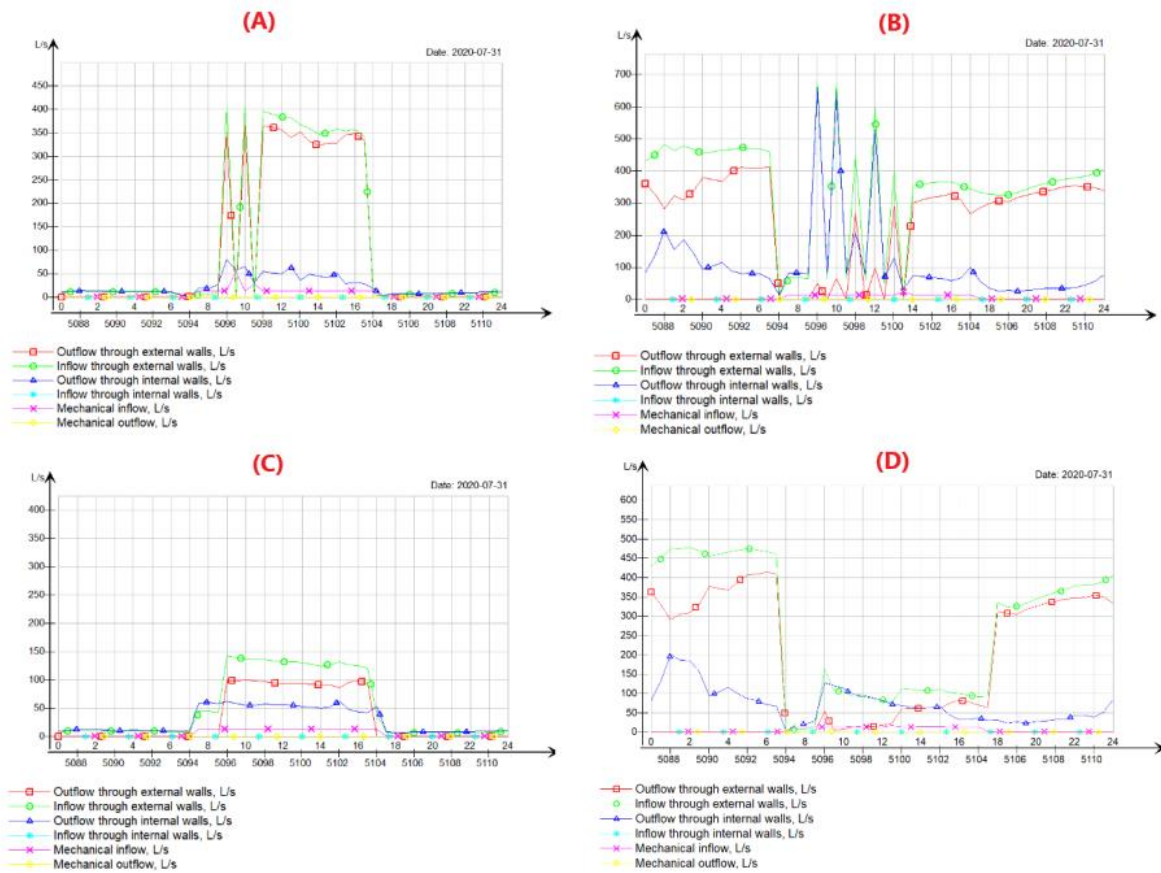
Figure 53: All airflows through the façade, internal walls, and mechanical ventilation for zone 16 for all window control algorithms for the 31. June of the BEM simulation. Where (A) is algorithm 1, (B) is algorithm 2, (C) is algorithm 3 and (D) is algorithm 4.

The inflow through the facades for algorithms 1 and 2 oscillates to close to zero when windows are closed, to a maximum of ~400 l/s for model 1 and ~650 l/s for model 2 when windows are fully open. Where with the variable window opening models, the inflow for model 3 is approximately 120 l/s – 140 l/s, and for model 4 is approximately 80 l/s – 160 l/s. However, the inflow through the facades for model 4 stays mainly around the 80 l/s -100 l/s range.

This inflow through external walls data supports what is previously addressed. Issues regarding draught are high for the ON/OFF models. Model 4 has a slight advantage over model 3 because a smaller window opening area is required to keep the operative temperature at an acceptable level.

8. Conclusion

The objective of the thesis work is based on two research questions: *"How do the wind pressure coefficients from databases compare to the on-site measured and calculated wind pressure coefficients for ZEB lab, and what is the optimal window cooling strategy for ZEB lab?"* To answer these two questions, an extensive literature study has been performed, a detailed BEM of the ZEB lab has been made, and on-site measurements used to calculate wind pressure coefficients for the ZEB lab are completed. And lastly, four proposed heuristic-based window opening control algorithms for the ZEB lab are evaluated and tested for optimal performance in the BEM.

The wind pressure coefficient values based on the on-site measurements were compared to the AIVC ones, which gave a clear indication that the new wind pressure coefficients much better represent how the wind interacts with ZEB labs building body. The wind pressure coefficients from AIVC consist of identical Cp for the north and south façades as with the west and east, giving unreasonable airflow patterns that the theory does not support. However, the new and measured Cp values produced more reasonable results when considering the well-known theory of building pressure profiles and wind-induced pressure differences. The Cp's are a long way from being accurate and should only be applied to get an overview of the building and not be used for a detailed analysis. Therefore, it is concluded that the measured Cp values should be applicable for evaluation of the window control algorithms performance.

The four proposed window control algorithms were tested in the BEM, giving essential information regarding the best approach for the ZEB lab to utilize operable windows for ventilative cooling. All four algorithms performed similarly in regards to thermal comfort. However, the night-cooling algorithms (2 and 4) show some more thermal discomfort due to too cold operative temperature in the mornings. However, all four models fulfilled all thermal comfort requirements from the adaptive thermal comfort model and the requirement from TEK17. The fully open/fully closed algorithms (1 and 2) show high draught risk, oscillating between the windows' fully open/closed position and reducing comfort for the occupants. Therefore, it is concluded that algorithms 3 and 4 are sub-optimal window opening strategies and should not be considered for implementation.

Furthermore, there were minor differences between algorithms 3 and 4, which utilize variable window opening areas, with some positive/negative sides with both algorithms found. The variable window opening with night cooling (algorithm 4) sees some discomfort due to too cold in the morning but may not need to open windows as much during the daytime due to the lower thermal mass of the ZEB lab. While algorithm 3 without night cooling requires a bigger window opening area when cooling but does not experience too cold operative temperatures in the mornings.

Night cooling can be implemented to give a small improvement in thermal comfort, by implementing a variable setpoint temperature for the nighttime cooling. But due to the relatively low thermal mass of ZEB lab the increased thermal comfort is low and when considering the and the time and cost of implementation and operation of such a system, it is not considered as the optimal strategy. Hence, with all this in mind it is therefore concluded that algorithm 3 is the ideal window control strategy, when considering the four proposed models.

Bibliography

[1]   "Climate change and the environment," *Norgesportalen*.
https://www.norway.no/en/missions/eu/values-priorities/climate-env/ (accessed Nov. 16,
2021).

[2]   T. Ahmad and D. Zhang, "A critical review of comparative global historical energy
consumption and future demand: The story told so far," *Energy Rep.*, vol. 6, pp. 1973–1991,
Nov. 2020, doi: 10.1016/j.egyr.2020.07.020.

[3]   "Norske utslipp og opptak av klimagasser." Miljødirektoratet, Apr. 17, 2022. [Online].
Available: https://miljostatus.miljodirektoratet.no/tema/klima/norske-utslipp-av-klimagasser/

[4]   "Emission Database for Global Atmospheric Research (EDGAR)." Accessed: Apr. 17,
2022. [Online]. Available: https://edgar.jrc.ec.europa.eu/country_profile/NOR

[5]   F. Goia, L. Finochiaro, and A. Gustavsen, "The ZEB Living Laboratory at the
Norwegian University of Science and Technology: a zero emission house for engineering and
social science experiments," Aug. 2015.

[6]   F. Goia, C. Schlemminger, and A. Gustavsen, "The ZEB Test Cell Laboratory. A
facility for characterization of building envelope systems under real outdoor conditions,"
Energy Procedia, vol. 132, pp. 531–536, Oct. 2017, doi: 10.1016/j.egypro.2017.09.718.

[7]   "About the ZEB Centre." http://zeb.no/index.php/en/about-zeb/about-the-zeb-centre
(accessed Apr. 20, 2020).

[8]   B. Time *et al.*, "ZEB Laboratory - Research Possibilities," 2019.
https://www.sintefbok.no/book/index/1232/zeb_laboratory_research_possibilities (accessed
Dec. 11, 2021).

[9]   "Direktoratet for byggkvalitet." https://dibk.no/regelverk/byggteknisk-forskrift-
tek17/13/ii/13-4/ (accessed Dec. 11, 2021).

[10]   N. Lolli, "Innovasjoner i ZEB-laboratoriet," p. 17.

[11]   "Inneklima og luftkvalitet på arbeidsplassen."
https://www.arbeidstilsynet.no/tema/inneklima/ (accessed Mar. 25, 2022).

[12]   S. Ingebrigtsen, *Ventilasjonsteknikk del 1*. Oslo: Skarland Press AS, 2016.

[13]   ASHRAE, "ASHRAE handbook Fundamentals ISBN: 9781615830015." ASHRAE,
2009.

[14]   P. Roghanchi, M. Sunkpal, and C. Kocsis, "Understanding the Human Thermal
Balance and Heat Stress Indices as They Apply to Deep and Hot US Mines," Jun. 2015.

[15]   P. O. Fanger, *Thermal comfort : analysis and applications in environmental
engineering*. Copenhagen: Danish technical press, 1970.

[16]   "Bygningers energiytelse Ventilasjon i bygninger Del 1: Inneklimaparametere for
dimensjonering og vurdering av bygningers energiytelse inkludert inneluftkvalitet, termisk
miljø, belysning og akustikk (Modul M1-6)." European Committee of Standardization., 2019.

[17]   "Ergonomi i termisk miljø Analytisk bestemmelse og tolkning av termisk
velbefinnende ved kalkulering av PMV- og PPD-indeks og lokal termisk komfort (ISO
7730:2005)." European Committee of Standardization., 2006.

[18]   M. A. Humphreys and J. Fergus Nicol, "The validity of ISO-PMV for predicting
comfort votes in every-day thermal environments," *Energy Build.*, vol. 34, no. 6, pp. 667–
684, Jul. 2002, doi: 10.1016/S0378-7788(02)00018-X.

[19]   R. Maiti, "PMV model is insufficient to capture subjective thermal response from Indians," *Int. J. Ind. Ergon.*, vol. 44, no. 3, pp. 349–361, May 2014, doi: 10.1016/j.ergon.2014.01.005.

[20]   J. Hoof, M. Mazej, and J. Hensen, "Thermal comfort: Research and practice," *Front. Biosci.*, vol. 15, pp. 765–788, Jan. 2010, doi: 10.2741/3645.

[21]   "ASHRAE 55." American Society of Heating, Refrigerating and Air-Conditioning Engineers, 2017.

[22]   C. T. Cheung, T. Parkinson, P. Li, and G. Brager, "Analysis of the accuracy on PMV – PPD model using the ASHRAE Global Thermal Comfort Database II," *Build. Environ.*, vol. 153, Feb. 2019, doi: 10.1016/j.buildenv.2019.01.055.

[23]   S. Moossavi, "Adaptive Thermal Comfort Model," Nov. 2012.

[24]   M. Humphreys and F. Nicol, "Understanding the adaptive approach to thermal comfort," *ASHRAE Trans.*, vol. 104, pp. 991–1004, Jan. 1998.

[25]   P. G. Schild, "Air-to-Air Heat Recovery in Ventilation Systems," p. 12, 2004.

[26]   M. Tobias, "Differences Between Constant and Variable Air Volume Systems." https://www.ny-engineers.com/blog/differences-between-constant-and-variable-air-volume-systems (accessed Oct. 05, 2021).

[27]   S. Kalaiselvam, S. V. Vidhya, S. Iniyan, and A. A. Samuel, "Comparative Energy Analysis of a Constant Air Volume (CAV) System and a Variable Air Volume (VAV) System for a Software Laboratory," *Int. J. Vent.*, vol. 5, no. 2, pp. 229–237, Sep. 2006, doi: 10.1080/14733315.2006.11683740.

[28]   K. Ahmed, J. Kurnitski, and P. Sormunen, "Demand controlled ventilation indoor climate and energy performance in a high performance building with air flow rate controlled chilled beams," *Energy Build.*, vol. 109, pp. 115–126, Dec. 2015, doi: 10.1016/j.enbuild.2015.09.052.

[29]   B. J. Wachenfeldt, M. Mysen, and P. G. Schild, "Air flow rates and energy saving potential in schools with demand-controlled displacement ventilation," *Energy Build.*, vol. 39, no. 10, pp. 1073–1079, Oct. 2007, doi: 10.1016/j.enbuild.2006.10.018.

[30]   P. Miri and P. Babakhani, "On the failure of the only vernacular windcatcher in the mountainous region of Western Iran: Opportunities for energy-efficient buildings," *J. Clean. Prod.*, vol. 295, p. 126383, May 2021, doi: 10.1016/j.jclepro.2021.126383.

[31]   R. T. Hellwig, S. Brasche, W. Bischof, and F.-S.-U. Jena, "Thermal Comfort in Offices – Natural Ventilation vs. Air Conditioning," p. 11.

[32]   H.-Y. Zhong *et al.*, "Single-sided natural ventilation in buildings: a critical literature review," *Build. Environ.*, vol. 212, p. 108797, Mar. 2022, doi: 10.1016/j.buildenv.2022.108797.

[33]   G. Carrilho da Graça, D. P. Albuquerque, M. Sandberg, and P. F. Linden, "Pumping ventilation of corner and single sided rooms with two openings," *Build. Environ.*, vol. 205, p. 108171, Nov. 2021, doi: 10.1016/j.buildenv.2021.108171.

[34]   S. Punyasompun, J. Hirunlabh, J. Khedari, and B. Zeghmati, "Investigation on the application of solar chimney for multi-storey buildings," *Renew. Energy*, vol. 34, no. 12, pp. 2545–2561, Dec. 2009, doi: 10.1016/j.renene.2009.03.032.

[35]   G. R. Hunt and P. F. Linden, "Displacement and mixing ventilation driven by opposing wind and buoyancy," *J. Fluid Mech.*, vol. 527, pp. 27–55, Mar. 2005, doi: 10.1017/S0022112004002575.

[36]   K. Gładyszewska-Fiedoruk and A. Gajewski, "Effect of wind on stack ventilation performance," *Energy Build.*, vol. 51, pp. 242–247, Aug. 2012, doi: 10.1016/j.enbuild.2012.05.007.

[37]   G. Carrilho da Graça and P. Linden, "Ten questions about natural ventilation of non-domestic buildings," *Build. Environ.*, vol. 107, pp. 263–273, Oct. 2016, doi: 10.1016/j.buildenv.2016.08.007.

[38]   H. Cho, D. Cabrera, S. Sardy, R. Kilchherr, S. Yilmaz, and M. K. Patel, "Evaluation of performance of energy efficient hybrid ventilation system and analysis of occupants' behavior to control windows," *Build. Environ.*, vol. 188, p. 107434, Jan. 2021, doi: 10.1016/j.buildenv.2020.107434.

[39]   "About Mixed-Mode." https://cbe.berkeley.edu/mixedmode/aboutmm.html (accessed Oct. 03, 2021).

[40]   M. Jenkins, "Stack Effect Ventilation& Bernoulli's Principle," *SimScale*, Aug. 30, 2019. https://www.simscale.com/blog/2019/08/stack-ventilation-bernoulli-effect/ (accessed Apr. 24, 2022).

[41]   H. E. Feustel and A. Raynor-Hoosen, "Fundamentals of the multizone air flow model - COMIS," p. 130.

[42]   P. R. Warren and L. M. Parkins, "Single-sided ventilation through open windows." 1985.

[43]   M. Santamouris and D. Asimakopoulos, *Passive Cooling of Buildings*. Earthscan, 1996.

[44]   C. M. Mak, J. L. Niu, C. T. Lee, and K. F. Chan, "A numerical simulation of wing walls using computational fluid dynamics," *Energy Build.*, vol. 39, no. 9, pp. 995–1002, Sep. 2007, doi: 10.1016/j.enbuild.2006.10.012.

[45]   A. Pfeiffer, V. Dorer, and A. Weber, "Modelling of cowl performance in building simulation tools using experimental data and computational fluid dynamics," *Build. Environ.*, vol. 43, no. 8, pp. 1361–1372, Aug. 2008, doi: 10.1016/j.buildenv.2007.01.038.

[46]   F. Jomehzadeh *et al.*, "A review on windcatcher for passive cooling and natural ventilation in buildings, Part 1: Indoor air quality and thermal comfort assessment," *Renew. Sustain. Energy Rev.*, vol. 70, pp. 736–756, Apr. 2017, doi: 10.1016/j.rser.2016.11.254.

[47]   S. Charisi, T. K.Thiis, and T. Aurlien, "Full-Scale Measurements of Wind-Pressure Coefficients in Twin Medium-Rise Buildings." 2019.

[48]   V. Picozzi, A. Malasomma, A. Maria Avossa, and F. Ricciardelli, "The Relationship between Wind Pressure and Pressure Coefficients for the Definition of Wind Loads on Buildings." 2022.

[49]   D. Cóstola, B. Blocken, and J. L. M. Hensen, "Overview of pressure coefficient data in building energy simulation and airflow network programs," *Build. Environ.*, vol. 44, no. 10, pp. 2027–2036, Oct. 2009, doi: 10.1016/j.buildenv.2009.02.006.

[50]   D. Costola, B. J. E. Blocken, and J. L. M. Hensen, "Uncertainties due to the use of surface averaged wind pressure coefficients." 2008.

[51]   S. Charisi, M. Waszczuk, and T. K. Thiis, "Investigation of the pressure coefficient impact on the air infiltration in buildings with respect to microclimate," *Energy Procedia*, vol. 122, pp. 637–642, Sep. 2017, doi: 10.1016/j.egypro.2017.07.362.

[52]   F. Allard, *Natural ventilation in buildings: a design handbook.* London: James & James, 1998.

[53]   J. Mao, W. Yang, and N. Gao, "The transport of gaseous pollutants due to stack and wind effect in high-rise residential buildings," *Build. Environ.*, vol. 94, pp. 543–557, Dec. 2015, doi: 10.1016/j.buildenv.2015.10.012.

[54]   M. Orme, M. W. Liddament, and A. Wilson, "Numerical Data for Air Infiltration and Natural Ventilation Calculations," p. 108.

[55]   D. K. Bhamare, M. K. Rathod, and J. Banerjee, "Passive cooling techniques for building and their applicability in different climatic zones—The state of art," *Energy Build.*, vol. 198, pp. 467–490, Sep. 2019, doi: 10.1016/j.enbuild.2019.06.023.

[56]   P. Engelmann, D. Kalz, and G. Salvalai, "Cooling concepts for non-residential buildings: A comparison of cooling concepts in different climate zones," *Energy Build.*, vol. 82, pp. 447–456, Oct. 2014, doi: 10.1016/j.enbuild.2014.07.011.

[57]   G. Carrilho da Graça, Q. Chen, L. R. Glicksman, and L. K. Norford, "Simulation of wind-driven ventilative cooling systems for an apartment building in Beijing and Shanghai," *Energy Build.*, vol. 34, no. 1, pp. 1–11, Jan. 2002, doi: 10.1016/S0378-7788(01)00083-4.

[58]   M. Kolokotroni, B. C. Webb, and S. D. Hayes, "Summer cooling with night ventilation for office buildings in moderate climates," *Energy Build.*, vol. 27, no. 3, pp. 231–237, Jun. 1998, doi: 10.1016/S0378-7788(97)00048-0.

[59]   S. Yuan, C. Vallianos, A. Athienitis, and J. Rao, "A study of hybrid ventilation in an institutional building for predictive control," *Build. Environ.*, vol. 128, pp. 1–11, Jan. 2018, doi: 10.1016/j.buildenv.2017.11.008.

[60]   D. P. Albuquerque, N. Mateus, M. Avantaggiato, and G. Carrilho da Graça, "Full-scale measurement and validated simulation of cooling load reduction due to nighttime natural ventilation of a large atrium," *Energy Build.*, vol. 224, p. 110233, Oct. 2020, doi: 10.1016/j.enbuild.2020.110233.

[61]   Y. Chen, Z. Tong, W. Wu, H. Samuelson, A. Malkawi, and L. Norford, "Achieving natural ventilation potential in practice: Control schemes and levels of automation," *Appl. Energy*, vol. 235, pp. 1141–1152, Feb. 2019, doi: 10.1016/j.apenergy.2018.11.016.

[62]   Y. Chen, L. K. Norford, H. W. Samuelson, and A. Malkawi, "Optimal control of HVAC and window systems for natural ventilation through reinforcement learning," *Energy Build.*, vol. 169, pp. 195–205, Jun. 2018, doi: 10.1016/j.enbuild.2018.03.051.

[63]   Y. Chen, Z. Tong, H. Samuelson, W. Wu, and A. Malkawi, "Realizing natural ventilation potential through window control: The impact of occupant behavior," *Energy Procedia*, vol. 158, pp. 3215–3221, Feb. 2019, doi: 10.1016/j.egypro.2019.01.1004.

[64]   Y. Zhang and P. Barrett, "Factors influencing the occupants' window opening behaviour in a naturally ventilated office building," *Build. Environ.*, vol. 50, pp. 125–134, Apr. 2012, doi: 10.1016/j.buildenv.2011.10.018.

[65]   R. K. Andersen, V. Fabi, and S. P. Corgnati, "Predicted and actual indoor environmental quality: Verification of occupants' behaviour models in residential buildings," *Energy Build.*, vol. 127, pp. 105–115, Sep. 2016, doi: 10.1016/j.enbuild.2016.05.074.

[66]   M. Schweiker, F. Haldi, M. Shukuya, and D. Robinson, "Verification of stochastic models of window opening behaviour for residential buildings," *J. Build. Perform. Simul.*, vol. 5, no. 1, pp. 55–74, Jan. 2012, doi: 10.1080/19401493.2011.567422.

[67]   K. Ackerly, "Occupant Response to Window Control Signaling Systems," Jan. 2012, Accessed: May 11, 2022. [Online]. Available: https://escholarship.org/uc/item/8043748x

[68]   "Expectation constrained stochastic nonlinear model predictive control of a batch bioreactor | Elsevier Enhanced Reader."

[69]   "Datasheet SDP8xx-Analog: Differential Pressure Sensor with Analog Output,"
SENSIRON, the sensor company, Version 1, Mar. 2018.

[70]   "Operating instructions, Data logger Item No. 2203101 (DL-250V: Voltage),"
VOLTCRAFT.

[71]   "SWI15-E Series Datasheet - Wall Plug," CUI Inc, Tualatin, Oregon, 1.05, Mar. 2021.

[72]   "Application Note for SDP800 Series differential pressure sensors Compensation of
pressure drop in a hose," SENSIRON, the sensor company, Version 1, 2019.

[73]   A. Førland-Larsen and T. L.L. Baxter, "ZEB Felxible lab Energikonsept,"
Unpublished internal document, 2020.

[74]   "ZEB Flexible lab - FB + 360 Ventilasjon," Unpublished internal document, 2020.

[75]   "Leveransebeskrivelse ZEB flexible lab," Unpublished internal document, 2018.

[76]   A. Førland-Larsen, "ZEB FLEXIBLE LAB STATUS ZEB-COM MÅLPRIS 2
DOKUMENTASJON," Unpublished internal document, 2017.

[77]   J. I. Vikan, "ZEB-laboratoriet i ferd med å tas i bruk." 2020. [Online]. Available:
https://static1.squarespace.com/static/5a156c44ccc5c5ef7b893553/t/5f33e60d29fb54274fd0cd
7c/1597236762372/1012_byggeindustrien.pdf

[78]   M. Sande, "Ventilative cooling potential of the ZEB laboratory." NTNU, 2021.

Appendices

Appendix A – Electrically operable windows for the façades of ZEB lab marked in red

Appendix A-1: Windows with automatic control on the north façade marked in red.

Appendix A-2: Windows with automatic control on the south façade marked in red
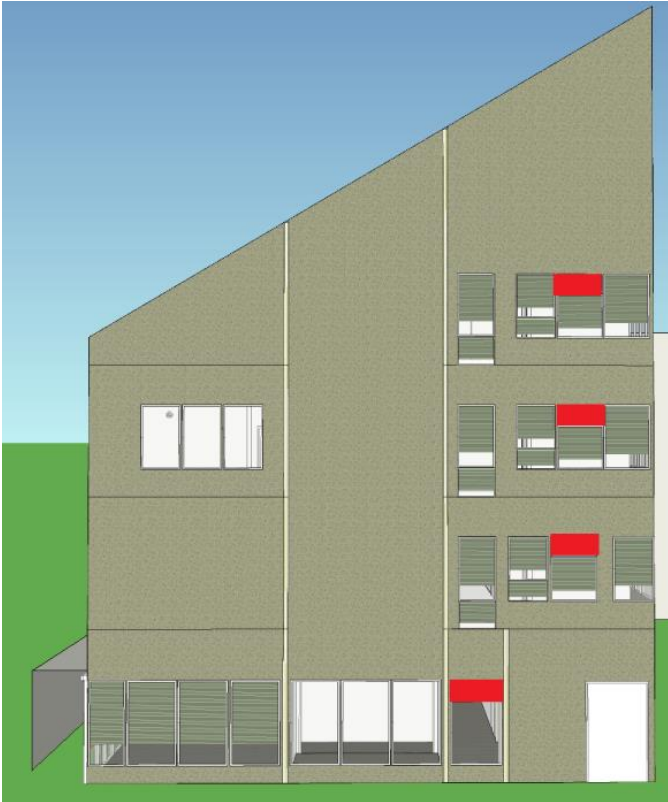
Appendix A-3: Windows with automatic control on the east façade marked in red
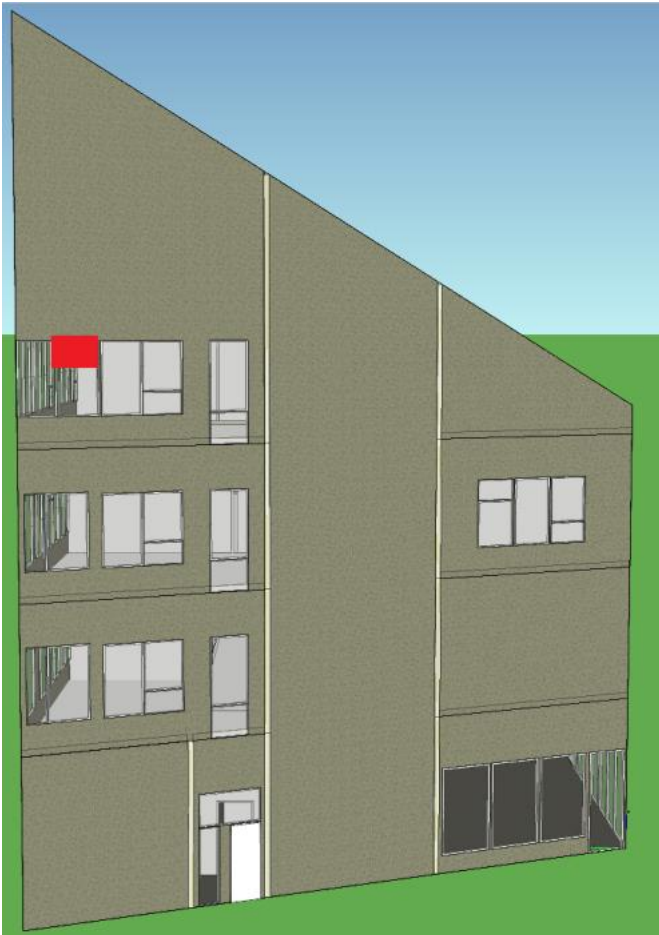
Appendix A-4: Windows with automatic control on the west façade marked in re

Appendix B – Overview of all zones, including airflow, schedules, and zone setpoints etc.

Name	Group	Floor height, m	Room height, m	Floor area, m2	Heat setp., °C	Cool setp., °C	AHU	System	Supply air, L/(s.m2)	Return air, L/(s.m2)	Occup., no./m2	Lights, W/m2	Lights, kWh/m2	Equipment, W/m2	Equipment, kWh/m2	Ext win. area, m2	Occup. schedule	Light schedule	Equipm. schedule
8 - Energy central	1st floor	0	4,45	54,89	21	22	Air Handling Unit	VAV, temp+CO2 control	5	0	0,01822	3	9,683	6	12,48	0	© Never present	Lighting unused rooms	© Equipment Schedule
7 - Stairwell	1st floor	0	4,45	21,87	21	22	No central AHU	n.a.	0	0	0,04572	3	9,683	6	3,135	10,79	Semi used zones	Lighting Schedule	Semi used zones
2 - Corridor	1st floor	0	4,45	72,57	21	22	Air Handling Unit	CAV	2	2	0,02756	3	9,683	6	3,135	3,695	Semi used zones	Lighting Schedule	Semi used zones
2 - Stairwell	1st floor	0	3,85	10,82	21	22	Air Handling Unit	CAV	0	2	0,09242	3	9,683	6	3,135	0	Semi used zones	Lighting Schedule	Semi used zones
14 - Stairwell	1st floor	0	4,45	144,1	21	22	Air Handling Unit	VAV, temp+CO2 control	4,8	151	0,4164	3	9,683	6	5,997	90,47	Cafeteria	Lighting Schedule	Cafeteria
6 - Cafeteria	1st floor	0	4,45	9,639	21	22	Air Handling Unit	VAV, temp+CO2 control	0	0	0,2074	3	9,683	6	8,818	4,177	Meeting/multirooms	Lighting Schedule	Meeting/multirooms
20 - Multiroom	2nd floor	4,45	3,85	176	21	22	Air Handling Unit	VAV, temp+CO2 control	1,6	0	0,07955	3	9,683	6	9,25	59,02	Offices	Lighting Schedule	Offices
15 - Hallway/office landscape	2nd floor	4,45	3,85	66,82	21	22	Air Handling Unit	VAV, temp+CO2 control	5	0	0,1647	3	9,683	6	8,818	15,98	© Never present	Lighting Schedule	© Never present
17 - Twin room research cell	2nd floor	4,45	3,85	21,65	21	22	Air Handling Unit	VAV, temp+CO2 control	5	0	0,2771	3	9,683	6	8,818	0	Meeting/multirooms	Lighting Schedule	Meeting/multirooms
18 - Meeting room	2nd floor	4,45	3,85	86,49	21	22	Air Handling Unit	VAV, temp+CO2 control	1,765	1,927	0,03468	3	9,683	6	8,818	0	© Never present	Lighting Schedule	© Never present
21 - Technical room	2nd floor	4,45	3,85	7,867	21	22	No central AHU	CAV	5	5	0,1271	3	5,45	6	3,135	0	Semi used zones	Lighting Schedule	Semi used zones
5 - Goods reception, wardrobes	1st floor	0	4,45	18,63	21	22	No central AHU	CAV	1,285	1,765	0,1792	3	9,683	6	3,135	0	Semi used zones	Lighting Schedule	Semi used zones
1 - Entrance	1st floor	0	4,45	5,581	21	22	No central AHU	n.a.	3,7	n.a.	0,2513	3	9,683	6	9,25	8,694	Offices	Lighting Schedule	Offices
3 - Elevator	1st floor	0	2,6	19,9	21	22	No central AHU	n.a.	7,09	n.a.	0,2552	3	9,683	6	3,135	0	Semi used zones	Lighting Schedule	Semi used zones
30 - Corner workspace	3rd floor	8,3	3,85	3,918	21	22	Air Handling Unit	CAV	2,2	0	0,1519	3	9,683	6	9,25	5,481	Semi used zones	Lighting Schedule	Semi used zones
35 - HCWC	3rd floor	8,3	3,85	52,67	21	22	Air Handling Unit	VAV, temp+CO2 control	11,31	0	0,407	3	9,683	6	3,135	0	Semi used zones	Lighting Schedule	Semi used zones
31 - Seperated workspace	3rd floor	8,3	3,85	2,457	21	22	Air Handling Unit	CAV	3,5	0	0,184	3	5,45	6	8,818	25,86	Meeting/multirooms	Lighting Schedule	Meeting/multirooms
39 - WC	3rd floor	8,3	3,85	32,61	21	22	Air Handling Unit	VAV, temp+CO2 control	1,413	0,9705	0,007764	3	5,45	6	3,135	0	Semi used zones	Lighting unused rooms	Semi used zones
32 - 2x multiroom	3rd floor	12,15	2,6	128,8	21	22	Air Handling Unit	CAV	0,6702	0,6702	0,01206	3	9,683	6	3,135	0	Semi used zones	Lighting unused rooms	Semi used zones
41 - Storage	4th floor	12,15	2,6	82,89	21	22	Air Handling Unit	VAV, temp+CO2 control	6,3	0	0,3683	3	9,683	6	8,818	44,65	Meeting/multirooms	Lighting Schedule	Meeting/multirooms
44 - Technical room/ventilation unit	4th floor	12,15	2,6	67,91	21	22	Air Handling Unit	CAV	1,995	10,27	0,04789	3	9,683	6	9,25	53,31	Offices	Lighting Schedule	Offices
42 - Classroom	4th floor	12,15	2,6	125,3	21	22	Air Handling Unit	VAV, temp+CO2 control	0	4,489	0,1616	3	9,683	6	3,135	0	Semi used zones	Lighting Schedule	Semi used zones
40 - Knowledge-center/hallway	4th floor	12,15	2,6	6,188	21	22	Air Handling Unit	CAV	0	0	0	3	5,45	6	3,135	0	© Never present	Lighting Schedule	© Equipment Schedule
43 - HCWC	4th floor	12,15	2,6	5,219	21	22	Air Handling Unit	CAV	3,949	3,949	0,1421	3	9,683	6	3,135	0	Semi used zones	Lighting unused rooms	Semi used zones
11 - Technical shaft	1st floor	0	12,15	7,035	21	22	Air Handling Unit	CAV	2,775	13,28	0,0999	3	9,683	6	3,135	0	Semi used zones	Lighting unused rooms	Semi used zones
4 - HCWC	1st floor	0	4,45	10,01	21	22	Air Handling Unit	CAV	0	13,28	0,478	3	9,683	6	3,135	0	Semi used zones	Lighting unused rooms	Semi used zones
19 - Copy room	1st floor	4,45	3,85	2,092	21	22	Air Handling Unit	CAV	0	0,478	0,478	3	9,683	6	3,135	0	Semi used zones	Lighting unused rooms	Semi used zones
12 - WC	1st floor	0	4,45	2,092	21	22	Air Handling Unit	CAV	0	0,478	0,1938	3	9,683	6	3,135	0	Semi used zones	Lighting unused rooms	Semi used zones
10 - WC	1st floor	0	4,45	5,214	21	22	Air Handling Unit	CAV	0	5,328	0,2038	3	9,683	6	3,135	2,85	Semi used zones	Lighting Schedule	Semi used zones
36 - HCWC	3rd floor	8,3	3,85	4,906	21	22	Air Handling Unit	CAV	2	2	0,1616	3	5,45	6	3,135	0	© Never present	Lighting Schedule	© Never present
9 - HCWC	1st floor	0	4,45	5,214	21	22	Air Handling Unit	CAV	2	2	0	3	5,45	6	3,135	0	Semi used zones	Lighting unused rooms	Semi used zones
13 - Entrance	1st floor	0	4,45	1,371	21	22	Air Handling Unit	CAV	2	2	0,2038	3	9,683	6	3,135	0	Semi used zones	Lighting Schedule	Semi used zones
28 - Meeting room	3rd floor	8,3	3,85	27,48	21	22	Air Handling Unit	VAV, temp+CO2 control	0	0	0,2911	3	9,683	6	8,818	13,13	Meeting/multirooms	Lighting Schedule	Meeting/multirooms
24 - Storage	2nd floor	4,45	3,85	1,371	21	22	Air Handling Unit	CAV	20,26	20,26	0,1624	3	9,683	6	12,48	0	Semi used zones	Lighting unused rooms	Semi used zones
23 - HCWC	2nd floor	4,45	3,85	4,111	21	22	Air Handling Unit	CAV	0	0	0,1012	3	9,683	6	9,25	39,99	Offices	Lighting Schedule	Offices
22 - HCWC	2nd floor	4,45	3,85	3,918	21	22	Air Handling Unit	CAV	1,8	6,757	0,2402	3	9,683	6	3,135	22,02	Offices	Lighting Schedule	Offices
37 - Storage	3rd floor	8,3	3,85	4,111	21	22	Air Handling Unit	CAV	0	7,09	0,2432	3	9,683	6	3,135	0	Semi used zones	Lighting Schedule	Semi used zones
29 - Workspace	3rd floor	8,3	3,85	20,25	21	22	Air Handling Unit	CAV	6,757	0	0,2432	3	9,683	6	3,135	0	Semi used zones	Lighting Schedule	Semi used zones
16 - Twin room research cell	2nd floor	4,45	3,85	21,64	21	22	Air Handling Unit	CAV	19,25	0	0,7294	3	9,683	6	8,818	0	© Never present	Lighting Schedule	© Equipment Schedule
26 - Hallway/office landscape	3rd floor	8,3	3,85	118,6	21	22	Air Handling Unit	VAV, temp+CO2 control	5	0	0,2911	3	9,683	6	8,818	15,98	Meeting/multirooms	Lighting Schedule	Meeting/multirooms
27 - Office landscape	3rd floor	8,3	3,85	49,94	21	22	Air Handling Unit	VAV, temp+CO2 control	1,8	0	0,1012	3	9,683	6	9,25	39,99	Offices	Lighting Schedule	Offices
38 - WC	3rd floor	8,3	3,85	2,511	21	22	Air Handling Unit	CAV	11,06	0	0,2402	3	9,683	6	3,135	22,02	Offices	Lighting Schedule	Offices
29 - Workspace	3rd floor	8,3	3,85	20,25	21	22	Air Handling Unit	VAV, temp+CO2 control	3	0	0,3982	3	9,683	6	3,135	0	Semi used zones	Lighting Schedule	Semi used zones
34 - Project workspace	3rd floor	8,3	3,85	21,64	21	22	Air Handling Unit	VAV, temp+CO2 control	5	0	0,1481	3	9,683	6	9,25	8,807	Offices	Lighting Schedule	Offices
33 - Hallway	3rd floor	8,3	3,85	41,97	21	22	No central AHU	n.a.	0	0	0,2773	3	9,683	6	8,818	0	Meeting/multirooms	Lighting Schedule	Meeting/multirooms
25 - Technical control room	2nd floor	4,45	3,85	32,58	21	22	Air Handling Unit	CAV	1,705	1,705	0,09207	3	9,683	6	3,135	0	Semi used zones	Lighting Schedule	Semi used zones

Appendix C – Detailed description of the automatic window control algorithms

Appendix C-1 shows window control algorithm 1, which is the typical ON/OFF window cooling control algorithm. To give a full depiction of how the control algorithm work, the key functions of the model are in a red box with a corresponding letter to it. Which is used for the step-by-step detailed description further below.
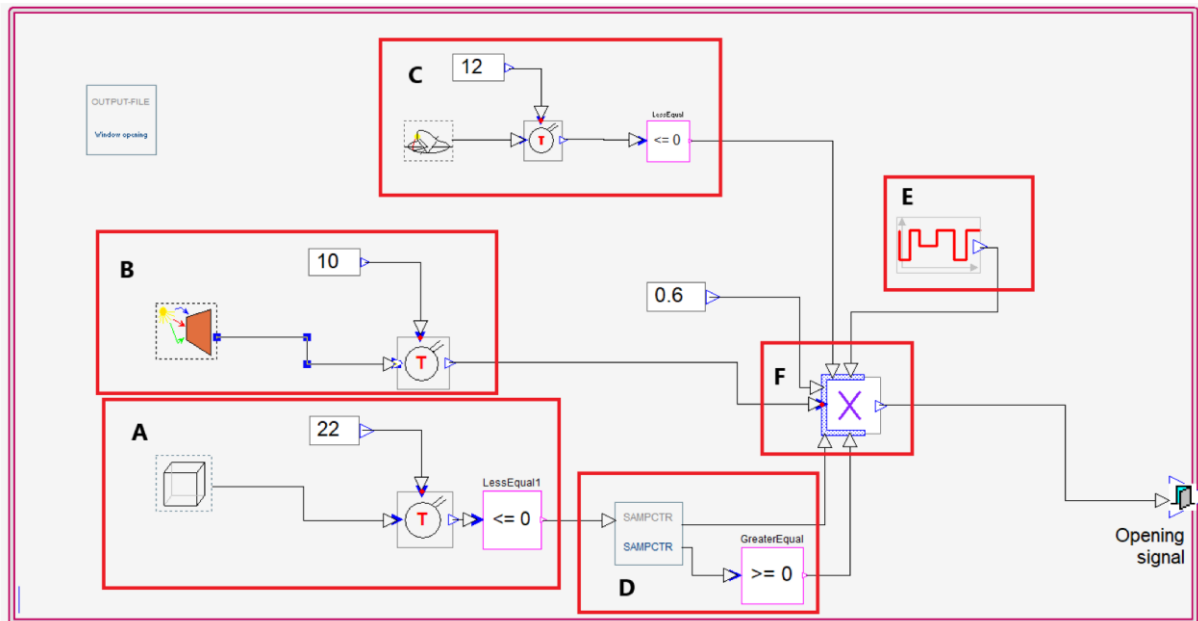
Appendix C-1: Window control algorithm 1 - Typical ON/OFF window cooling control algorithm

This window opening control algorithm is based on the following criteria's being true, if all is true then window opens to 60% of the geometrical window area. If not true window is fully closed.

Criteria's:

A – Returns true if inside air temperature is over 22 °C
B – Returns true if wind speed is less than 10 m/s
C – Returns true if outside air temperature is over 12 °C
D – Functionality of this block is to only update the output signal once per 0.5h
E – Returns true if it is daytime (07-18)
F – Multiplication block, if all other criteria is true (which is equal to 1) the output signal is multiplied by 0.6 (geometrical opening area), and the window is open. If any criteria is not met the window stays closed.

Appendix C-2 shows window control algorithm 2, which is the typical ON/OFF window cooling control algorithm that includes night cooling. To give a full depiction of how the control algorithm work, the key functions of the model are in a red box with a corresponding letter to it. Which is used for the step-by-step detailed description further below.
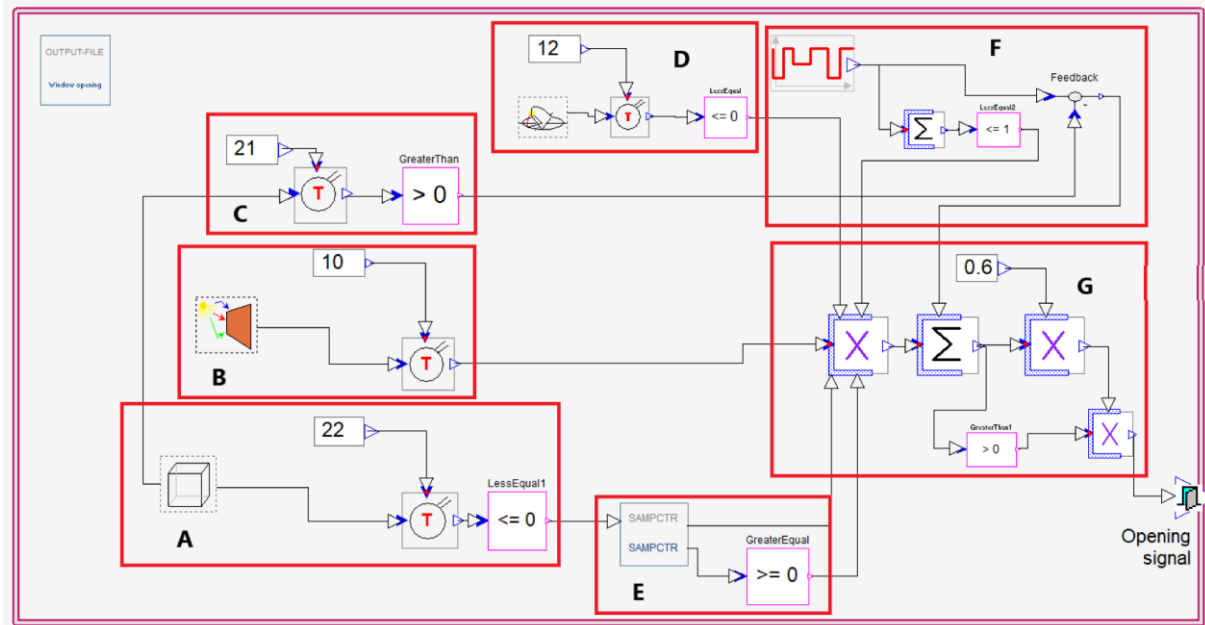
Appendix C-2: Window control algorithm 2 - Typical ON/OFF window cooling control algorithm with night cooling

This window opening control algorithm is based on the following criteria's being true, if all is true then window opens to 60% of the geometrical window area. If not true window is fully closed.

Criteria's:

A – Returns true if inside air temperature is over 22 °C
B – Returns true if wind speed is less than 10 m/s
C – Returns true if outside air temperature is over 21 °C, which is used as a night cooling criteria
D - Returns true if outside air temperature is over 12 °C
E - Functionality of this block is to only update the output signal once per 0.5h
F – Returns true if it is daytime (07-18), and true in the nighttime if temperature requirement in C is met
G – Multiplication and addition blocks to switch between daytime and nighttime window opening. Addition block either receives true from the daytime criteria's or nighttime criteria's and is further multiplied by 0.6 for geometrical opening area.

Appendix C-3 shows window control algorithm 3, which is the variable window opening cooling control algorithm. To give a full depiction of how the control algorithm work, the key functions of the model are in a red box with a corresponding letter to it. Which is used for the step-by-step detailed description further below.
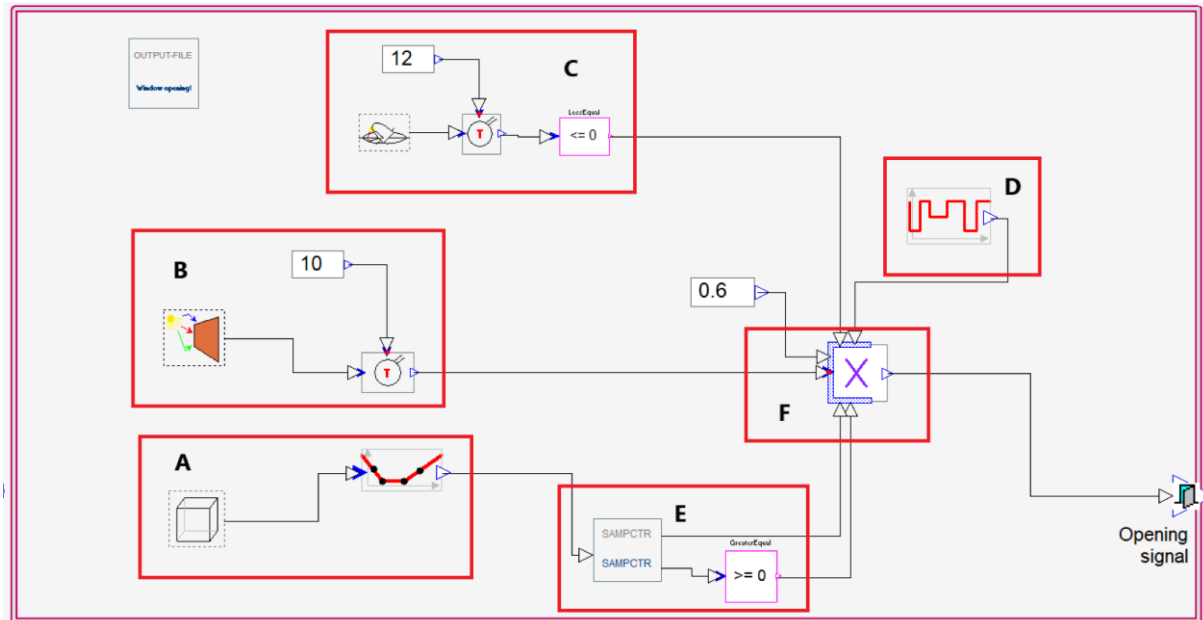
Appendix C-3: Window opening algorithm 3 - Variable window opening

This window opening control algorithm is based on the following criteria's being true, if all is true then window opens to 60% of the geometrical window area. If not true window is fully closed.

Criteria's:

A – Returns a value in the range of 0-1 if the indoor air temperature is over 22 °C. The output is linear: 0.2 at 22 °C – 1 at 25 °C
B – Returns true if wind speed is less than 10 m/s
C – Returns true if outside air temperature is over 12 °C
D – Returns true if it is daytime (07-18)
E – Functionality of this block is to only update the output signal once per 0.5h, and change it if the new value is greater than 0.1 different from the current configuration
F – Multiplication block, if all other criteria is true (which is equal to 1) the output signal is multiplied by 0.6 (geometrical opening area), and the window is open. If any criteria is not met the window stays closed.

Appendix C-4 shows window control algorithm 4, which is the which is the variable window opening cooling control algorithm that includes night cooling. To give a full depiction of how the control algorithm work, the key functions of the model are in a red box with a corresponding letter to it. Which is used for the step-by-step detailed description further below.
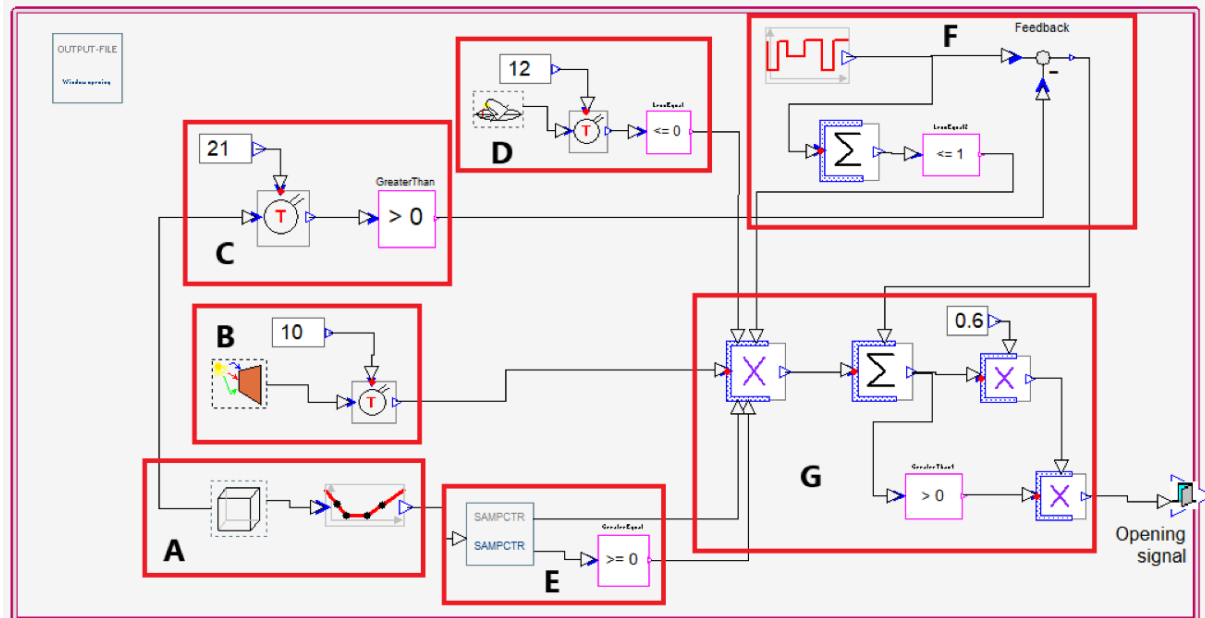
Appendix C-4: Window opening algorithm 3 - Variable window opening with night cooling

This window opening control algorithm is based on the following criteria's being true, if all is true then window opens to 60% of the geometrical window area. If not true window is fully closed.

Criteria's:

A – Returns a value in the range of 0-1 if the indoor air temperature is over 22 °C. The output is linear: 0.2 at 22 °C – 1 at 25 °C

B – Returns true if wind speed is less than 10 m/s

C – Returns true if outside air temperature is over 21 °C, which is used as the only night cooling criteria

D - Returns true if outside air temperature is over 12 °C

E - Functionality of this block is to only update the output signal once per 0.5h, and change it if the new value is greater than 0.1 different from the current configuration

F – Returns true if it is daytime (07-18), and true in the nighttime if temperature requirement in C is met

G – Multiplication and addition blocks to switch between daytime and nighttime window opening. Addition block either receives true from the daytime criteria's or nighttime criteria's and is further multiplied by 0.6 for geometrical opening area.

Appendix D – raw output data in voltage from the DP-sensors
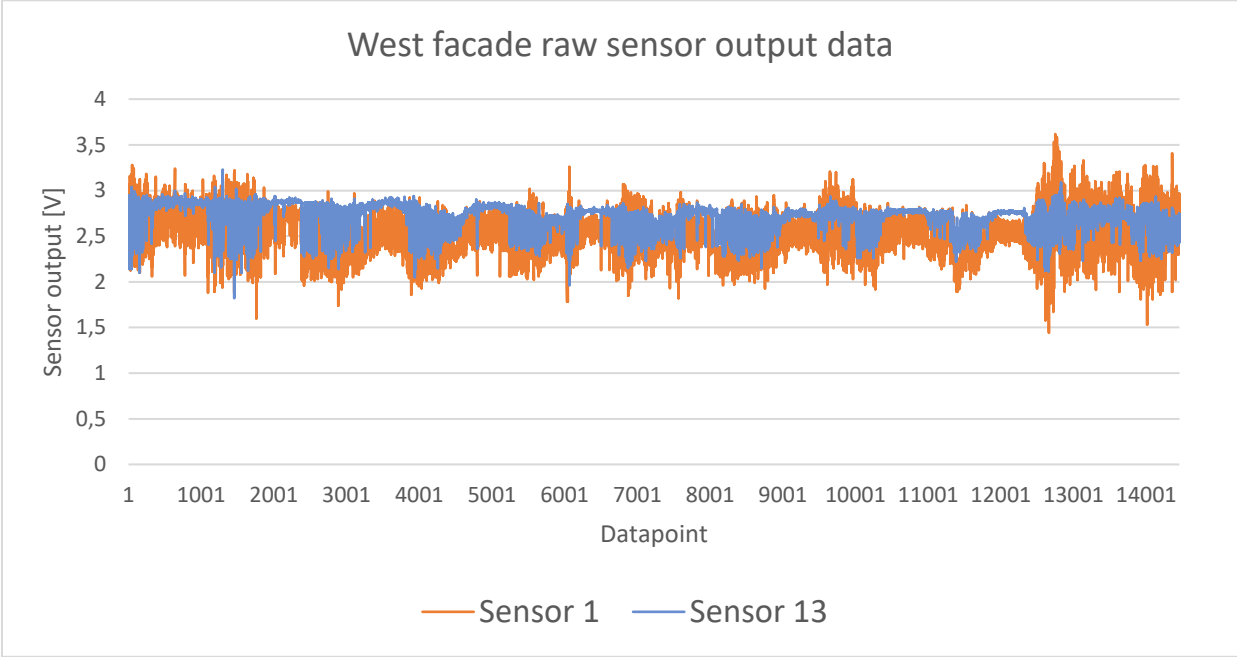
Appendix D- 1: Raw output data in voltage from the DP-sensors at the west facade
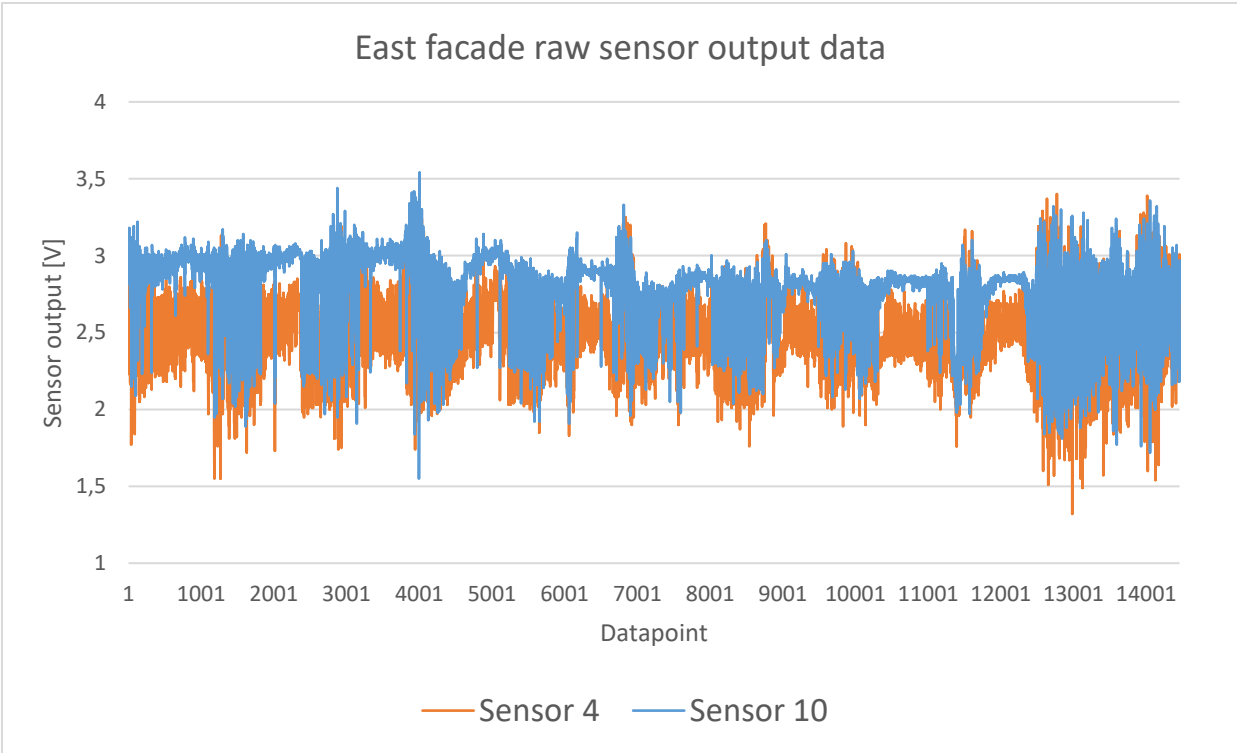
Appendix D- 2: Raw output data in voltage from the DP-sensors at the east facade
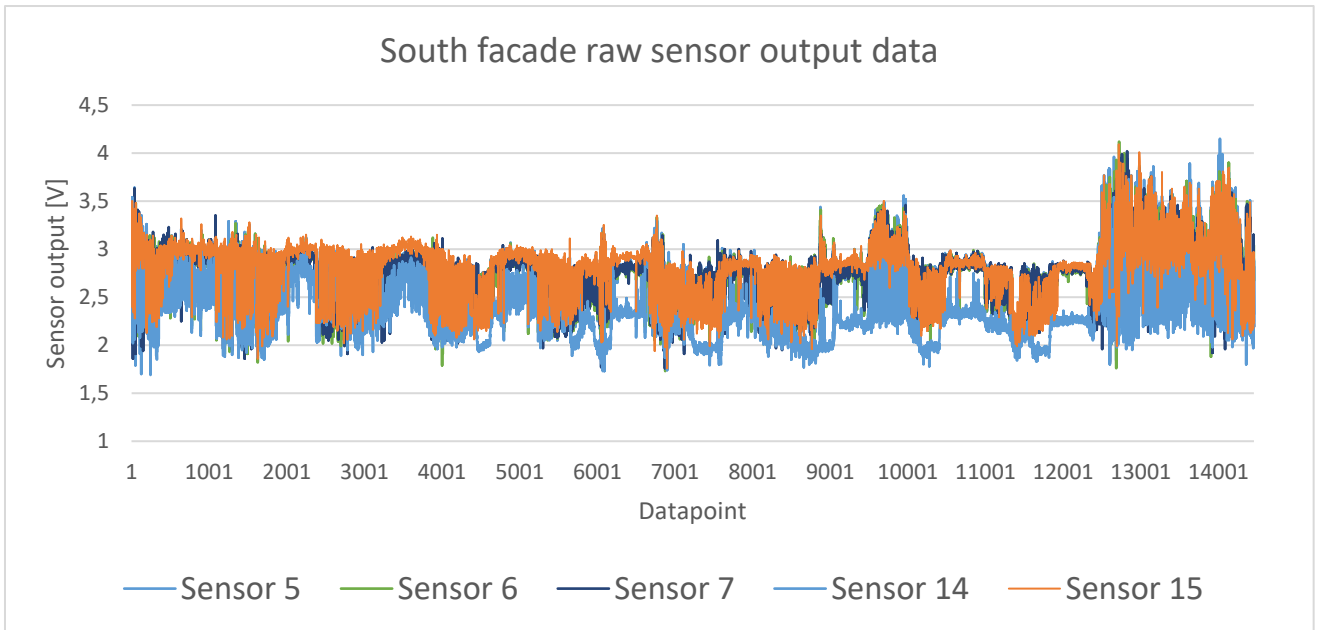
Appendix D- 3: Raw output data in voltage from the DP-sensors at the south facade
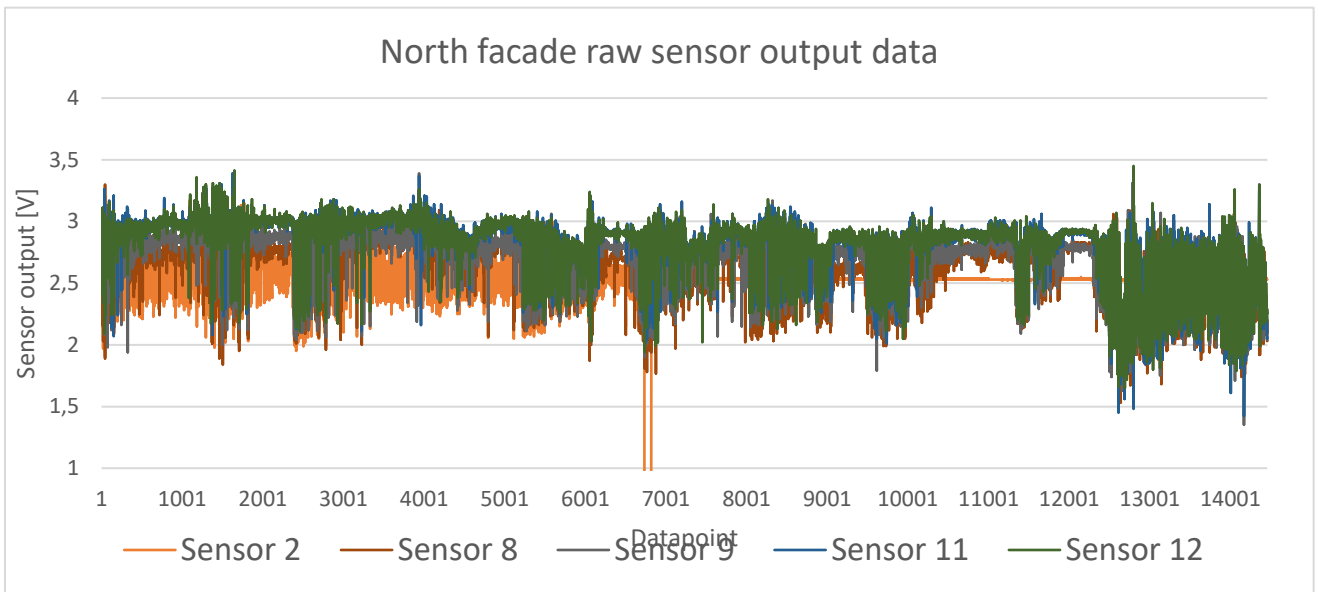
Appendix D- 4: Raw output data in voltage from the DP-sensors at the north facade

Appendix E – Thermal environment comparison of wind pressure coefficients from AIVC vs on-site

AIVC Pc model	Minimum op temp	Max op temp	PPD	Temp over 26
1 - Entrance	20,93	21,99	17,23	0
2 - Corridor	21,55	22,81	13,58	0
3 - Elevator	21,71	22,59	17,19	0
4 - HCWC	21,84	22,42	13,99	0
5 - Goods reception, wardrobes	21,55	22,24	13,81	0
6 - Cafeteria	21,62	26,12	13,77	14,6
7 - Stairwell	21,64	22,9	20,79	0,9
9 - HCWC	22,25	22,91	14,33	0
10 - WC	22,12	22,83	14,48	0
12 - WC	21,94	22,78	14,51	0
13 - Entrance	21,62	23,42	14,97	4,8
14 - Stairwell	21,83	22,67	14,89	0
15 - Hallway/office landscape	20,63	25,69	14,99	0
16 - Twin room research cell	21,22	26,33	13,54	4
17 - Twin room research cell	21,27	26,46	13,51	5
18 - Meeting room	21,61	25,31	12,94	0
19 - Copy room	22,19	22,69	14,08	0
20 - Multiroom	21,25	25,72	13,57	0
22 - HCWC	22,41	22,86	13,69	0
23 - HCWC	22,46	22,83	13,75	0
25 - Technical controlroom	22,49	22,79	13,16	0
26 - Hallway/office landscape	20,59	26,2	14,27	1,6
27 - Office landscape	21,16	27,28	14,2	6,4
28 - Meeting room	19,91	27,13	20,69	12,1
29 - Workspace	20,19	27,7	16,48	6,5
30 - Corner workspace	19,62	28,31	24,61	12,6
31 - Seperated workspace	20,91	27,04	13,53	10,8
32 - 2x multiroom	21,51	24,5	12,99	0
33 - Hallway	21,84	22,98	14,67	3,5
34 - Project workspace	21,03	26,61	13,88	5,7
35 - HCWC	21,94	22,57	13,86	0
36 - HCWC	21,83	22,28	13,96	0
38 - WC	21,6	22,18	13,9	0
39 - WC	21,58	22,12	13,89	0
40 - Knowledge-center/hallway	21,19	25,63	15,13	0
41 - Storage	21,81	22,54	24,83	0
42 - Classroom	21,02	27,34	13,82	20,4
43 - HCWC	21,83	22,56	17,37	0
44 - Technical room/ventilation unit	22,18	22,77	13,98	0

On-site Pc model	Minimum op temp	Max op temp	PPD	Temp over 26
1 - Entrance	20,96	22,01	17,21	0
2 - Corridor	21,63	22,84	13,55	0
3 - Elevator	21,75	22,66	17,19	0
4 - HCWC	21,87	22,45	14	0
5 - Goods reception, wardrobes	21,56	22,28	13,81	0
6 - Cafeteria	21,62	26,07	13,3	13,8
7 - Stairwell	21,71	22,93	20,8	0
9 - HCWC	22,31	22,96	14,32	0
10 - WC	22,19	22,88	14,46	0
12 - WC	22,03	22,84	14,49	0
13 - Entrance	21,64	23,47	14,96	4,9
14 - Stairwell	21,82	22,81	14,88	0
15 - Hallway/office landscape	21	25,62	14,95	0
16 - Twin room research cell	21,22	26,07	13,56	2,5
17 - Twin room research cell	21,27	26,31	13,53	4,4
18 - Meeting room	21,68	25,23	12,81	0
19 - Copy room	22,21	22,74	14,07	0
20 - Multiroom	21,25	25,7	13,57	0
22 - HCWC	22,46	22,96	13,7	0
23 - HCWC	22,51	22,95	13,76	0
25 - Technical controlroom	22,5	22,8	13,16	0
26 - Hallway/office landscape	21,05	26	14,25	1,1
27 - Office landscape	21,16	26,97	14,21	5,7
28 - Meeting room	19,88	26,85	20,75	7,8
29 - Workspace	20,58	27,39	19,7	6,1
30 - Corner workspace	19,78	28,13	23,32	11,4
31 - Seperated workspace	20,9	26,75	13,53	9,2
32 - 2x multiroom	21,57	24,43	12,9	0
33 - Hallway	21,92	22,8	14,65	2,2
34 - Project workspace	21,24	26,31	13,89	2
35 - HCWC	21,99	22,53	13,85	0
36 - HCWC	21,87	22,28	13,94	0
38 - WC	21,61	22,21	13,91	0
39 - WC	21,59	22,14	13,91	0
40 - Knowledge-center/hallway	21,19	25,61	15,09	0
41 - Storage	21,87	22,35	24,93	0
42 - Classroom	21,05	27,18	13,85	20,7
43 - HCWC	21,85	22,58	17,39	0
44 - Technical room/ventilation unit	22,24	22,75	13,98	0

Appendix F – IDA ICE simulation result for automatic window control algorithms

Zone	Group	Zone multiplier, M	Min temp, °C	Max temp, °C	Min op temp, °C	Max op temp, °C	Max heat supplied, W/m2	Room unit heat, W/m2	Max heat removed, W/m2	Room unit cool, W/m2	Dry vent cool, W/m2	Max sup airflow, L/(s m2)	Max rtn airflow, L/(s m2)	Max solar gain, W/m2	Min rel hum, %	Max rel hum, %	Max CO2, ppm (vol)	Max PPD, % air, h	Max age of air, h	In use, h	h of T_op>26, h	h of T_op>27, h	Occ. hours, h	PDH, h	Unmet hours (cooling)	Unmet hours (heating)
1 - Entrance	1st floor	1	20.64	25.49	20.96	22.01	38.4	105.7	41.22	0	9.311	2.006	2.014	19.27	14.78	83.81	628.7	14.49	12.067	446.5	0	0	174	14.52	175.2	0
2 - Corridor	1st floor	1	20.42	25.74	21.63	22.84	34.68	30.56	94.16	0	0	0	0	22.94	14.87	75.09	635	15.28	3.912	446.5	0	0	348	32.8	157.21	0
3 - Elevator	1st floor	1	20.05	24.21	21.75	22.66	98.23	114.4	113.6	0	0	0	0	17.19	15.41	75.27	618.2	4.104	446.5	0	0	174	17.9	119.8	0	
4 - HCWC	1st floor	1	20.72	23.47	21.87	22.45	13.32	41.95	24.09	0	16.87	3.962	3.935	14	14.72	78.73	468.2	2.598	446.5	0	0	174	18.45	19.34	0	
5 - Goods reception, wardrobes	1st floor	1	20.34	23.74	21.56	22.28	30.39	81.3	21.88	0	5.744	1.289	1.92	14.76	75.72	478.4	13.81	3.936	446.5	0	0	522	51.26	20.26	0	
6 - Cafeteria	1st floor	1	20.39	27.02	21.62	26.07	25.82	64.53	44.01	0	29.81	4.799	39.87	14.92	72.34	837	13.3	4.083	872.1	13.8	3.8	19967	1457	256.4	27.91
7 - Stairwell	1st floor	1	19.6	25.99	21.71	22.93	84.04	45.72	290.6	0	0	0	130.4	14.98	73.96	622.6	20.8	4.298	446.5	0	0	174	16.82	181.4	0	
8 - Energicentral	1st floor	1	20.18	24.1	22.31	26.07	10.01	18.22	23.63	0	21.37	4.965	15.01	72.38	400.2	8.196	0	0	0	256.4	49.11	0					
9 - HCWC	1st floor	1	20.76	24.4	22.11	22.8	13.07	33.54	20.41	0	0	5.309	14.85	73.29	684.3	14.32	5.207	446.5	0	0	174	16.14	145.2	0		
10 - WC	1st floor	1	20.7	24.37	22.19	22.88	23.28	76.91	46.26	0	0	0	14.85	73.96	692.6	14.46	4.003	446.5	0	0	174	16.32	145.1	0		
11 - Technical shaft	1st floor	1	20.98	24.06	23.28	13.49	4.212	26.1	0	11.65	2.006	1.994	15.29	72.21	400	10.28	0	0	0	156.1	0						
12 - WC	1st floor	1	20.69	27.21	22.03	22.84	27.5	87.65	47.75	0	12.58	2.007	14.85	74.18	604.2	14.49	4.004	446.5	4.9	174	16.41	136.9	0			
13 - Entrance	1st floor	1	20.4	27.21	21.64	23.47	28.64	81.88	66	0	1993	14.1	70.29	604.2	14.96	3.618	446.5	1	174	14.72	427.5	0				
14 - Stairwell	1st floor	1	19.9	25.79	21.82	22.81	199.6	101.5	252.2	0	150.6	15.09	72.83	654.3	1.88	4.519	446.5	0	174	16.06	203.7	0.2355				
15 - Hallway/office landscape	2nd floor	1	19.69	25.76	21	25.62	19.38	32.02	101.2	0	8.648	1.6	14.86	75.07	657.1	14.95	4.983	870	0	7185	607	188.5	1.958
16 - Twin room research cell	2nd floor	1	20.37	26.37	21.22	26.07	22.04	74.03	78.05	0	7.663	1.53	18.87	14.98	76.06	770.6	13.56	7.841	870	2.5	5646	465.8	197.1	0
17 - Twin room research cell	2nd floor	1	20.21	26.56	21.27	26.31	24.8	73.59	79.59	0	8.035	1.522	19.16	14.98	75.83	770.6	13.53	8.186	870	4.4	5646	454.5	232.2	0
18 - Meeting room	2nd floor	1	20.97	25.38	21.68	25.23	2.215	23.03	0	14.69	2.392	15.79	72.58	796.1	12.81	14.99	957	0	2936.3	196.1	332.4	0				
19 - Copyroom	2nd floor	1	20.58	23.65	22.21	22.74	12.13	37.65	21.05	0	13	2.784	14.72	77.27	466.7	14.07	3.318	446.5	0	174	17.75	46.87	0			
20 - Multiroom	2nd floor	1	20.69	25.77	21.25	25.7	13.93	32.46	34.38	0	30.59	4.997	42.25	14.98	73.36	903.7	13.57	6.886	957	0	978.8	71.41	257.9	0
21 - Technical room	2nd floor	1	20.32	24.16	26.99	93.16	40.08	0	9.696	1.771	14.69	73.3	450	4.781	0	0	0	153	0							
22 - HCWC	2nd floor	1	20.81	24.56	22.46	22.96	14.23	28.56	26.52	0	0	7.065	14.96	73.51	694.4	13.7	5.263	446.5	0	174	15.26	150	0			
23 - HCWC	2nd floor	1	20.73	24.46	22.51	22.95	14.39	23.59	25.13	0	0	6.733	14.96	73.61	694.3	13.76	5.318	446.5	0	174	15.41	128.6	0			
24 - Storage	2nd floor	1	20.67	24.6	32.41	75.35	60.15	0	0	20.19	14.94	74.54	631.1	4.628	0	0	0	133.3	0							
25 - Technical controlroom	2nd floor	1	20.97	24.15	22.5	22.8	5.872	2.796	14.07	0	8.809	1.711	14.97	73.94	494.9	13.16	5.717	446.5	0	522	45.37	101	0
26 - Hallway/office landscape	3rd floor	1	19.8	26.11	21.05	26	30.89	62.09	90.55	0	10.05	1.801	40.93	14.89	72.71	651.5	14.25	4.763	870	1.1	6159	501.1	202	0.3031
27 - Office landscape	3rd floor	1	19.31	27.1	21.16	26.97	59.37	162.2	179.7	0	3.959	1.327	32.6	14.88	74.72	787.9	14.21	4.672	870	5.7	0.4	6159	505.8	168.1	2.438
28 - Meeting room	3rd floor	1	16.41	27.03	19.88	26.85	69.98	100	323.3	0	28.88	4.998	82.71	14.91	75.7	904.1	20.75	4.78	957	7.8	3915	301.6	174.1	5.455
29 - Workspace	3rd floor	1	17.32	27.63	20.58	27.39	104.1	96.54	413	0	14.61	3.001	32.67	14.88	77.41	750.3	19.7	4.679	870	6.1	1.6	1539.9	130.1	158.4	5.477
30 - Corner workspace	3rd floor	1	17.35	23.56	19.78	28.13	58.14	103.3	297.7	0	22.61	3.708	120.4	14.19	69.84	904.9	23.22	4.414	870	11.4	3.9	2566.5	192.9	567.7	4.129
31 - Seperated workspace	3rd floor	1	17.6	27.41	20.9	26.75	60.53	93.49	176.3	0	14.64	2.204	68.18	14.39	70.36	658.5	13.53	4.683	870	9.2	4107	307.3	544.4	6.012
32 - 2x multiroom	3rd floor	1	20.98	24.7	21.57	24.43	2.748	2.741	22.95	0	17.05	3.495	16.21	75.27	909.5	12.9	15.33	957	0	2596.3	222.1	100.1	0
33 - Hallway	3rd floor	1	19.96	26.82	21.92	22.8	79.03	99.17	250.5	0	0	14.81	74.44	670.2	14.65	4.645	446.5	2.2	348	31.3	168.4	0.09142			
34 - Project workspace	3rd floor	1	20.74	26.39	21.24	26.31	35.3	27.44	127.6	0	25.79	5.001	10.82	14.81	73.71	679.9	13.89	4.793	957	2	2936.3	238	178.3	0
35 - HCWC	3rd floor	1	20.81	24.08	21.99	22.53	17.86	49.62	37.52	0	34.79	7.114	0	14.66	78.57	471.3	13.85	1.92	446.5	0	174	17.85	74.45	0
36 - HCWC	3rd floor	1	20.65	23.88	21.87	22.28	18.32	45.63	34.37	0	31.6	6.78	0	14.66	78.87	468.8	13.94	2.067	446.5	0	174	18.07	60.3	0
37 - Storage	3rd floor	1	20.45	24.28	49.54	100.2	89.79	0	90.66	19.31	14.62	81.09	400	0.5415	0	0	0	76.32	0							
38 - WC	3rd floor	1	20.69	23.65	21.61	22.21	28.72	91.28	51.34	0	45.8	11.09	0	14.63	79.15	493.3	13.91	1.979	446.5	0	174	18.2	24.03	0
39 - WC	3rd floor	1	20.69	23.52	21.59	22.14	30.41	92.67	50.75	0	45.34	11.35	0	14.63	79.23	494.6	13.91	2.021	446.5	0	174	18.26	19.32	0
40 - Knowledge-center/hallway	4th floor	1	20.36	26.04	21.19	25.61	46.27	64.64	92.81	0	12.04	2.002	65.62	14.86	72.8	585.6	15.09	3.993	870	0	3081	261.8	196.6	0
41 - Storage	4th floor	1	18.71	23.63	21.87	22.35	7.555	7.795	20.33	0	6.742	1.418	16.42	75.81	409.9	24.93	3.063	870	0	174	19.78	56.04	204.6	0.9731
42 - Classroom	4th floor	1	18.47	28.1	21.05	27.18	48.89	57.65	187	0	15.82	2.57	67.16	14.88	72.46	786.1	13.85	7.256	957	20.7	4.9	12234	933.3	596.1	14.93
43 - HCWC	4th floor	1	19.49	23.57	21.85	22.58	60.73	76.57	54.04	0	0	4.488	15.56	73.48	621.5	17.39	6.584	446.5	0	174	17.25	74	42.24
44 - Technical room/ventilation unit	4th floor	1	20.6	23.89	22.24	22.75	19.01	41.83	17.11	0	3.689	0.6723	0.6677	14.97	70.2	479.2	13.98	10.55	446.5	0	0	174	16.32	130.4	0

Appendix F-1: Automatic window control algorithm 1. Cropped from IDA ICE

Zone	Group	Zone multiplier, M	Min temp, °C	Max temp, °C	Min op temp, °C	Max op temp, °C	Max heat supplied, W/m2	Room unit heat, W/m2	Max heat removed, W/m2	Room unit cool, W/m2	Dry cool, W/m2	Max sup airflow, L/s m2	Max rtn airflow, L/s m2	Max solar gain, W/m2	Min rel hum, %	Max rel hum, %	Max CO2, ppm (vol)	Max PPD, %	Max age of air, h	In use, h	h of T_op>26, h	h of T_op>27, h	Occ. hours, h	PDH, h	Unmet hours (cooling)	Unmet hours (heating)
1 - Entrance	1st floor	1	20,02	24,36	21,28	22,44	38,61	105,7	45,77	0	0			17,06	14,78	73,03	615,7	14,74	13,74	445,8	0	0	174	15,05	101	0
2 - Corridor	1st floor	1	20,04	25,74	21,04	21,2	35,52	30,56	83,73	0	8,344	2,006	1,992	22,5	14,85	82,14	694,7	15,54	2,774	445,8	0	0	348	33,06	74,32	0
3 - Elevator	1st floor	1	20,02	24,09	21,09	22,03	151,1	114,4	112,7	0	0				15,46	81,34	623,9	17,28	2,268	445,8	0	0	174	18,69	45,33	0
4 - HCWC	1st floor	1	20,67	23,43	21,37	22,32	14,6	45,8	31,37	0	16,25	3,962	3,935	0	14,71	78,78	468,2	14,4	3,05	445,8	0	0	174	18,53	10,72	0
5 - Goods reception, wardrobes	1st floor	1	20,22	23,49	21,4	22,14	33,51	86,96	26,95	0	5,366	1,289	1,92	0	14,75	76,69	481,5	14,18	5,662	445,8	0	1,9	522	50,96	11,15	0
6 - Cafeteria	1st floor	1	20,25	27,01	21,63	26,06	29,96	78,56	42,03	0	28,16	4,799		39,85	14,91	76,35	855,6	13,23	3,96	871,6	10,7		19966	1439,6	202,6	0
7 - Stairwell	1st floor	1	20,41	26,02	20,9	21,45	128	45,72	192,2	0	20,5	4,956		130,4	14,98	82,32	635,7	15,91	2,541	445,8	0	0	174	16,3	88,61	0
8 - Energycentral	1st floor	1	20,02	24,04			11,24	18,22	20,13	0	0				14,99	71,56	403,3	13,27	0	0	0	0	0		40,08	0
9 - HCWC	1st floor	1	20,71	24,14	21,71	22,73	11,38	34,29	25,55	0			5,309	0	14,85	74,86	682,7	14,52	4,4	445,8	0	0	174	16,68	71,1	0
10 - WC	1st floor	1	20,68	24,3	21,49	22,63	23,37	45,55	24,35	0	10,84	2,006	2,006	0	15,28	75,39	696,1	14,62	3,2	445,8	0	0	174	16,81	68,71	0
11 - Technical shaft	1st floor	1	20,57	23,78	21,3	22,52	13,45	5,183		0	0				15,28	73,71	400		10,29	0	0	0	0	0		64,79	0
12 - WC	1st floor	1	20,67	24,46	21,3	22,52	22,2	62,76	42,42	0	0	2,007		0	14,83	75,64	696,1	14,62	3,2	445,8	0	0,7	174	16,91	65,82	0
13 - Entrance	1st floor	1	20,26	26,86	21,16	23,21	33	97,23	59,19	0	11,76	2,007	1,993	166,3	14,14	71,57	600,6	15,28	2,816	445,8	3,4		174	15,05	308,6	0
14 - Stairwell	1st floor	1	20,09	25,69	21,21	22,36	197	101,5		0	0		150,6	1,447		77,96	659,2	15,76	2,393	445,8	0	0,7	174	17,3	115	0
15 - Hallway/office landscape	2nd floor	1	19,51	25,69	21,12	25,58	27,3	32,02	95,01	0	7,125	1,6		31,82	14,84	81,04	658,4	14,71	2,289	870	0	0	7185	609,1	82,97	77,23
16 - Twin room research cell	2nd floor	1	18,22	26,45	21,34	26,15	60,02	100	74,71	0	6,423	1,529		18,87	14,96	83,16	771,3	16,3	3,701	870	1,9		5646	477,4	112,1	386,1
17 - Twin room research cell	2nd floor	1	18,22	26,62	21,25	26,37	61,68	100,5	81,08	0	6,389	1,541		19,17	14,96	82,92	771,7	16,28	3,796	870	2,6		5646	468,9	118,8	385,6
18 - Meeting room	2nd floor	1	20,97	25,19	21,33	25,02	2,236	5,242	21,37	0	13,92	2,392		0	15,79	73,65	796,1	13,16	17,39	957	0	0	2936,1	206,5	144,8	0
19 - Copy room	2nd floor	1	20,52	23,42	21,81	22,56	14,24	40,93	28,58	0	11,99	2,784		0	14,72	78	466,7	14,87	3,757	870	0	0	174	18,14	16,5	0
20 - Multiroom	2nd floor	1	20,62	25,69	21,19	25,53	15,35	35,06	32,93	0	27,75	4,993		42,28	14,96	73,96	902,6	14,35	9,442	957	0	0	978,6	74,94	174,2	0
21 - Technical room	2nd floor	1	20,15	23,99			32,07	104,5	61,54	0	9,175	1,771	1,759	0	14,68	74,45	437,5		5,187	0	0	0	0	81,85		0
22 - HCWC	2nd floor	1	20,77	24,19	21,92	22,7	14,22	33,13	26,82	0			7,065	0	14,94	74,34	695,5	14,19	3,387	445,8	0	0	174	16,09	76,15	0
23 - HCWC	2nd floor	1	20,67	24,1	21,87	22,71	14,46	27,88	25,66	0			6,733	0	14,94	74,48	695,1	14,61	3,455	445,8	0	0	174	16,32	73,45	0
24 - Storage	2nd floor	1	20,59	24,43	21,87	22,71	32,71	91,83	58,3	0		20,19		0	14,92	77,28	633,8		2,471	0	0	0	0	73,23		0
25 - Technical controlroom	2nd floor	1	20,97	23,94	22,32	22,66	5,583	2,815	13,03	0	8,505	1,711	1,699	0	14,56	74,63	494,9	13,19	5,723	870	0	0	522	46,91	50,77	0
26 - Hallway/office landscape	3rd floor	1	19,37	26,13	21,2	25,98	46,83	62,1	86,75	0	8,338	1,797		40,96	14,9	83,19	664,8	14,27	1,978	870	0,7	0	6159	511,6	94,91	247,7
27 - Office landscape	3rd floor	1	18,4	27,19	21,02	26,99	102,2	162,2	137,9	0	26,12	4,099	1,383	32,62	14,9	85,9	790,5	14,33	1,955	870	4,9	0,5	6159	526,4	89,17	138,8
28 - Meeting room	3rd floor	1	18,03	27,33	20,56	26,91	61,32	100	244,9	0	26,12	4,98		82,46	14,89	86,04	901,8	15,35	5,662	957	6,1	0,1	3915	324,1	100,7	844,6
29 - Workspace	3rd floor	1	19,13	27,82	21,07	27,39	116,1	96,54	277,5	0	12,31	2,99		32,69	14,9	89,9	774,6	14,68	2,303	870	5,9	1,7	1539,9	138,1	80,78	234,1
30 - Corner workspace	3rd floor	1	18,4	28	20,64	27,7	61,56	103,3	238,7	0	20,54	3,703		120,4	14,29	79,65	901,8	18,76	1,46	870	8,3	3,5	2566,5	201,7	230,3	270,5
31 - Seperated workspace	3rd floor	1	18,27	26,98	20,59	26,54	56,14	93,49	170,4	0	13,04	2,2		68,18	14,5	77,57	673	14,76	1,711	870	6,2		4107	327,9	217,5	323,8
32 - 2x multiroom	3rd floor	1	20,98	24,67	21,31	24,4	2,933	2,624	21,32	0	16,24	3,493		0	16,27	75,68	910	13,18	16,56	957	0	0	2936,1	226,2	58,52	22,31
33 - Hallway	3rd floor	1	19,74	26,94	21,36	21,39	88,92	99,4	193,8	0	0		7,184	11,03	14,82	85,8	685	14,86	2,065	445,8	1,8	0	348	32,33	83,7	
34 - Project workspace	3rd floor	1	20,49	26,5	21,17	26,31	48,01	100	101	0	21,21	4,981			14,82	84,06	696,5	14,02	2,007	957	3,3	0	2936,1	245,8	87,57	0
35 - HCWC	3rd floor	1	20,77	24,04	21,5	22,37	17,01	53,88	41,17	0	33,51	7,114		0	14,65	79,06	471,1	14	1,518	445,8	0	0	174	18,15	41,08	0
36 - HCWC	3rd floor	1	20,6	23,85	21,45	22,17	17,38	49,94	39,21	0	30,65	6,78		0	14,65	79,01	468,7	14,67	1,593	445,8	0	0	174	18,28	31,45	0
37 - Storage	3rd floor	1	20,35	24,23	21,38	22,07	51,71	100,2	95,48	0	88,11	19,31		0	14,62	81,42	404,6	0,5711	0,5711	445,8	0	0	0		41,27	0
38 - WC	3rd floor	1	20,64	23,62	21,36	22,04	30,14	99,44	57,35	0	43,65	11,09		0	14,63	79,65	495,4	14,34	0,577	445,8	0	0	174	18,19	17,9	0
39 - WC	3rd floor	1	20,64	23,49	21,36	22,04	30,88	100,9	58,4	0	43,39	11,35		0	14,62	79,98	496,8	14,33	0,956	445,8	0	0	174	18,23	12,59	0
40 - Knowledge-center/hallway	4th floor	1	19,7	26,08	21,19	25,48	58,44	64,64	73,94	0	10,36	2,002	10,24	65,62	14,84	80,78	588,3	15,88	3,082	870	0	0	3081	272	100,2	11,56
41 - Storage	4th floor	1	18,45	23,4	21,43	22,21	7,753	7,795	26,16	0	6,123	1,418	0,9744		16,71	77,18	409,9	27,53	4,505	870	0	0	272	22,92	25,49	393,4
42 - Classroom	4th floor	1	18,73	27,42	20,56	26,86	50,39	57,65	193,1	0	10,37	2,49		67,16	14,84	82,11	784,2	16,58	2,068	957	10,5		12234	1012,7	161,8	277,3
43 - HCWC	4th floor	1	19,12	23,32	21,66	22,46	76,57	76,57	81,88	0	10,37	4,491		0	15,78	75,37	620,2	19,97	7,045	445,8	0	0	174	18,68	12,52	131,6
44 - Technical room/ventilation unit	4th floor	1	20,52	23,67	21,77	22,56	23,08	45,78	25,29	0	3,316	0,6723	0,6677	0	14,95	71,92	431,6	14,65	11,46	445,8	0	0	174	17,15	43,71	0

Appendix F-2: Automatic window control algorithm 2. Cropped from IDA ICE

Zone	Group	Zone multiplier, M	Min temp, °C	Max temp, °C	Min op temp, °C	Max op temp, °C	Max heat supplied, W/m2	Room unit heat, W/m2	Max heat removed, W/m2	Room unit cool, W/m2	Dry vent cool, W/m2	Max sup airflow, L/(s m2)	Max rtn airflow, L/(s m2)	Max solar gain, W/m2	Min rel hum, %	Max rel hum, %	Max CO2, ppm (vol)	Max PPD, %	Max age of air, h	In use, h	h of T_op>26, h	h of T_op>27, h	Occ. hours, h	PDH, h	Unmet hours (cooling)	Unmet hours (heating)
1 - Entrance	1st floor	1	20,12	24,78	21,4	22,72	35,95	104,9	33,83	0	0			17,31	14,78	71,09	591,9	14,03	9,478	447,9	0	0	174	14,38	276,1	0
2 - Corridor	1st floor	1	20,49	25,79	21,79	23,14	28,52	30,56	97,22	0	10,87	2,006	1,992	22,47	14,87	73,77	712,8	15,22	3,935	447,9	0	0	348	32,4	219,2	0
3 - Elevator	1st floor	1	20,05	24,45	21,86	22,89	99,96	114,4	118,8	0	0			15,46	14,72	74,42	581,2	17,1	4,146	447,9	0	0	174	17,77	173,9	0
4 - HCWC	1st floor	1	20,71	23,58	21,72	22,5	13,4	43,45	25	0	17,23	3,962	3,935	14,72	14,13	78,59	468,7	14,13	2,503	447,9	0	0	174	18,23	25,11	0
5 - Goods reception, wardrobes	1st floor	1	20,31	23,89	21,46	22,36	31,11	84,41	21,88	0	5,879	1,289	1,92	14,75	14,92	75,14	480,6	13,55	3,646	447,9	0	0	522	49,36	35,31	0
6 - Cafeteria	1st floor	1	20,35	27,22	21,67	26,24	26,26	74,26	44,48	31	4,799			39,87	14,92	71,56	847,6	14,25	3,984	872,7	17,4	4,8	19968	1422,3	315,3	0
7 - Stairwell	1st floor	1	20,47	26,02	21,85	23,27	66,3	45,72	229,8	0	130,4			72,67	14,99	72,88	639,7	15,5	4,301	447,9	0	0	174	15,52	272,3	0
8 - Energycentral	1st floor	1	20,15	24,2	22,28	23,08	11,13	18,22	23,96	21,81	4,965		5,309	15,01	14,87	72,67	400	14,33	7,697	0	0	0			57,16	0
9 - HCWC	1st floor	1	20,76	24,7	22,28	23	31,76	31,76	20,33	0	0			20,33	14,87	72,45	647,9	14,33	5,172	447,9	0	0	174	15,87	223,8	0
10 - WC	1st floor	1	20,73	24,7	22,19	23	23,05	58,13	39,36	0	0			39,36	14,85	73,12	658,4	14,34	3,975	447,9	0	0	174	16,08	194,4	0
11 - Technical shaft	1st floor	1	20,98	24,28			13,52	4,206	26,81	0	12,17	2,006	1,994	15,31	10,28	10,97	658,4		0	0			0		234	0
12 - WC	1st floor	1	20,73	24,75	22,1	22,99	21,65	58,27	37,98	0	0			14,85	73,39	658,4	14,34	3,975	447,9	0	0	174	16,13	202,5	0		
13 - Entrance	1st floor	1	20,37	27,48	21,49	23,6	28,01	90,68	59,21	0	13,45	2,007	1,993	166,3	14,15	69,54	581,4	16,66	3,659	447,9	5,2	1,1	174	14,43	510,7	0
14 - Stairwell	1st floor	1	20,23	26,07	21,81	23,05	15,23	101,5	159,8	0	150,6			1,145	15,14	71,66	659,2	15,92	4,323	447,9	0	0	174	15,81	332,7	0
15 - Hallway/office landscape	2nd floor	1	20,47	25,91	21,07	25,74	15,23	32,02	77,56	0	9,415	1,6		31,83	14,85	73,3	660,9	14,76	5,028	870	0	0	7185	598,2	278	0
16 - Twin room research cell	2nd floor	1	20,61	26,69	21,34	26,45	15,41	73,47	73,47	0	6,524	1,447		18,87	14,99	72,46	769,3	13,89	7,518	870	4,6	0	5646	446,3	320	0
17 - Twin room research cell	2nd floor	1	20,68	26,83	21,3	26,6	12,56	36,67	76,74	0	6,934	1,47		19,17	14,99	72,02	770	13,94	7,867	870	5,4	0	5646	432,5	383,4	0
18 - Meeting room	2nd floor	1	20,97	25,59	21,35	25,43	2,413	5,727	23,45	0	15,04	2,39		15,78	13,22	71,95	796,1	13,22	14,78	956,8	0	0	2936,1	197,1	456,6	0
19 - Copy room	2nd floor	1	20,57	23,8	22,2	22,85	12,39	39,1	21,74	0	13,05	2,784		14,72	76,75	467	14,52	3,287	447,9	0	0	174	17,53	66,53	0		
20 - Multiroom	2nd floor	1	20,67	25,85	21,27	25,73	14,18	33,6	35,27	0	32,01	5,001		42,28	14,98	72,95	905,1	14,13	6,396	956,8	0	0	978,6	72,55	300,3	0
21 - Technical room	2nd floor	1	20,3	24,35		26,92	99,29	40,16	0	10,03		1,771	14,69	72,04	463,5	14,69	5,025	447,9	0	0	174	15,4	211,7	0		
22 - HCWC	2nd floor	1	20,8	24,77	22,54	23,19	14,23	30,3	22,35	0	1,759			14,97	72,38	676,1	14,11	5,058	447,9	0	0	174	15,4	267,6	0		
23 - HCWC	2nd floor	1	20,72	24,65	22,55	23,18	14,52	24,96	23,94	0	0	7,065		6,733	14,96	72,71	676	14,43	5,125	447,9	0	0	174	15,59	225,3	0
24 - Storage	2nd floor	1	20,66	24,71		22,9	32,2	84,17	55,98	0	0		20,19	14,95	73,54	619,6	13,94	4,146	0	0	0		0	201,4	0		
25 - Technical controlroom	2nd floor	1	20,97	24,3	22,56	22,9	6,096	2,748	14,47	0	9,012	1,711	1,699	14,97	73,36	495,2	13,13	5,722	447,9	0	0	522	44,81	115,1	0
26 - Hallway/office landscape	3rd floor	1	20,66	26,14	21,22	26,08	14,94	30,91	74,87	0	10,9	1,801		40,91	14,97	73,13	669,9	14,27	4,777	870	1,5	0	6159	488,3	325,1	0
27 - Office landscape	3rd floor	1	20,45	27,12	21,21	27	47,74	162,2	181	0	4,223	1,362		32,6	14,91	73,05	789,2	14,37	4,65	870	6	0,7	6159	515,7	220,7	0,9203
28 - Meeting room	3rd floor	1	19,51	27,1	21,37	26,96	43,92	100	170,7	0	29,56	4,998		80,64	14,9	74,97	901,5	13,85	4,283	956,8	9,4	0	3915	295,4	238,1	0
29 - Workspace	3rd floor	1	18,59	27,58	20,63	27,35	80,44	96,54	382,3	0	15,48	3,001		32,69	14,91	75,44	746	14,78	4,658	870	6,2	1,6	1539,9	138,8	191,2	13,06
30 - Corner workspace	3rd floor	1	20,09	29,7	21,31	28,21	28,46	103,3	81,81	0	23,34	3,706		120,4	14,3	68,81	898,8	25,35	3,911	870	11,8	4,2	2566,5	196,5	660,6	0
31 - Seperated workspace	3rd floor	1	20,69	27,76	21,29	26,94	13,75	37,95	66,03	0	15,69	2,204		68,16	14,45	70,26	677,3	14,1	4,584	870	15,4	1,1	4107	301,7	762,2	0
32 - 2x multiroom	3rd floor	1	20,98	24,85	21,31	24,54	2,667	2,885	23,28	0	17,44	3,498		16,23	74,95	908,7	13,32	14,92	956,8	0	0	2936,1	221,3	119,5	0	
33 - Hallway	3rd floor	1	20,66	26,82	22,04	23,2	65,55	99,4	220,7	0	0	3,498		7,081	14,82	73,63	690,2	14,32	4,628	447,9	2,9	0	348	31,11	221,3	0
34 - Project workspace	3rd floor	1	20,9	26,41	21,23	26,35	28,53	106,3	23,28	0	28,02	5,001		11,16	14,8	73,74	698,6	13,89	4,792	956,8	2,8	0	2936,1	234,4	260,6	0
35 - HCWC	3rd floor	1	20,8	24,19	21,86	22,64	17,77	51,35	38,62	0	35,58	7,114		14,65	77,93	469,8	13,9	1,814	447,9	0	0	174	17,67	95,31	0	
36 - HCWC	3rd floor	1	20,65	24	21,77	22,39	18,17	47,14	36,05	0	32,35	6,78		14,65	78,47	468,9	14,45	1,96	447,9	0	0	174	17,91	65,63	0
37 - Storage	3rd floor	1	20,43	24,41	21,86	22,64	51,85	100,2	92,41	0	93	19,31		14,61	80,24	400	13,9	0,4996	447,9	0	0	0		87,47	0
38 - WC	3rd floor	1	20,68	23,74	21,55	22,31	28,38	94,07	51,97	0	46,28	11,09		14,63	79,18	488,8	14,04	1,85	447,9	0	0	174	18,02	30,78	0
39 - WC	3rd floor	1	20,68	23,62	21,49	22,22	30,1	55,44	51,81	0	45,54	11,35		14,63	79,19	490	14,03	1,894	447,9	0	0	174	18,09	22,73	0
40 - Knowledge-center/hallway	4th floor	1	20,28	26,05	21,14	25,54	38,56	64,64	62,97	0	12,79	2,002	10,24	65,55	14,85	71,85	561,2	15,14	3,971	870	0	0	3081	254,6	329,8	431
41 - Storage	4th floor	1	18,32	23,8	21,75	22,48	7,04	7,795	25,16	0	6,761	1,418	0,9744	0	16,89	74,96	409,9	29,08	2,752	447,9	0	0	174	21,66	61,65	0
42 - Classroom	4th floor	1	19,47	28,43	20,88	27,51	33,69	57,65	155,9	0	13,05	2,114		67,16	14,87	68,44	775,9	16,58	6,892	956,8	28,4	7,4	12234	888,1	865,8	18,91
43 - HCWC	4th floor	1	19,28	23,74	21,71	22,69	61,76	76,57	60,23	0	0		4,489	0	15,68	72,55	587,4	18,95	6,491	447,9	0	0	174	17,51	139,5	101,2
44 - Technical room/ventilation unit	4th floor	1	20,59	24,08	22,18	22,88	19,81	43,77	19,86	0	3,741	0,6723	0,6677	0	14,97	69,23	442,5	14,26	10,53	447,9	0	0	174	16,07	205	0

Appendix F-3: Automatic window control algorithm 3. Cropped from IDA ICE

Zone	Group	Zone multiplier, M	Min temp, °C	Max temp, °C	Min op temp, °C	Max op temp, °C	Max heat supplied, W/m2	Room unit heat, W/m2	Max heat removed, W/m2	Room unit cool, W/m2	Dry vent cool, W/m2	Max sup airflow, L/(s m2)	Max rtn airflow, L/(s m2)	Max solar gain, W/m2	Min rel hum, %	Max rel hum, %	Max CO2, ppm (vol)	Max PPD, % air, h	Max age of air, h	In use, h	h of T_op>26, h	h of T_op>27, h	Occ. hours, h	PDH, h	Unmet hours (cooling)	Unmet hours (heating)
1 - Entrance	1st floor	1	20,31	24,99	20,67	21,77	39,8	105,1	32,5	0	0	2,006	2,014	16,74	14,77	83,91	630,1	14,58	9,182	445	0	0	174	14,97	191,08	0
2 - Corridor	1st floor	1	20,1	25,72	21,02	21,26	35,56	30,56	88,54	0	9,961		2,006	23,18	14,88	82,65	639,2	15,2	2,797	445	0	0	348	33,1	171,53	0
3 - Elevator	1st floor	1	20,02	24,05	21,08	22,1	114,4	108	46,76	0	15,45		2,007		15,45	81,79	593,9	17,05	2,254	445	0	0	174	18,85	46,33	0
4 - HCWC	1st floor	1	20,68	23,41	21,53	22,34	153,7	114,4	0	0	14,72	3,962	3,935	14,07	78,79	468,5	14,07	3,053	445	0	0	174	18,72	11,78	0
5 - Goods reception, wardrobes	1st floor	1	20,26	23,55	21,43	22,18	14,3	44,43	31,26	0	16,11	1,289		14,76	76,96	484,9	13,73	5,672	445	0	0	522	53,45	9,799	0
6 - Cafeteria	1st floor	1	20,33	27,03	21,64	26,06	33,47	84,17	27,84	0	5,424	4,799	1,92	13,34	76,52	815,9	13,86	4,098	445	3,2	3,2	19966	1470,7	194,8	0
7 - Stairwell	1st floor	1	19,53	26	20,96	21,55	130	69,87	41,96	0	29,25		4,956	130,4	15,01	82,62	627,8	21,25	2,549	445	10,8		19966	1470,7	93,75	29,89
8 - Energycentral	1st floor	1	20,1	24,05			18,22	45,72	20,17	0	20,6				15,02	71,72	403,3	14,6	14,6	0	0	0	0	0	40,39	0
9 - HCWC	1st floor	1	20,73	24,27	21,76	22,72	11,16	34,96	26,08	0	4,956		5,309		14,88	75,02	688,1	14,4	4,396	445	0	0	174	16,84	72,24	0
10 - WC	1st floor	1	20,67	24,25	21,51	22,6	80,16	46,76	20,17	0			13,23		14,86	75,74	696,2	14,61	3,211	445	0	0	174	17,01	70,67	0
11 - Technical shaft	1st floor	1	20,96	23,88			13,56	5,382	24,64	0	10,83		1,994		15,31	73,45	400	10,29	4,396	0	0	0	0	0	72,3	0
12 - WC	1st floor	1	20,67	24,41	21,28	22,49	27,09	43,62		0			2,006		14,86	76,04	696,2	15,2	3,211	445	0	0	174	17,2	67,09	0
13 - Entrance	1st floor	1	20,67	27,03	21,19	23,23	85,23	101,5	67,37	0	11,68	2,007	1,993	0,9211	14,13	71,77	611,8	14,62	2,861	445	3,2	0,8	174	15,23	284,6	0
14 - Stairwell	1st floor	1	20,31	25,7	21,36	22,51	33,84	206	67,37	0			150,6	15,13	14,62	77,56	652,8	15	2,397	445	0	0	174	16,02	123,4	0
15 - Hallway/office landscape	2nd floor	1	20,35	25,65	21,13	22,55	197,6	67,92	32,02	0	7,92	1,595	31,83	14,88	15	81,32	654,3	14,58	2,261	870	0	0	7185	650,1	81,69	74,24
16 - Twin room research cell	2nd floor	1	19,52	21,13	21,1	25,53	27,55	59,62		0	6,155	1,531	18,87	15	82,09	771,4	16,17	1,952	870	2,3		5646	447,7	141,4	383
17 - Twin room research cell	2nd floor	1	18,21	26,53	21,1	26,24	61,48	100	59,62	0	6,395	1,547	19,16	15	82,09	771,9	16,28	1,941	870	4		5646	437,6	147,3	378,9
18 - Meeting room	2nd floor	1	20,97	25,2	21,08	25,05	3,449	5,081	21,39	0	14,03	2,39		15,85	73,7	796	12,88	17,46	957	0	0	2936,1	204	155	0
19 - Copy room	2nd floor	1	20,53	23,49	21,96	22,62	13,98	28,35	28,35	0	11,9	2,784		14,73	78,17	466,8	14,23	3,757	445	0	0	174	18,34	14,12	0
20 - Multiroom	2nd floor	1	20,67	25,67	21,25	25,5	15,56	34,35	32,06	0	28,22	4,996	42,29	14,99	74,2	905,1	13,93	8,978	957	0	0	978,6	73,55	173,1	0
21 - Technical room	2nd floor	1	20,19	24,1			33,43	98,59	60,09	0	9,303	1,771		14,69	73,96	466,7		5,189	0	0	0	0	0	90,32	0
22 - HCWC	2nd floor	1	20,78	24,37	22,09	22,79	13,96	31,34	25,11	0		1,759		14,98	74,55	679	13,7	3,38	445	0	0	174	15,96	78,06	0
23 - HCWC	2nd floor	1	20,63	24,26	22,06	22,78	14,38	26,3	23,92	0	0	6,733	20,19	14,97	74,84	678,7	13,76	3,447	445	0	0	174	16,25	72,76	0
24 - Storage	2nd floor	1	20,97	24,38	21,09	22,71	32,71	82,93	57,91	0	0			14,96	77,68	620,9	2,49		0	0	0	0	0	75,31	0
25 - Technical controlroom	2nd floor	1	20,67	24,03	22,38	22,7	5,574	2,903	13,25	0	8,524	1,711	0	14,98	74,56	495	13,21	5,724	445	0	0	522	46,55	52,41	0
26 - Hallway/office landscape	3rd floor	1	20,19	26,11	21,21	25,95	46,84	62,1	74,67	0	9,646	1,794	40,97	14,92	83,22	657,3	15,09	2,355	870	0,5	0	6159	536	106,5	244,8
27 - Office landscape	3rd floor	1	20,78	27,18	21,09	27	106,8	162,1	147,2	0	4,313	1,37	32,6	14,92	85,87	790,1	14,39	2,239	870	5,5	0,6	6159	542,3	93,12	148,1
28 - Meeting room	3rd floor	1	19,26	27,36	21,28	26,96	31,68	100	158	0	25,75	4,998	80,53	14,91	86,12	904,5	14,28	5,697	957	6,7	0,2	3915	310,2	112,9	782,4
29 - Workspace	3rd floor	1	18,42	27,78	20,8	27,36	111,6	96,54	286,7	0	12,34	2,978	32,68	14,91	90,03	738,5	14,62	2,48	870	5,9	1,6	1339,9	144,6	85,46	192,5
30 - Corner workspace	3rd floor	1	18,6	28,11	21,14	27,82	61,26	103,3	132,9	0	21,21	3,707	120,4	14,24	79,5	904,9	20,08	1,492	870	3,6	3,6	2566,5	202,2	242,7	277,2
31 - Seperated workspace	3rd floor	1	19,12	26,98	21,13	26,54	62,84	93,49	83,08	0	13,94	2,2	68,2	14,5	77,08	666,2	15,03	2,254	870	6,8	0	4107	323,1	244,2	277,2
32 - 2x multiroom	3rd floor	1	18,56	24,67	21,55	24,4	2,921	2,624	21,23	0	16,33	3,493	0	16,28	75,66	910	12,87	17,05	957	0	0	2936,1	225,9	60,69	0
33 - Hallway	3rd floor	1	18,29	26,93	21,41	21,67	71,38	99,4	201,7	0	7,15		10,87	14,84	85,86	678,3	14,74	2,205	445	1,5	0	348	33,26	90,21	29,47
34 - Project workspace	3rd floor	1	20,98	26,48	21,24	26,28	49,21	100	105,9	0	24,94	4,978	10,87	14,84	84,08	683,5	14,05	2,295	957	2,9	0	2936,1	252	55,82	0
35 - HCWC	3rd floor	1	19,76	24,03	21,66	22,44	15,86	52,45	41,32	0	33,44	7,114	0	14,65	79,07	470,4	13,86	1,518	445	0	0	174	18,23	41,86	0
36 - HCWC	3rd floor	1	20,78	23,84	21,6	22,23	16,27	48,46	39,41	0	30,58	6,78	0	14,65	79,01	468,8	14,11	1,593	445	0	0	174	18,36	32,86	0
37 - Storage	3rd floor	1	20,39	24,22			50,12	100,2	95,84	0	87,96	19,31	0	14,62	81,36	406,1		0,5711	0	0	0	0	0	41,07	0
38 - WC	3rd floor	1	20,64	23,6	21,48	22,14	29,4	57,43	11,09	0	43,41	11,09	0	14,63	79,63	493,4	14,06	0,977	445	0	0	174	18,36	18,02	0
39 - WC	3rd floor	1	20,65	23,47	21,44	22,09	30,13	98,13	58,32	0	43,06	11,35	0	14,63	80	494,7	14,06	0,956	445	0	0	174	18,4	12,1	0
40 - Knowledge-center/hallway	4th floor	1	19,69	26,04	21,09	25,43	58,17	64,64	63,2	0	11,51	2,002	65,62	14,86	81,1	559	15,13	3,397	870	0	0	3081	280,5	100,4	7,546
41 - Storage	4th floor	1	18,8	23,52	21,51	22,3	7,549	7,795	25,64	0	6,161	1,418	0	16,4	77	409,9	24,12	4,507	445	0	0	174	20,6	26,9	229,7
42 - Classroom	4th floor	1	18,61	27,5	21,12	27,03	47,93	57,65	167,2	0	11,88	2,399	67,18	14,88	80,65	782,4	15,35	2,279	957	11,1	2,3	12234	957,4	216	248,2
43 - HCWC	4th floor	1	19,31	23,38	21,76	22,56	62,99	81,06	0	0	0		4,489	15,67	75,43	589,6	18,01	7,292	445	0	0	174	18,19	16,5	59,79
44 - Technical room/ventilation unit	4th floor	1	20,54	23,77	21,97	22,66	22,89	24,43	24,43	0	3,324	0,6723	0,6677	0	14,98	71,57	475,4	14,19	11,46	445	0	0	174	17,06	47,55	0

Appendix F-4: Automatic window control algorithm 4. Cropped from IDA ICE